

1A01

STUDY OF ELUCIDATING AN EFFECT OF
MATERIAL PERMITTIVITY TO CURRENT-
VOLTAGE CHARACTERISTICS OF
ANTHOCYANIN-BASED DYE-SENSITIZED
SOLAR CELL

NURUL ATIKAH BINTI MOHAMAD ASRI

BACHELOR OF ELECTRICAL
ENGINEERING WITH HONOURS

UNIVERSITI MALAYSIA PAHANG

UNIVERSITI MALAYSIA PAHANG

DECLARATION OF THESIS AND COPYRIGHT

Author's Full Name : NURUL ATIKAH BINTI MOHAMAD ASRI

Date of Birth : 30 MAY 1997

Title : 1A01 STUDY OF ELUCIDATING AN EFFECT OF MATERIAL PERMITTIVITY TO CURRENT-VOLTAGE CHARACTERISTICS OF ANTHOCYANIN-BASED DYE-SENSITIZED SOLAR CELL

Academic Session : SEMESTER 2 ACADEMIC SESSION 2020/2021

I declare that this thesis is classified as:

- CONFIDENTIAL (Contains confidential information under the Official Secret Act 1997)*
- RESTRICTED (Contains restricted information as specified by the organization where research was done)*
- OPEN ACCESS I agree that my thesis to be published as online open access (Full Text)

I acknowledge that Universiti Malaysia Pahang reserves the following rights:

1. The Thesis is the Property of Universiti Malaysia Pahang
2. The Library of Universiti Malaysia Pahang has the right to make copies of the thesis for the purpose of research only.
3. The Library has the right to make copies of the thesis for academic exchange.

Certified by:

NURUL ATIKAH

NURUL ATIKAH BINTI
MOHAMAD ASRI

970530-04-5386
Date: 11 February 2022


(Supervisor's Signature)

DR. AHMAD SYAHIMAN BIN
MOHD SHAH
Date: 11 February 2022

NOTE: * If the thesis is CONFIDENTIAL or RESTRICTED, please attach a thesis declaration letter.



SUPERVISOR'S DECLARATION

I hereby declare that I have checked this thesis and in my opinion, this thesis is adequate in terms of scope and quality for the award of the Bachelor of Electrical Engineering with Honours.

A handwritten signature in black ink, appearing to read 'A. S. M. S.', is written over a horizontal line.

(Supervisor's Signature)

Full Name : DR. AHMAD SYAHIMAN BIN MOHD SHAH

Position : SENIOR LECTURER

Date : 11 FEBRUARY 2022

(Co-supervisor's Signature)

Full Name :

Position :

Date :



STUDENT'S DECLARATION

I hereby declare that the work in this thesis is based on my original work except for quotations and citations which have been duly acknowledged. I also declare that it has not been previously or concurrently submitted for any other degree at Universiti Malaysia Pahang or any other institutions.

NURUL ATIKAH

Full Name : NURUL ATIKAH BINTI MOHAMAD ASRI

ID Number : EC18003

Date : 11 FEBRUARY 2022

1A01

STUDY OF ELUCIDATING AN EFFECT OF METRIAL PERMITTIVITY TO
CURRENT-VOLTAGE CHARACTERISTICS OF ANTHOCYANIN-BASED
DYE-SENSITIZED SOLAR CELL

NURUL ATIKAH BINTI MOHAMAD ASRI

Thesis submitted in fulfillment of the requirements
for the award of the
Bachelor of Electrical Engineering with Honours.

College of Engineering
UNIVERSITI MALAYSIA PAHANG

FEBRUARY 2022

ACKNOWLEDGEMENTS

First of all, thanks to Allah S.W.T for his mercy and guidance in giving full strength to me in complete this project. Even I faced with some difficulties in completing this project. But I still manage to complete it. Also, thanks to Allah S.W.T for giving a good health condition for me to have ability and strength in completing the project during the given time by a lecturer.

I would like to express the appreciation feeling to all lecturers that give me guidance and support throughout in completing this project. Moreover, the lecturer subject which is BEE4724 Engineering Project 2 lecturer who are Dr. Nur Huda Binti Ramlan and Dr. Ikhwan Bin Muhammad Ridzuan. Then, I would like to express my deepest appreciation to a special gratitude I give to my supervisor, Dr. Ahmad Syahiman Bin Mohd Shah who's supported my project under his guidance, gave me a great opportunity to involve in this project.

Besides that, I also grateful to my senior colleague that give suggestion and advises admitting continuously. Thanks to always spend time to sharing a knowledge that related to my project and give the best explanation to all questions that I asked. Last but not least, thanks a lot towards my family for the nonstop support and always love me. Thanks to my parent gives who love and guidance me in whatever I pursue. They are the ultimate role model.

ABSTRAK

Untuk mendapatkan pengetahuan bagaimana pemrosesan dan pengukuran dalam projek ini berdasarkan beberapa menjalankan eksperimen mengenai sel solar peka pewarna (DSSC). Ia memasifkan yang berkaitan dengan aktiviti fotokatalitik (PCA) yang dipujuk oleh fotoelektrod dan elektrod balas yang memulakan penghinaan pewarna. Dalam wujud, pigmen pewarna buah yang diekstrak digunakan sebagai antosianin yang diekstrak daripada beberapa buah untuk menyelongkar radikal bebas (antioksidan) yang dimulakan akibat PCA. Justifikasi penerokaan dalam penyelidikan adalah untuk merayu proses pengekstrakan untuk mengekstrak antosianin daripada beberapa buah dan untuk mengawal aspek utama yang terlibat dalam proses perizinan bahan. Pengekstrakan mekanikal dan pengekstrakan tangan merupakan teknik pengekstrakan berasaskan antosianin daripada beberapa buah yang mewajarkan dalam kajian ini. Elemen yang memerlukan eksperimen dalam penyiasatan ini ialah kategori penyediaan DSSC, pengukuran kemiringan berdasarkan resonator, pengukuran voltan litar terbuka (V_{oc}) dan pengukuran voltan litar terbuka (V_{oc}) pada beban. Dalam penyiasatan ini, kepekatan antosianin diukur dengan menggunakan Ultraviolet-Visible Spectrophotometer (UV-Vis). Sebagai tambahan, CST Studio Suite 2019 telah digunakan untuk membina ukuran reka bentuk resonator dengan pewarna isian dan semua analisis data untuk berasaskan antosianin akan mengenal pasti melalui pemalar dielektrik keluaran ϵ dan kehilangan dielektrik. Nilai frekuensi terbahagi kepada dua bahagian iaitu pengukuran dengan bahan pewarna dan pengukuran dengan bahan udara yang kedua-duanya adalah berkorelasi antara satu sama lain dalam kebolehtepatan pengukuran. Berdasarkan eksperimen, semakin tinggi kepekatan dalam berasaskan antosianin dalam pewarna yang diekstrak, semakin tinggi kesannya kepada kebolehtepatan pengukuran yang berkaitan dengan prestasi voltan semasa. Oleh itu, pengukuran kemiringan adalah mencapai pewarna dalam nilai maksimum penyerapan.

ABSTRACT

To gain the knowledge how the processing and measurement in this project based on several conducting experimental regarding dye-sensitized solar cells (DSSC). It is passivating the related to the photocatalytic activity (PCA) persuade by photoelectrode and counter electrode that initiate dye humiliation. In the existent, fruit coloring pigments extracted is used as an anthocyanin extracted from several fruit to rummage the free radicals (antioxidant) initiate as a result of PCA. The justification of the exploration in research is to appeal extraction process to extract anthocyanin from several fruit and to regulate the foremost aspect involved in the material permittivity process. Mechanical extraction and by hand extraction are a technique of extracting anthocyanin-based from several fruit that justify in this study. The element be in need of an experiment in this investigation were category of preparation of DSSC, measurement of permittivity based on resonator, measurement of open circuit voltage (V_{oc}) and measurement of open circuit voltage (V_{oc}) at load. In this investigation, the concentration of anthocyanin was measured by using an Ultraviolet-Visible Spectrophotometer (UV-Vis). In additional, CST Studio Suite 2019 was used to construct the design measurement of resonator with fill dye and all the data analysis for anthocyanin-based will identify by output dielectric constant ϵ and dielectric losses. The value of frequency divided into two part which measurement with material dye and measurement with material air that both are them was correlated each other in measurement permittivity. Based on experiment, the higher concentration in anthocyanin-based in extracted dye, the higher effected to measurement permittivity that related to the current-voltage performance. Therefore, permittivity measurement is accomplishing the dyes' in the maximum value of absorption

TABLE OF CONTENT

DECLARATION	
TITLE PAGE	
ACKNOWLEDGEMENTS	ii
ABSTRAK	iii
ABSTRACT	iv
TABLE OF CONTENT	v
LIST OF TABLES	ix
LIST OF FIGURES	x
LIST OF SYMBOLS	xiv
LIST OF ABBREVIATIONS	xv
CHAPTER 1 INTRODUCTION	1
1.1 Background of the Study	1
1.2 Problem Statement	3
1.3 Objective	4
1.4 Scope of Study	5
CHAPTER 2 LITERATURE REVIEW	9
2.1 Photovoltaic-System Solar Energy	9
2.2 The Application of Anthocyanin in Solar Cells	10
2.2.1 Overview of Anthocyanin	10
2.2.2 Characteristics of Solar Cell	11
2.3 DSSC Fabrication Categorization	13

2.3.1	Extraction of Photosensitizer	13
2.3.2	Photoanode and Counter Electrode Preparation	14
2.3.3	Dye Loading to TiO ²	15
2.3.4	Electrolyte	16
2.3.5	Assembly of DSSC	16
2.3.6	Measurement of DSSC Performance	16
2.4	Measurement of Permittivity	17
2.4.1	Sensor design	17
2.4.2	Fabrication of the Prototype and Measurement of Set-up	18
CHAPTER 3 METHODOLOGY		20
3.1	Flow of Methodology	20
3.2	Selection of Apparatus and Material	22
3.2.1	Apply for Measurement Absorbance	22
3.2.2	Apply for Measurement Permittivity	24
3.2.3	Apply for Measurement Dye-Sensitized Solar Cells Fabrication (DSSC)	26
3.3	Extraction of Photosensitizer	30
3.3.1	Type of Dye's Extraction Fruit for First Batch	30
3.3.2	Type of Dye's Extraction Fruit for Second Batch	31
3.4	Preparation or Arrangement of Extraction	31
3.4.1	Extraction Fruit for First Batch	32
3.4.2	Summarize for Flow Whole Procedure First Batch	34
3.4.3	Extraction Fruit for Second Batch	34
3.4.4	Summarize for Flow Whole Procedure for Second Batch	37
3.5	Measurement of Absorbance by Ultraviolet-Visible Spectrophotometer	38

3.5.1	Absorbance for Extraction Fruit First Batch	39
3.5.2	Summarize for Flow Whole Procedure for First Batch	42
3.5.3	Absorbance for Extraction Fruit Second Batch	43
3.5.4	Summarize for Flow Whole Procedure for Second Batch	46
3.6	Measurement of Permittivity based on Resonator	47
3.6.1	Permittivity for the Extraction Fruit First Batch	48
3.6.2	Summarize for Flow Whole Procedure for First Batch	53
3.6.3	Permittivity for the Extraction Fruit Second Batch	54
3.6.4	Summarize for Flow Whole Procedure for Second Batch	59
3.7	Preparation of Dye Sensitized Solar Cell (DSSC)	59
3.7.1	DSSC for First Batch	60
3.7.2	Summarize for Flow Whole Procedure for First Batch	65
3.7.3	DSSC for Second Batch	66
3.7.4	Summarize for Flow Whole Procedure for Second Batch	70
CHAPTER 4 RESULTS AND DISCUSSION		74
4.1	Graphical of Absorbance by Ultraviolet-Visible Spectrophotometer	74
4.1.1	First Batch Graph of Absorbance versus Wavelength	74
4.1.2	Second batch Graph of Absorbance versus Wavelength	76
4.1.3	Summarized of Measurement Absorbance	81
4.2	Software CST Studio Suite 2019	81
4.2.1	Dimensioning of Resonator	81
4.2.2	Measurement of Resonator	82
4.2.3	Summarized of Measurement Permittivity	83
4.3	Summarize of Completeness of Titanium Oxide on FTO glass	84
4.3.1	Completeness TiO_2 for the First Batch	84

4.3.2	Completeness TiO ² for the Second Batch	85
4.4	Measurement of Open-Circuit Voltage, Voc	86
4.4.1	First Batch on Open Circuit Voltage, Voc	86
4.4.2	Second Batch on Open Circuit Voltage, Voc	87
4.4.3	Summarize for Measurement Dye-sensitized Solar Cells	89
4.4.4	Open Circuit Voltage at Load	90
4.5	Summarize of Measurement Project	91
	CHAPTER 5 CONCLUSION AND RECOMMENDATION	92
	REFERENCES	93
	APPENDIX A GANTT CHART	96
	APPENDIX B LITERATURE REVIEW	97

LIST OF TABLES

Table 1. 1: Several type of selection fruit	6
Table 1. 2: Surface of Photoelectrode and Counter Electrode	7
Table 3. 1: Equipment and material are used in measurement absorbance	22
Table 3. 2: Equipment and material are used in measurement permittivity	24
Table 3. 3: Equipment and apparatus are used in measurement DSSC	26
Table 4. 1: The data Strawberry of three sample with different dilution	74
Table 4. 2: The data Strawberry of the actual value and the value dilution	75
Table 4. 3: The data Mango of two sample with different dilution	76
Table 4. 4: The data Mango of the actual value and the value dilution	76
Table 4. 5: The data Dragon fruit of two sample with different dilution	77
Table 4. 6: The data Dragon Fruit of the actual value and the value dilution	78
Table 4. 7: The data Black Grapes of two sample with different dilution	78
Table 4. 8: The data Black Grapes of the actual value and the value dilution	79
Table 4. 9: The data Water Melon of two sample with same dye without dilution	80
Table 4. 10: The data for overall measurement absorbance	81
Table 4. 11: The data from Network Analyzer Material Dye & Air	83
Table 4. 12: The calculation of differences frequency	83
Table 4. 13: The calculation of differences Q factor of a resonant	83
Table 4. 14: The data excel from CST Studio Suite 2019	83
Table 4. 15: The data for Overall Measurement Permittivity	83
Table 4. 16: Differences value Voc depends on the difference's places measured	89
Table 4. 17: Differences value Voc depend on differences equipment	90
Table 4. 18: The value of Current-Voltage Characteristics	90
Table 4. 19: Summarize of the Measurement Project	91

LIST OF FIGURES

Figure 1. 1: Fluorine-doped Tin Oxide with thin layer	8
Figure 1. 2: Measurement of Open-Circuit Voltage, Voc	8
Figure 2. 1: Schematic diagram of semi-transparent solar cell based SBS PV/T	9
Figure 2. 2: Astaxanthin act as capping layer around anthocyanin pigment	10
Figure 2. 3: The flow how the anthocyanin process	11
Figure 2. 4: The pH of the liquid influences the appearance anthocyanin	11
Figure 2. 5: The structure of dye-sensitized solar cells	12
Figure 2. 6: The scheme of natural dye-sensitized solar cells	13
Figure 2. 7: Dyes extraction was filtrate	14
Figure 2. 8: The construction of dye-sensitized solar cell	15
Figure 2. 9: Schematic view of the transmission line plane	18
Figure 2. 10: Ground plane of the metamaterial-based liquid detector	18
Figure 2. 11: The transmission line view	18
Figure 2. 12: The ground plane view of fabricated sensor	19
Figure 2. 13: Set-up for the sole metamaterial	19
Figure 2. 14: Metamaterial with glass capillary	19
Figure 3. 1: Fakultas Teknologi kejuruteraan Elektrik & Elektronik (FTKKE)	20
Figure 3. 2: Fakultas Teknologi Kejuruteraan Kimia & Proses (FTKKP)	21
Figure 3. 3: The flow of methodology procedure	21
Figure 3. 4: Selection fruit dyes extraction for first batch	30
Figure 3. 5: Selection fruit dyes extraction for second batch	31
Figure 3. 6: First batch dyes extraction	32
Figure 3. 7: The process of dyes extraction by hand	32
Figure 3. 8: All dyes extraction is filled in the bottle	33
Figure 3. 9: Wrapped each of the bottle for the first batch	33
Figure 3. 10: Efficiently arrangement for the first batch	34
Figure 3. 11: The flow whole procedure dyes extraction first batch	34
Figure 3. 12: Second batch dyes extraction	34
Figure 3. 13: The process of dyes extraction by mixer	35
Figure 3. 14: The indicate part of mechanical extraction which is mixer	35
Figure 3. 15: All the dyes extraction is filled in the bottle	36
Figure 3. 16: Wrapped each of the bottle for the second batch	37
Figure 3. 17: Efficiently arrangement for the second batch	37

Figure 3. 18: The flow whole procedure dyes extraction second batch	37
Figure 3. 19: The indicate part of Ultraviolet-Visible Spectrophotometer	38
Figure 3. 20: All the dyes extraction first batch is filled in the bottle	39
Figure 3. 21: Display on Ultraviolet-Visible Spectrophotometer	39
Figure 3. 22: Initial procedure with distilled water (Blank)	39
Figure 3. 23: Pour dyes first batch into cuvette by using dropper	40
Figure 3. 24: Exchanging the cuvette with different dyes extraction	40
Figure 3. 25: Comparison liquid before & after dilute process first batch	40
Figure 3. 26: Graphical Strawberry representation measurement absorbance	41
Figure 3. 27: Graphical Cherry representation measurement absorbance	41
Figure 3. 28: Graphical Blueberry representation measurement absorbance	41
Figure 3. 29: Graphical Water Melon representation measurement absorbance	41
Figure 3. 30: The flow whole procedure measurement absorbance first batch	43
Figure 3. 31: All the dyes extraction second batch is filled in the bottle	43
Figure 3. 32: Pour dyes second batch into cuvette by using dropper	44
Figure 3. 33: Wipes the surrounding the cuvette	44
Figure 3. 34: Comparison liquid before & after dilute process second batch	45
Figure 3. 35: Graphical Dragon Fruit representation measurement of absorbance	45
Figure 3. 36: Graphical Black Grapes representation measurement of absorbance	45
Figure 3. 37: Graphical Mango representation measurement of absorbance	46
Figure 3. 38: Graphical Water melon representation measurement of absorbance	46
Figure 3. 39: The flow whole procedure measurement absorbance second batch	47
Figure 3. 40: Calibration Network Analyzer	48
Figure 3. 41: Calibration Open, Short & Load of Network Analyzer	49
Figure 3. 42: Calibration Thru of Network Analyzer	49
Figure 3. 43: Calibration of Isolator of Network Analyzer	49
Figure 3. 44: Loose the screw at waveguide	50
Figure 3. 45: Loose the screw at Resonator	50
Figure 3. 46: Fill the dyes first batch into holder dye	51
Figure 3. 47: Placed the holder dye first batch into Resonator	51
Figure 3. 48: The flow whole procedure measurement permittivity first batch	54
Figure 3. 49: Using tight kit to tightness port Network Analyzer	54
Figure 3. 50: Tightness the port at Resonator by using tight kit	56
Figure 3. 51: Fill the dyes second batch into holder dye	56
Figure 3. 52: Placed the holder dye first batch into Resonator	56

Figure 3. 53: The flow whole procedure measurement permittivity second batch	59
Figure 3. 54: Weighing TiO_2 powder by using Analytical Balance for First Batch	60
Figure 3. 55: Perform work in Fume Hood Chamber	60
Figure 3. 56: Cleansing the conductive test	60
Figure 3. 57: Stir the mixture all together	61
Figure 3. 58: Planning the length & width of FTO glass	61
Figure 3. 59: Checking the conductive side of FTO glass	61
Figure 3. 60: A drop of TiO_2 on the FTO glass and using Doctor Blade Method	62
Figure 3. 61: Various area of FTO glass	62
Figure 3. 62: Baked FTO glass 450°C for 45 minutes for first batch	62
Figure 3. 63: Immerse the FTO glass into dyes extraction first batch	63
Figure 3. 64: Keep FTO glass first batch into dark places	63
Figure 3. 65: FTO glass after take it out immerse first batch	63
Figure 3. 66: Shaded Counter electrode for first batch with graphite	64
Figure 3. 67: Assembly the Photoelectrode & Counter Electrode for First Batch	64
Figure 3. 68: Dye-sensitized solar cells for First Batch fabricated	64
Figure 3. 69: The flow whole procedure DSSC for First Batch	66
Figure 3. 70: Weighing TiO_2 powder by Analytical Balance for second batch	66
Figure 3. 71: Stir the mixture all together for the second batch	66
Figure 3. 72: Doctor Blade Method for second batch	67
Figure 3. 73: Record how many rolling is apply	67
Figure 3. 74: Baked FTO glass 450°C for 45 minutes for Second Batch	67
Figure 3. 75: Immerse the FTO glass into dyes extraction second batch	68
Figure 3. 76: Keep FTO glass Second Batch into dark places	68
Figure 3. 77: Rinse and clean the debris at FTO glass for Second Batch	68
Figure 3. 78: FTO glass after take it out immerse Second Batch	68
Figure 3. 79: Shaded Counter Electrode for Second Batch with graphite	69
Figure 3. 80: Assembly the Photoelectrode & Counter Electrode for Second Batch	69
Figure 3. 81: Dye-sensitized solar cells for Second Batch fabricated	69
Figure 3. 82: The flow whole procedure DSSC for Second Batch	71
Figure 3. 83: Several sample of Dye-Sensitized Solar Cells	71
Figure 3. 84: A drop of Potassium Iodide	71
Figure 3. 85: Measurement of V_{oc} under shading area	72
Figure 3. 86: Measurement of V_{oc} under direct sunlight	72
Figure 3. 87: Measurement of V_{oc} by uses differences equipment solar	72

Figure 3. 88: Measurement of voltage at load	73
Figure 4. 1: The graph Strawberry of three sample with different dilution	74
Figure 4. 2: The graph Strawberry of the actual value and value of dilution	75
Figure 4. 3: The graph Mango of two sample with different dilution	76
Figure 4. 4: The graph Mango of the actual value and the value dilution	77
Figure 4. 5: The graph Dragon Fruit of two sample with different dilution	77
Figure 4. 6: The graph Dragon Fruit of the actual value and the value dilution	78
Figure 4. 7: The graph Black Grapes of two sample with different dilution	79
Figure 4. 8: The graph Black Grapes of the actual value and the value dilution	80
Figure 4. 9: The graph Water melon of two sample with same dye without dilution	80
Figure 4. 10: The design of Sensor Resonator	82
Figure 4. 11: Measurement Permittivity with Material Dye	82
Figure 4. 12: Measurement Permittivity with Material Air	82
Figure 4. 13: Before immerse from First Batch	84
Figure 4. 14: After immerse from First Batch	84
Figure 4. 15: Before immerse from Second Batch	85
Figure 4. 16: After immersed from Second Batch	85
Figure 4. 17: Open Circuit Voltage for First Batch	86
Figure 4. 18: Measurement Open Circuit Voltage for Condition 1	87
Figure 4. 19: Measurement Open Circuit Voltage for Condition 2	88
Figure 4. 20: Measurement Open Circuit Voltage with difference equipment Solar	89
Figure 4. 21: The value of Black Grapes in I-V characteristics	91

LIST OF SYMBOLS

$^{\circ}\text{C}$	Degree Celsius
%	Percentage
g	Gram
ε	Permittivity

LIST OF ABBREVIATIONS

DSSC	Dye-Sensitized Solar Cells
PCE	Power Conversion Efficiency
TiO ²	Titanium Oxide
NP	Nanoparticle
FTO	Fluorine-Doped Tin Oxide
Pt	Platinum
I ⁻	Iodide
I ³⁻	Triiodide
HOMO	Highest Inhabited Molecular Orbit
LUMO	Lowest Inhabited Molecular Orbit
I-V	Current-Voltage
Voc	Open Circuit Voltage
PV	Photovoltaic
IEA	International Energy Agency
SBS	Solar Cell-Based Spectral Beam
NS	Nanospheres
OH	Hydroxyl
CE	Counter Electrode
FTKEE	Fakulti Teknologi Kejuruteraan Elektrik & Elektronik
FTKKP	Fakulti Teknologi Kejuruteraan Kimia & Proses
H ² O	Distilled Water
AVG	Average
CAL	Calibration
BW	Bandwidth
CENT	Centre
Q	Quality
Isc	Short Circuit Current
L	Length
W	Width
KI	Potassium Iodide

CHAPTER 1

INTRODUCTION

1.1 Background of the Study

Dye-sensitized solar cells (DSSC) are contemplated to be one of the predominant next-generation solar cells in view of the fact that of their proportional high-power conversion efficiency (PCE), tranquil fabrication, and low fabricate cost (O'regan and Gratzel, 1991, Kavan and Gratzel, 1995). Dye-sensitized solar cell is utilized natural dyes have shown encouraging results in construct green energy at inexpensive cost since no expensive apparatus or vacuum structure is essential for fabrication. The natural dyes for DSSC are compose from a variation of plant and algal pigments. The pigment necessarily present especial element for the plant metabolism and growing (N., Prabavathy., 2021)

However, a DSSC comprise of an extracted dyes' that absorbed Titanium Oxide (TiO_2) nanoparticle (NP) integrate thin film fabricated on the surface of a conductive side of Fluorine-doped Tin Oxide (FTO) as the photoelectrode while Platinum (Pt) coated of FTO as the counter electrode. In additional, Iodide/triiodide (I^-/I_3^-) as the liquid electrolyte. The electrolyte that fill to overflowing between the photoelectrode and counter electrode (Guiming Fu., 2018). DSSC are implement that convert light energy from the source sun to electricity with the make use of dyes' anthocyanin-based as active materials. For the structure DSSC are the photoelectrode, or called active material (absorbing layer), counter electrode and the electrolyte. For the absorbing layer (dye) occupy light that flow through photoelectrode and the electrons charge locomote from the highest inhabited molecular orbital (HOMO) to the lowest inhabited molecular orbital (LUMO) of the extracted dyes. (Sabastine C., 2021).

The comprehension concerning the variation of plant pigments that comprise the dye preparation for the several extractions of unique pigment. This intensify PCA which

degenerate the organic dyes that come in contact with anthocyanin-based with TiO_2 nanoparticles (N., Prabavathy., 2021). However, the assembly of such as a dye is overpriced, multiplex and dangerous to humans and the habitat. Due to this, pigments or natural dyes are extracted from plants such as (chlorophyll, anthocyanin, carotenoid, etc.). Therefore, natural dyes degenerate simply, major to low performance of the cells. Hence, in the midst the natural pigments, anthocyanin take shape to be a magnificent another for use in DSSC. Anthocyanin-based wealthy batch comprise strawberry, cherry, berries, red cabbage, eggplant, to name a several. The utilization of anthocyanin has enlarged drastically in the two decades since of their colour and anti-oxidant belongings and as contamination appeal to and photoprotective agents, conserve plant DNA from destruction convince by UV irradiation. Anthocyanin pigment is established close by the surface of cells in fruit and vegetables (Glennise Faye C. Mejica., 2022). Anthocyanin-based is a water-soluble molecule and it is the one of the natural pigments the most largely thoughtful due to its especial possessions. This pigment is extremely pH-dependent. Furthermore, the greatest light to electricity transformation effectiveness was observed at pH 9, with an effectiveness of 0.1021%, an electric current of $0.0682\text{mW}/\text{cm}^2$. Therefore, the absorbance possessions of the natural organic dye are enhanced (Glennise Faye C., 2022).

In the second quadrant of the current-voltage characteristics of DSSC, the continuously flow by forward currents and towards more negative voltages the operating voltage points moderately shift. These exchanges are assigning to the increment in the ratio of iodide to tri-iodide in the dye-sensitized solar cells. For the electrolyte preferably than to the decomposition and constituent material by coupling reactions. In addition, these exchanges are adjustable reactions that can be discover based on the exchanges in electrolyte colour or current-voltage measurement (Shiro Iwata., 2018). Begin a one-dimensional electrical model taking into consideration all conduct and electrochemical response elaborate in an operating device to graphical the current-voltage characteristics. Later, by enlarge the works to a two-dimensional model taking into considering a very thin film of a dyes' solar cell. Avail oneself of impedance spectroscopy to draw out equivalent circuit component that can be used to relevant the current-voltage characteristics (Subarna Rudra., 2019).

Spectrum is well known to its capability of execute like microwave and infrared on condition that the element of radiating as wave in line, corresponding. This frequency spectrum is these days existence traverse for applications like medicine, security surveillance in speedy sensing and imaging, telecommunication and evolution of high data shift wireless system. Recently, the propose procedure for build on the far-field variable like radiation effectiveness and acquire with regulate lord it over the utilization of metal or dielectric based radiator and make use of the graphene material with some non-resonant component (Vishwanath., 2022).

1.2 Problem Statement

Representative DSSC current-voltage (I-V) characteristics for the similar sizing of photodetector but the dissimilar colours and transmission of photodetector due to sensitizers and thickness of photodetectors surface. For the example, I-V characteristics of a module be made up of the cells that connected in series. For the other investigate are carried out such as designate that dissimilar in DSSC element has a widely domination on short-circuit currents that an open-circuit voltage or fill factors. All independent cells are working in the first quadrant due the power control circuit for photovoltaic generation. In dissimilarity, when the module give rise to electrical power on the working point cell. For investigate that working in first quadrant, whereas cell has the lowered short circuit current is working in the second quadrant. In the research, a backwards voltage is appeal to cell. When the backwards voltage extends 1500mV the dye and electrolyte element of DSSC have been disclose to moulder (Shiro Iwata., 2018).

TiO² and ZnO high-rise pure 2-inch ceramic select were acquire from Nanobazar. In order to deposit the thin film, 3 cathodes were employed by RF hesitant structure hence there was no be on need of two aperture the vacuum due the deposition of multilayer surface, therefore the coated procedure was bringing about with the lowered contaminate. As well known, in a DSSC construction, the electrolyte is divided from the conductive oxide by the photoelectrode semiconductor element. Moreover, these components should have a mesoporous habitat to absorb dye molecules. Hence, the liquid electrolyte can proceed throughout the holes of semiconductor element and attracted with the FTO, which effected recombination. Situate a dense block surface between the confluence head off them the FTO/ electrolyte interchange and reverse electron through and rise up the DSSC efficiency (Ahmad Zatirostami. 2020).

At this part, there are a lot of literatures are focusing priority on improving the output performance of environmental performance of dye-sensitized solar cells based on natural dyes. The most ordinary natural photosensitizers extracted from plants be in the hands of two carotenoids, anthocyanin, betalains and chlorophylls have been lately experimental. However, up to at the moment DSSC construct on natural sensitizers had solar to electric transformation effectiveness less than 3%. The Hitherto dissimilar plan of action to upgrade the effectiveness and steadily of DSSC with natural sensitizers have been investigate such as discriminating purification by column chromatography, discriminating extraction, the mixing with other natural dyes and dissimilar variety of electrolyte additives to defeat the dark current. For specimen, the execution of anthocyanin DSSC were upgrade succeeding elimination of organic compound (non-pigments). Moreover, solar cells sensitized with the anthocyanin and betalain combine appear the high-rise effectiveness and upgrade photostability over those sensitized with set apart dyes (Alfred Blaszczyk., 2021).

The specification of dielectric component of element under test has a critical part in industrial applications, scientific and pharmacological. The quantification system used for regulate the dielectric element of characteristics in two representation as resonant and non-resonant technique. For broad-band particular non-resonant detection are required, while resonant technique is avail oneself of for spectral components over a narrow frequency scale. Resonant technique is generally employed since of its proportionate unexpensive coat, tiny electrical sizing, real-time quantification alternative, high sensitivity and uncomplicated integration to components electronic. On the other hand, the resonant apprehension technique. In the resonator technique, the situate interior a cavity and its electromagnetic element are acquired from the exchange of the resonance frequency and quality (Q) factor (or S_{21}) of the cavity (Mustafa Suphi Gulsu., 2021).

Up to recent, there are no studies regarding the material permittivity's properties that are correlated to the output characteristics of dye-sensitized solar cells (DSSCs).

1.3 Objective

The most important thing in this project are focuses to the main objective that should been done by achieved that to elucidate an effect of material permittivity to current-voltage performance of dye-sensitized solar cell (DSSCs) based on several extracted

dyes' fabrication. The DSSCs involved several basic steps such as light absorption, electron injection, transportation of carrier, and collection of current. Furthermore, to analyse the relationship between the material's permittivity and dye's absorption from the linear graph representation the related between of them.

A re-entrant cavity resonator equipment was used for the establishment of dielectric permittivity by determined several extracted dyes in anthocyanin-based. The measurement of resonator is determined measured by used network analyzer with a dye extricate. In the resonator method, the place interior a cavity and its electromagnetic element are acquired from the exchange of the resonance frequency and quality (Q) factor (or S_{21}) of the cavity. The data analysis from the network analyzer are categorized into two part which is measurement with material dye and other part is measurement with material air. From data execution with both measurements will come out into several element value such as bandwidth, centre of frequency, low of frequency, high frequency, quality factor and loss. In additional, for the measurement permittivity are included the software part which is well known CST Studio Suite 2019. This software is execution for designing, analyzing and optimizing electromagnetic (EM) waves.

The ultraviolet-visible spectrophotometer is a major ordinary analytical equipment that evaluate the concentration of segment due their absorption of light at particular definite wavelengths where dissimilar substances absorb and consider these wavelengths especial. UV-Vis are conduct software and computers for data relationship and investigation can accessibility. Thereby with the dissimilar concentration of anthocyanin-based can be observed that the higher concentration liquid in dyes achieved the maximum value of absorbance. In fact, the lowered concentration of the liquid in dyes achieved the minimum value of absorbance.

1.4 Scope of Study

At these points, the scopes of these project are conducting at several aspect. The following are the scopes of this research such as sample of dyes are chosen on several fruit from anthocyanin-based. At this element present, the all-encompassing investigation on the combination of natural pigments has been to supply a possible to dye-sensitizer as a photosensitizer for dye-sensitized solar cells (DSSC). Hence, this research work is the initiate of its category to conduct an investigation into how the performance different

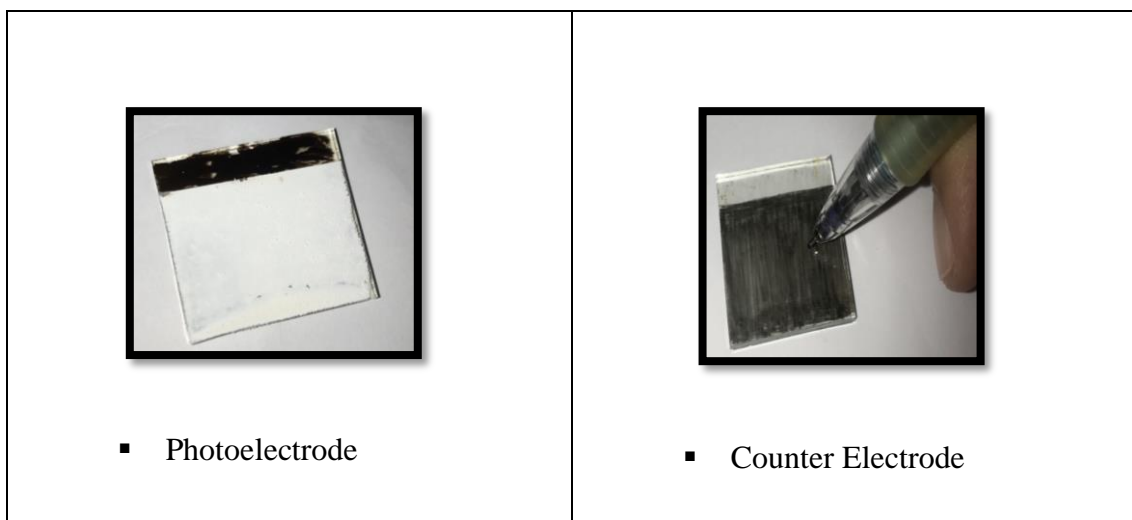
extracted dyes' will be come out the result based on this study. Therefore, several fruits are chosen for investigate for all performance based on this study. The selection of fruit that have been carry out is in category anthocyanin-based such as:

Table 1. 1: Several type of selection fruit

 <ul style="list-style-type: none">▪ Strawberry	 <ul style="list-style-type: none">▪ Blueberry
 <ul style="list-style-type: none">▪ Cherry	 <ul style="list-style-type: none">▪ Water Melon
 <ul style="list-style-type: none">▪ Mango	 <ul style="list-style-type: none">▪ Dragon Fruit
 <ul style="list-style-type: none">▪ Black Grapes	

Dye-sensitized solar cell be made up of transparent conductive side that have been used in this study fluorine-doped tin oxide (FTO) as operating electrode substrates to covering TiO_2 nanomaterial. In the midst of which FTO is would rather due to its high-rise steadiness and lowered sheet resistance. An accretion in porosity and surface area for the nanomaterial which is TiO_2 layer starting point a magnification in photon to electricity transformation throughout increment dye loading and absorption of the solar spectrum. However, recombining of photoelectrode due to layer TiO_2 surface and counter electrode due to layer graphite influence the lowering of photovoltaic performance of dye-sensitized solar cell.

Table 1. 2: Surface of Photoelectrode and Counter Electrode



Establish a high-density TiO_2 dense layer between the FTO confluence has been hypothetically and experimentally inveterate as an effectual tool for blocking charge electron reunification via indirect pathways. Semiconductors such as TiO_2 have also been experimented as a blocking layer for the fabrication of DSSC. Apart from the blocking consequence, a thoroughly dense TiO_2 layer along with a sizeable active area and improved abidance between the TiO_2 surface and FTO surface clear the way for higher charges electron transfer and eventually increment the performance efficiency. Furthermore, the size of solar cell which FTO (active area) approximately (2cm x 2cm) per sample. For the reason that, in the procedure fabrication dye-sensitized solar cell have the step which is well known Doctor Rolling Blade are used to rolling above FTO with thin layer.

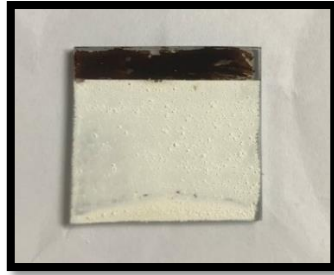


Figure 1. 1: Fluorine-doped Tin Oxide with thin layer

However, the accomplishment of the independent solar cells is not at all times consistently to be contrived by shadows, clouds, and dirt when place outdoor. Particularly, the outputs of the solar cells in DSSC are frequently non-uniform in view of the fact that different used of fruit anthocyanin and transparent surface at FTO by layer TiO_2 surface. Hence, dye-sensitized solar cell specify that the difference used of fruit by extracted the dye impact the components element of open-circuit voltage, short circuit currents and fill factors.



Figure 1. 2: Measurement of Open-Circuit Voltage, V_{oc}

CHAPTER 2

LITERATURE REVIEW

2.1 Photovoltaic-System Solar Energy

Based on high-speed growth of metropolis, sun gather for rectify the environment and restore traditional energy has enhance growingly critical. In the midst of the several solar energy transformation automations, photovoltaic (PV) cells have exhausted consequential observation. On the report of to the most recent study outcome from International Energy Agency (IEA) (2019), the renewable power capacity is place to enlarge by 50% from 2019 to 2024, and solar PV resolve description for estimation 60% of this speculate magnification (Jung Fang., 2020). In this research, the recommendation of make use of a single piece of PV to synchronize the emission conduct of the full solar spectrum for perceive the co-generation of electricity and high-rise category thermal energy is initiate. A semi-transparent solar cell with a sawtooth trench construction at its base was construct. The solar cell can transform 400-800nm wavelength photons to electricity, and observe 800-2500nm wavelength photons on a small-scale mark to construct high-rise temperature thermal energy. Hence, the transferred irradiance can be provided with easy construction in semi-transparent solar cell-based spectral beam splitting (SBS) PV/T system (Huaxu Liang., 2022).

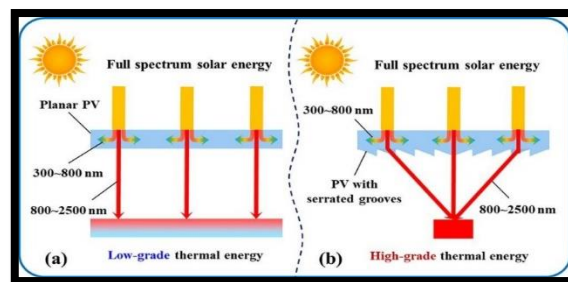


Figure 2. 1: Schematic diagram of semi-transparent solar cell based SBS PV/T

2.2 The Application of Anthocyanin in Solar Cells

The dye sensitized solar cells were constructed depend on anthocyanins as sensitizer at varied concentrations. Then, electron transferred variable were then make use by to describe solar cell execution. It was study that, solar cell execution provided with incremental in concentration of anthocyanin. The high-rise effectiveness acquire was 0.145% with concentration of 1.18mg/ml. The development in solar cell execution was due to incremental in re-together resistance at the anode as application of anthocyanin increases (Alex Okello., 2021). Within the situation magmatic assemble silicate TiO_2 nano-construction that seem as disfigure TiO_2 nanospheres (NS) and the enervate ratio is enhance for greatest astaxanthin effectiveness. The less molecular interconnectivity of astaxanthin with anthocyanins as resolute from dignified life time research indicate that astaxanthin surround anthocyanins as a defence opposed to photodegradation. The construction of DSSC with FTO, TiO_2 , NS/algal buffer surface/ co-sensitized dyes (Rose: -70:30)/ iodide-iodide/ pt shown a high-rise effectiveness of 2.82%. Comparatively high-rise effectiveness of 3.31% was also conduct for DSSC with 3% TiO_2 nanorods as photoelectrode (N., Prabavathy., 2021).

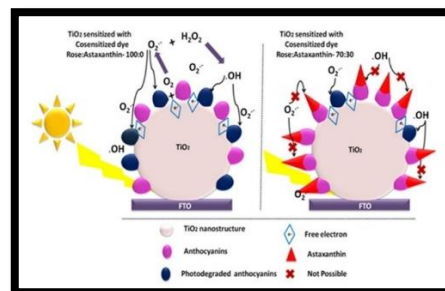


Figure 2. 2: Astaxanthin act as capping layer around anthocyanin pigment

2.2.1 Overview of Anthocyanin

From the research, based on combination of natural pigments have been carry out to analyse to dye as a photosensitizer for DSSC. Therefore, this study operate is the one of its variety to experimental how influence the steadily of anthocyanin pigments acquire from extracted several fruits as a photosensitizer and enlarge DSSC by using graphite coated surface as a counter electrode activated with TiO_2 surface act as photoelectrode. The prime pigments that sensitize the nano-material TiO_2 film have been evaluate as

anthocyanin-based. Furthermore, anthocyanin is a water-soluble molecule and is first of the natural pigments widely conscientiously research based on to especial element. This pigment is high-rise pH value of the liquid. As the come out the analyse, the absorption components of the natural organic dye are developed. At pH 9 transformation effectiveness was analyse that is the best light to light electricity. In additional, efficiency of 0.1021%, a current electric is 0.0682mA and a voltage is 0.4877V and power density is 0.0227mW/cm². The pH of the liquid influences the appearance of the anthocyanin in the extraction, which scale from magenta to red in acidic to neutral situation and from purple to yellow in fundamental situation. As the pH 1-12 arise, the colour of the anthocyanin extracted from red to purple to blue to green to yellow (Glennise Faye C. Mejica., 2022).

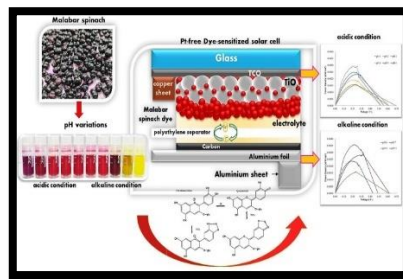


Figure 2. 3: The flow how the anthocyanin process

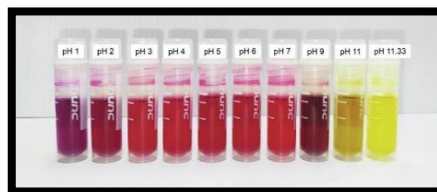


Figure 2. 4: The pH of the liquid influences the appearance anthocyanin

2.2.2 Characteristics of Solar Cell

In the midst of accessible renewable energy origin, sun would be comfortably change to make use by energy solar cell the reason of that has no operating parts, few of maintenance condition, expected energy output, silent working, and speed installing. Solar cells are category into three dissimilar generation. Generally, they are first, second and third. The dye-sensitized solar cell (DSSC) has variety high-tech lead on top of silicon and thin-film solar cells. DSSC have captivate general observation the reason of

that of their cheap manufacture cost, uncomplicated fabrication procedure, least energy fabrication procedure, great cell performance under absorption light conditions, and ecologically initiate. Dye sensitizer has main part in the cell transform effectiveness of a DSSC (Fahmid Kabir., 2022).

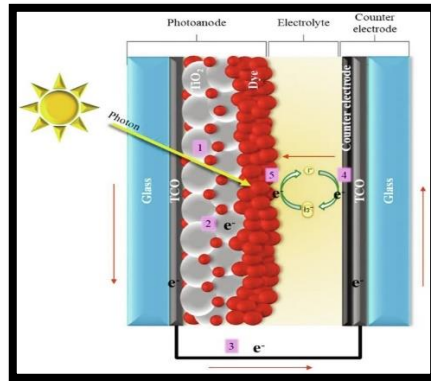


Figure 2. 5: The structure of dye-sensitized solar cells

Dye-sensitized solar cell is a third-generation solar cell possess high-rise execution and operate in low light visible environment among to other generation solar cells. The current study is observation on put a value on effectual DSSC with high-rise robustness and transform effectiveness. The utilization of dye components is high-rise in a great many sector such as chemical, furniture, paints and textile industries. Currently, the latest oxidation procedure is enlarging for the degradation of dyes. The appliance of this technique is, formation of powerful hydroxyl (OH) reformer for the severance of multiplex molecules in the company of the assist of solar energy and this forming of OH radicals get hold of position due the photocatalysis process.

Semiconducting metal oxide nano-components (TiO_2 , ZnO , SnO , ZrO_2 etc.) accompanied by an extensive bandgap make use absorption solar energy in the UV region and have a diversified scale of element outstanding to their wealthy constructional diversity. Amidst the dissimilar semiconducting metal oxide nano-components, TiO_2 is an reassure element for variety inquiry via to its non-toxic nature, great optical and electrical element and observe high-rise steadily in DSSC and photocatalytic inquiry (T. raguram., 2022).

2.3 DSSC Fabrication Categorization

Dye-sensitized solar cells (DSSC) are equipment for the transform from visible light into electricity depend on sensitization of most band-gap semiconductor nano-material. (O'Regan and Graetzel,1991). A representative DSSC, are combination situate in progression a translucent photoanode, an electrolyte mixture is consisting a redox structure and counter electrode (CE). Typically, the photoanode containing of a film of TiO_2 nano-material displacement into a transparent conductive oxide (TCO) glass keep up, sensitizer with extracted dye molecules. The operation electrolyte organization, situate in the middle of the two electrodes (Giuseppe Calogero., 2012).

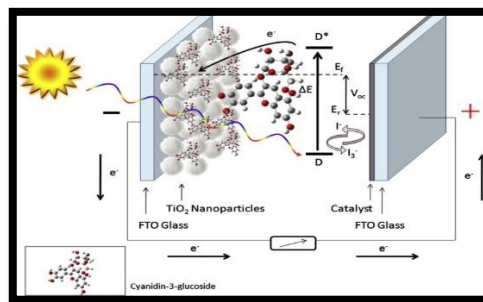


Figure 2. 6: The scheme of natural dye-sensitized solar cells

2.3.1 Extraction of Photosensitizer

The extraction procedure used was affect and improve. First, the fruit Malabar spinach were set apart from the stem. The plant representation was then wash out with water, air-dried at room temperature, squash into smaller pieces, and combine with an organic solvent. Eventually, the liquid was put down in a beaker and left-hand at room temperature for 10 minutes. Finally, the solid remnant was filtrate with whatman filtrate paper, and the dye extracted was placed in a container (Glennise Faye C. mejica., 2022).

The natural dye was composed due revise technique based on the exchange is made up by granulate the inflamed element into powder in rules to incremental water-insoluble of the fresh element in solution and amplify the pigment of extraction. Fresh *P. rubra* flowers and *S. androgynous* leaf were self-possessed and dice into small slices. The flower is wash out several times with distilled water to remove dirt. The dry flower and leaf were crush into powder by using a grinder. The nano-material were combined together consist of ethanol (95%, HmbG chemical) in container with 1:5 ratio. The

container was enclosed and heating at 40°C for 2 hours for the purpose of incremental pigment extraction by using a hot plate. Finally, the dye solution was filtrated by using filter paper to separate residues (Wan Almaz Dhafina., 2020).



Figure 2. 7: Dyes extraction was filtrate

2.3.2 Photoanode and Counter Electrode Preparation

Subsequently, variety procedure was used to assemble the photoanode, also well known as the operating electrode. Foremost, the FTO glass was cleaned with three dissimilar liquids (methanol, distilled H₂O and soap) for 10 minutes per liquid. The FTO glass was then air-dried before actually investigating for the conductive side by evaluating its resistance, and the four-corner side conductive surface of FTO glass was stuck to reach the wanted layer area of 3cm². Simultaneously, the TiO₂ paste was assembled by minimizing the molecule size of the TiO₂ powder in a vibrating mixer for 1 hour. Concurrently, 5g TiO₂ powder ratio, 10ml of 5% acetic acid and 0.5 surfactants were absolutely combined for 1 hour by using a magnetic stirrer and then placed in a sealed container to avoid evaporation. Lastly, by using the doctor blade technique, the TiO₂ paste was deposited on the glass. Continuing with that, the annealing procedure was experimental by heating it at a constant temperature of 300°C for 1 hour and then cooling it. Activated carbon (AC) was made and used as a counter electrode component. It was made by mixing 1g of AC, 5g of adhesive glue, and 5ml of 70% ethanol. Furthermore, an active area of 3cm² was generated by covering the AC paste on the aluminum foil. Finally, it was heated for 10 minutes at 200°C (Glennise Faye C. Mejica., 2022).

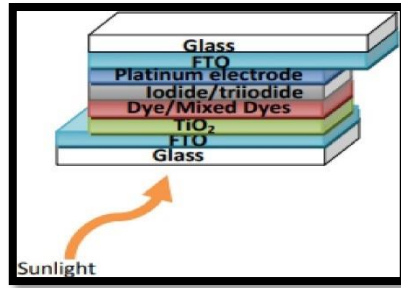


Figure 2. 8: The construction of dye-sensitized solar cell

FTO glass substrates were immersing in a bath of helmanex III (1%) for 20 minutes in an ultrasonic bath and then wash out three times with deionized water. After then, the electrodes were soak in ultra-sonic bath of acetone for 20 minutes and 2-propanol for 20 minutes. Titanium paste was assembly by combine 4g of commercialized TiO_2 nano-powder, 8ml of 0.1M nitric acid liquid and polyethylene glycol and Triton X-100. The solution was thoroughly cause in porcelain mortar to formation a paste. The compose TiO_2 paste was deposited by technique slot coating. Displacement was on the conducting side of the FTO glass substrate on an of area 36mm^2 elucidate by a scorch tape. The displacement TiO_2 was strengthen at 450°C in an open-air tube furnace for 20 minutes. When it had chill to about 30°C , the anode was immersed in anthocyanins for 16 hours. The cathode was composing by coating FTO glass substrates with a Platinum. An art brushes was immersed in plastisol, a platinum precursor and appeal onto FTO glass substrate. Platinum catalyst was operating by strengthening in the tube furnace for 20 minutes. The counter electrode was left-hand to chill naturally in air environment (Alex Okello., 2021).

2.3.3 Dye Loading to TiO_2

Acknowledge it to dry for 5 minute and Malabar spinach dyes under dissimilar pH value photosensitizer were filled into TiO_2 by steadily flow in 10 drops of the dye. Replicate the process twice more. Separate any excess dye from the FTO glass after it has been dyed step (Glennise Faye C. mejica., 2022). The construct TiO_2 paste was situated at the boundary of the secured FTO coated glass and cruise or rolling swiftly by used glass rod to outspread on above of the conductive glass of FTO (Abebe Reda Woldu., 2020).

2.3.4 Electrolyte

In the solution electrolyte devising procedure embrace from 20ml of ethylene glycol diversified with 80ml of acetonitrile was situate in a beaker. And the, 0.21g of iodine was combine into the liquid solution. Then 1.08g of potassium iodide was put in. Lastly, the solution that have been mixture with the glass rod up until there is no iodine or potassium iodide grist were apparent (Glennise Faye C. mejica., 2022). In electrolyte based was filled up with a redox that are consisting 0.5M lithium iodide (99.9% Sigma Aldriich) and 0.05M iodine (Fluka Analyticals) in acetonenitrile (Wan Almaz Dhafina., 2018).

2.3.5 Assembly of DSSC

The review of the fabricated DSSC in this study was conduct that was construct by attach the copper sheet (6cm x 0.5cm) to the TiO_2 conductive layer as photoanode's uncoated. The dye surface was then enveloped with a polyethylene (PE) divider that had been immerse in electrolyte. After that, the activated carbon was coated by aluminum foil and then placed on top of PE divider. The (6cm x 0.5cm) aluminum sheet was reinforced by aluminum foil. Lastly, after the appliance had been gather, it was situated inside the transparent plastic and sealed. Moreover, after the DSSC was assembly, all variable was dignified instantly to covered any exchanging in the dye and PV element bring about aging (Glennise Faye C. mejica., 2022).

The anodes, filled with the dyes were harvest from their receptacle and cleanse with ethanol. The anodes were situated with manage side facing keep up. Meltonix, lacerate with a pore of about 8mm by 8mm was situate that the depositing TiO_2 supplied with the dye was inside the pores. The compose counter electrode, was situate on above of the anode that correspondence to solar cells were adequate for appeal copper tape to provide electrical contact and equate crocodile clips. Sew up was accomplish make by use a hot solder iron, hold down on above of the counter electrode, ahead the edges of the solar cell. The two pores behind the counter electrode was injected by electrolyte, Iodolyte-AN 50 and the pore sew up with cell cups and meltonic as before (Alex Okello., 2021).

2.3.6 Measurement of DSSC Performance

Using a solar detector, intensity of light was set at $1000\text{W}/\text{m}^2$. The measurement of open circuit voltage, short circuit current and fill factor are determined by use a Keithley

equipment (Model 2400, 4066884, C32) (Alex Okello., 2021). Electrochemical computation was executed in Zhenium Zahner potentiostat apparatus with solar detector on condition that by using xenon lamp. Later, the electrochemical impedance spectroscopy (EIS) investigate were produce in the frequency scale from 10mHz and 10kHz with an irradiance of 100mW cm^{-2} under grade illumination of air-mass 1.5 world (AM 1.5 G) and agitation of 10mV. A biased from scale 0 and 750mV that is higher that measurement Voc (Sabastine C. Ezike., 2021).

The Photo catalytic task quantification were sustained by using UV. An origin lamp and the spectrophotometer were used to determined concentration of dye. Furthermore, photoluminescence spectra were set down by used PerkinElmer LS 45 Fluorescence Spectrometer. Current-voltage observation was intent on Top solar detector PECELL-L01. Dye-sensitized solar cell by used UV filter are analyzer at wavelength cut off 417nm (N. Prabavathy., 2019).

2.4 Measurement of Permittivity

This research is based on operating using a microwave re-entrant cavity resonator that organization with a design acquire based the cavity evolve by Goodwin et al. Hence procedure of calibrated the re-entrant cavity to decompose for temperature and highly pressure-convince deformation to its designing based on well accepted technique which is involvement in vacuum and helium (Gergana Tsankova., 2019).

2.4.1 Sensor design

A shift ground transmission line with a shift defected plane consist a slot resonator on lo least loss substrate with dielectric constant that designing of the liquid sensor. The characteristics of liquid pass is perceiving from the middle point of the detector throughout a drilled hole to purposed glass capillary tube is flow over. The width of the construction microstrip is arrangement such as 4.80mm to have 50Ω input based on impedance. A fault with width of 0.4mm is structure with the length of 9.8mm is attach from microstrip in rules to minimize the top band bandwidth and come out on that high-rise the interconnectivity of the electromagnetic waves with the liquid (Mustafa Suphi Gulsu., 2021).

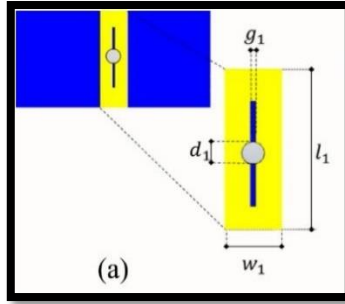


Figure 2. 9: Schematic view of the transmission line plane

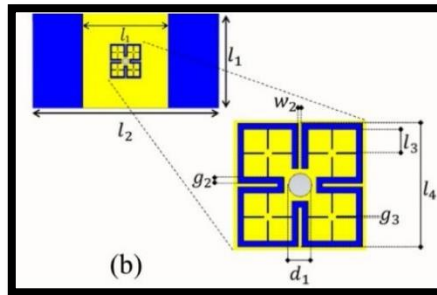


Figure 2. 10: Ground plane of the metamaterial-based liquid detector

2.4.2 Fabrication of the Prototype and Measurement of Set-up

The indicator be made up of spiral drills with 0.1mm and 0.2mm diameter values, 0.2mm diameter of stubs end mills, 1mm and 2mm by counter router. The procedure of fabrication is consisting of etching by Rogers RT/ duroid 5880 in double-sided copper-plated.

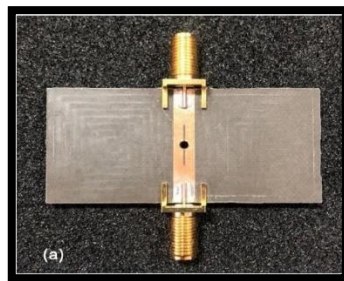


Figure 2. 11: The transmission line view

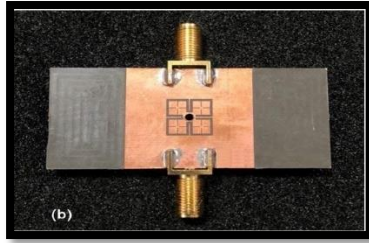


Figure 2. 12: The ground plane view of fabricated sensor

Furthermore, the spectral detector of the fabricated response with the Rohde & Schwarz ZVL13 by used network analyzer. Hence, it is competent of observation in a frequency in the middle from 9kHz to 13.6GHz. Computation are conducting at the first in the absence of capillary tube and then later absence the capillary tube by insert ethanol-water, methanol-water and ethanol-methanol solution. (Mustafa Suphi Gulsu., 2021).

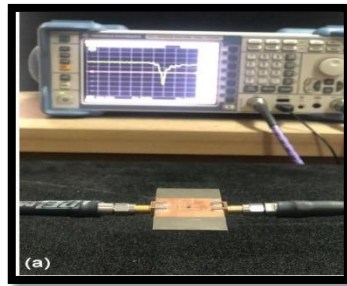


Figure 2. 13: Set-up for the sole metamaterial

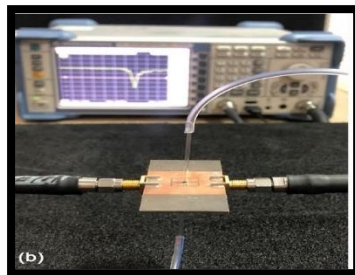


Figure 2. 14: Metamaterial with glass capillary

CHAPTER 3

METHODOLOGY

3.1 Flow of Methodology

The flow of methodology for whole process in this research has been illustrated in the Figure 3.1. Foremost, for this project was conducting by several apparatus and material that used for three measurement consists of measurement absorbance, measurement permittivity and measurement dye-sensitized solar cells (DSSC). Subsequently, for the measurement absorbance and measurement DSSC are successfully accomplish at UMP Gambang which is Fakulti Teknologi Kejuruteraan Kimia & Proses (FTKPP) laboratory. In addition, for the measurement permittivity is done at UMP Pekan which is Fakulti Teknologi Kejuruteraan Elektrik & Elektronik (FTKEE) laboratory.



Figure 3. 1: Fakulti Teknologi kejuruteraan Elektrik & Electronik (FTKEE)



Figure 3. 2: Fakulti Teknologi Kejuruteraan Kimia & Proses (FTKKP)

In this research, it was initiate procedure with extraction of photosensitizer well known are called dye. The element of dyes is intercorporate with nano-material which is in anthocyanin-based material. There are several fruits that have been chosen to extraction fruit that categorization into two part for the first batch and second batch by using different extract analyse. For the preparation or arrangement of extraction in this study was analysing with different procedure but the purpose is that to achieve the dyes from extraction fruit in anthocyanin-based. Therefore, in this research was conducting also measurement of absorbance versus wavelength by make use of Ultraviolet-Visible Spectrophotometer. Hence, to become acquainted with the quantity of light absorbed by used a liquid which dyes anthocyanin-based. Measurement of permittivity is also experimental in this research by used the equipment that are called resonator. Finally, preparation of dye-sensitized solar cells (DSSC) that have been carried out in this research has divided two part which first batch and second batch.

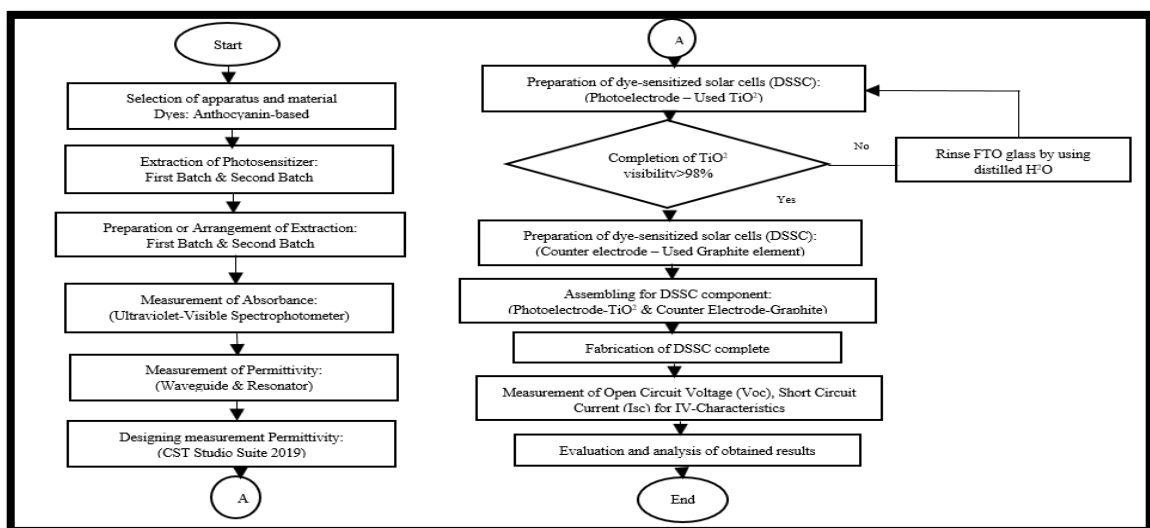





Figure 3. 3: The flow of methodology procedure


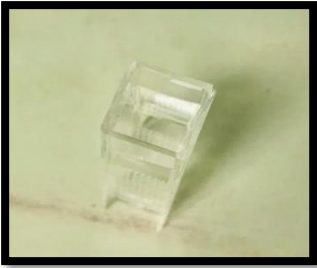

3.2 Selection of Apparatus and Material

The material and equipment are listed in the table based on the factor need to be examine in this research.

3.2.1 Apply for Measurement Absorbance


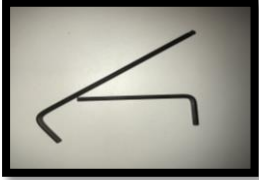

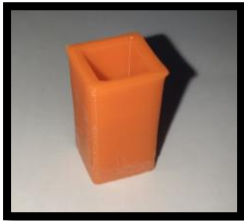
Table 3. 1: Equipment and material are used in measurement absorbance



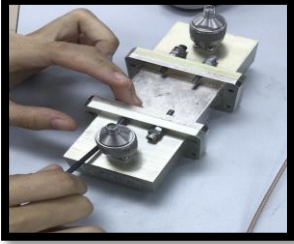
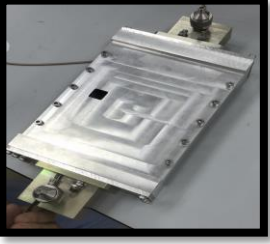
No.	Equipment/ Material	Functioning
1.	 Ultraviolet-Visible Spectrophotometer	To measure dyes for the absorbance values
2.	 Dropper	To inject and take it out the liquid properties
3.	 Wipes Tissue	To wipe the excess solution surrounding the cuvette

4.	 <p data-bbox="603 562 802 595">Holder Cuvette</p>	To place the cuvette into the holder on Ultraviolet-Visible Spectrophotometer
5.	 <p data-bbox="671 1032 775 1066">Cuvette</p>	To fill the dyes extraction
6.	 <p data-bbox="464 1525 979 1603">Distilled Water, Test Tube, Holder Test Tube & Beaker</p>	Included the process of dilution on measurement absorbance

3.2.2 Apply for Measurement Permittivity




Table 3. 2: Equipment and material are used in measurement permittivity


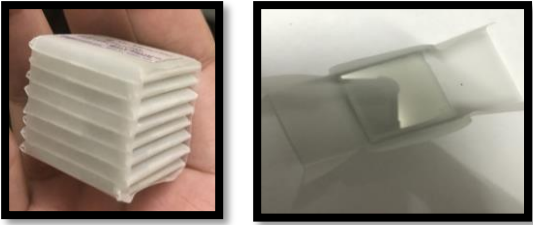


No.	Equipment/ Material	Functioning
1.	 Wire	Used to transfer the data
2.	 Loose Screw	Used to loosen screw at resonator & waveguide and tight the screw at resonator & waveguide
3.	 Syringe	Used to inject or take out fluid
4.	 Holder Dye	As placed for dyes extraction




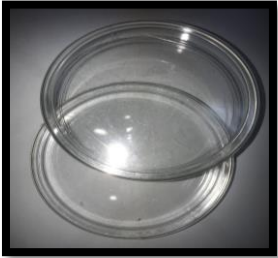
5.	 <p style="text-align: center;">Calibration Kit</p>	Used for the initial procedure calibration Network Analyzer
6.	 <p style="text-align: center;">Network Analyzer</p>	To measure and display magnitude and phase information across frequency range
7.	 <p style="text-align: center;">Waveguide</p>	To carry high frequency and electromagnetic waves
8.	 <p style="text-align: center;">Resonator</p>	As generate waves of specific frequency





3.2.3 Apply for Measurement Dye-Sensitized Solar Cells Fabrication (DSSC)

Table 3. 3: Equipment and apparatus are used in measurement DSSC

No.	Equipment/ Material	Functioning
1.	 <p>Fume Hood</p>	Fabrication work is performed experimental under room temperature 27°C
2.	 <p>Analytical Balance</p>	Used to weighing TiO^2 with 2 grams
3.	 <p>Hot Plate</p>	Sample baked (TiO^2 – coated FTO glass)

4.	 <p data-bbox="692 524 775 555">Mixer</p>	To crush the fruit
5.	 <p data-bbox="558 949 908 981">Fluorine-Doped Tin Oxide</p>	As conductive glass for Dye-Sensitized Solar Cells
6.	 <p data-bbox="620 1386 836 1417">Aluminium Foil</p>	To avoid from oxidized
7.	 <p data-bbox="652 1818 804 1850">Multimeter</p>	To checking conductivity side and measure the electrical element

8.	 <p data-bbox="563 504 903 539">Porcelain Mortar & Pestle</p>	To crush the fruit
9.	 <p data-bbox="668 981 786 1016">Filtering</p>	Used to filter the piece of fruit
10.	 <p data-bbox="684 1420 772 1456">Bottle</p>	To place the dyes after extraction
11.	 <p data-bbox="652 1879 786 1915">Petri Dish</p>	Used to immersed the FTO in dyes

12.	 <p data-bbox="684 510 743 546">Clip</p>	To bind the combination between FTO glass
13.	 <p data-bbox="628 954 823 990">Crocodile Clip</p>	Act as clip between polarity charge
14.	 <p data-bbox="571 1402 849 1438">Potassium Iodide, KI</p>	Act as electrolyte
15.	 <p data-bbox="603 1850 839 1886">Chemical Solvent</p>	There is vinegar, ethanol, methanol, distilled water, beaker, glass rod, syringe, test tube, dropper and holder test tube

3.3 Extraction of Photosensitizer

This step is the most important thing that include experimental procedure dye-sensitized solar cell. Therefore, about several fruit in based-anthocyanin have been chosen in this figure below. The fruit were appropriately washed with distilled water (H^2O) and then rinse in ethanol solution. The reason of that to removal any nano-particles are not certainly consists in dye extracted later. Furthermore, ethanol is make used for the terminate the solvent shell that encircling the environment.

Moreover, in this step extraction fruit (dyes) categorization divided into two part which is for the first batch by used extraction by hand while for the second batch by used mechanical extraction (mixer) to come in for dyes anthocyanin-based.

3.3.1 Type of Dye's Extraction Fruit for First Batch

In this research, there are identifying several aspects to observe how to determination based on the different dyes will come out for the output. Hence, initiate by chosen several fruits in based-anthocyanin that are best sample will used in this session. Strawberry, blueberry, cherry and water melon are the grouping in the based anthocyanin regarding from the research would made before.



Figure 3. 4: Selection fruit dyes extraction for first batch

3.3.2 Type of Dye's Extraction Fruit for Second Batch

Foremost, experimental dye's extraction is repeat once more to making an observation regarding the result would outcome based on the make used different extraction dye. For the example, water melon, mango, black grapes and dragon fruit are the group fruit have been chosen in this process which us dyes extraction. The reason why divided into second batch is make an observation into many data and made a summarized about the output from different dye used.

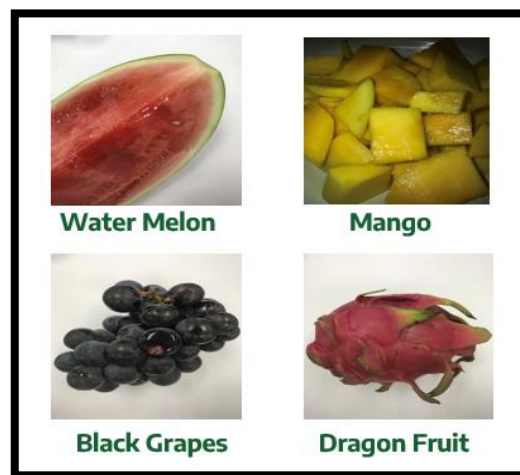


Figure 3. 5: Selection fruit dyes extraction for second batch

3.4 Preparation or Arrangement of Extraction

Provided that, there are some procedure ways how to provide the preparation or arrangement of extraction have been made before. It was the easily understanding when it elaborates one by one step in this procedure moreover for the step of first batch and second batch are exactly the same procedure but different technique will used. Referring the categorization for the first batch make used by extraction by hand while for the second batch make used by extraction by hand. The comparison between in this different technique will discuss in the part result outcome. From that, it will know how the finalized result could make the analysing based on used different fruit selection.

3.4.1 Extraction Fruit for First Batch



Figure 3. 6: First batch dyes extraction

Initially, the procedure of dyes extraction would start with selection dyes material in different fruit extraction in anthocyanin-based. It is depending on the experimental owner what type of the fruit would made decision to chosen the fruit. Moreover, regarding the research that mostly are correctly information have been made great solution extraction such as water melon, blueberry, cherry and strawberry have been chosen. After that the process will continue by extraction stage that the most important thing dyes extraction by hand. There are some cases that while conducting the extraction process strawberry is the difficult dyes extraction among the other fruit. This is because strawberry is the hard-outer fruit compare the blueberry, cherry and water melon. Furthermore, water melon is the easily dyes extraction among the other fruit for the reason that water melon is the juicy more water extraction among the selection fruit



Figure 3. 7: The process of dyes extraction by hand

Likewise, after dyes extraction for the blueberry, cherry, water melon and strawberry it will place the dye into bottle. The proving of dyes extraction it could make referring from the figure below shows that the level of solution dyes in the bottle. From that proves, strawberry is the least level solution dye while water melon is the high-level solution dye and for the blueberry and cherry has similar characteristics intermediate easily to extracted the fruit to make of dye anthocyanin-based.



Figure 3. 8: All dyes extraction is filled in the bottle

Aluminum foil has the most important element that consist in this study dye-sensitized solar cell. To provide the dyes extraction in the good condition it must be protect by used something covered. Therefore, aluminum foil is the best solution to covered the dyes extraction since aluminum foil has characteristics to avoid any material or components from any oxidation. While each of the bottle that filled the different dye such as strawberry, blueberry and water melon and cheery compulsory to wrapped by aluminum foil.



Figure 3. 9: Wrapped each of the bottle for the first batch

Last but not least, all the dyes extraction for the first batch has been successfully extraction and efficiently arrangement. In additional, each of the bottle has been made placed the mark or sticker to rename each dyes extraction.



Figure 3. 10: Efficiently arrangement for the first batch

3.4.2 Summarize for Flow Whole Procedure First Batch

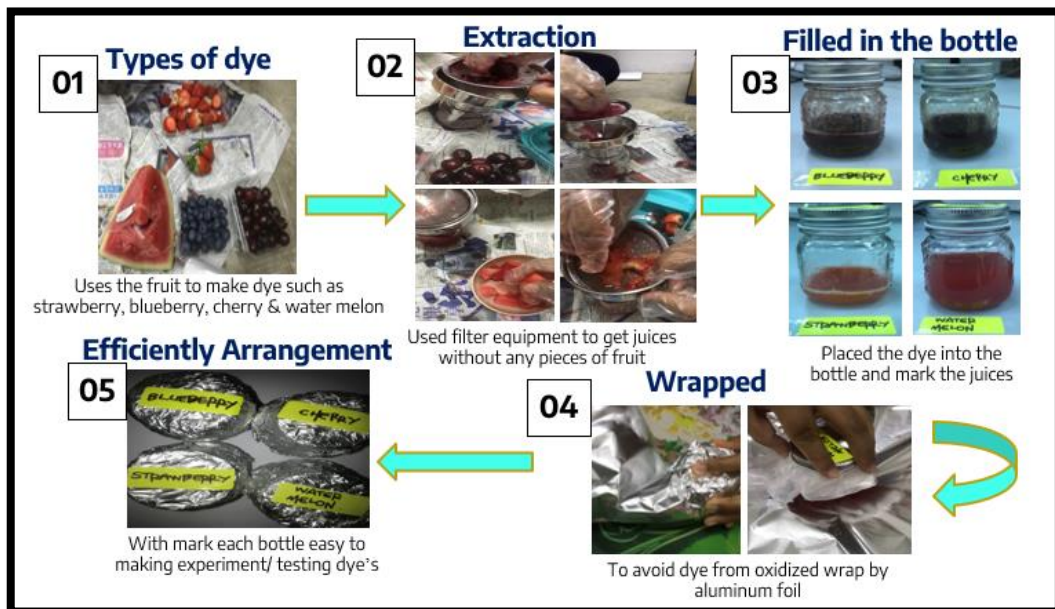


Figure 3. 11: The flow whole procedure dyes extraction first batch

3.4.3 Extraction Fruit for Second Batch



Figure 3. 12: Second batch dyes extraction

For begin the procedure dyes extraction would be the same as the first batch dyes extraction but dissimilar of uses selection of the fruit. In this part, dragon fruit, black grapes, mango and water melon have been chosen for the dyes extraction regarding the research most are them are categorization are mostly the good experimental in dye-sensitized solar cells to would testing and also popular in anthocyanin-based extraction photosensitizer.

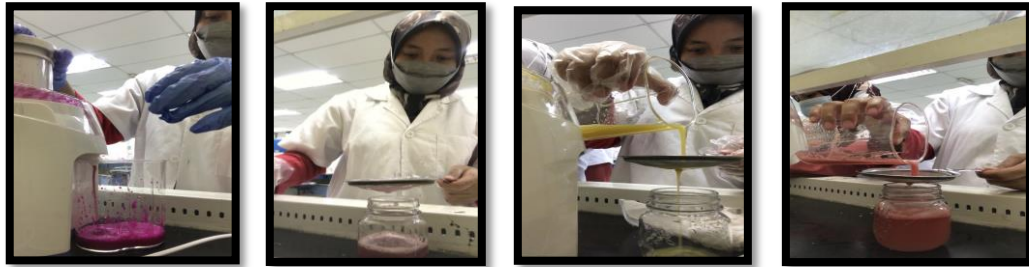


Figure 3. 13: The process of dyes extraction by mixer

Regarding the dyes extraction it would show that the different part which is in this part the uses of mechanical extraction by mixer to made of dyes from fruit. It is easily technique to crush the fruit comparing based on extraction fruit by hand also the uses of mortar pestle.

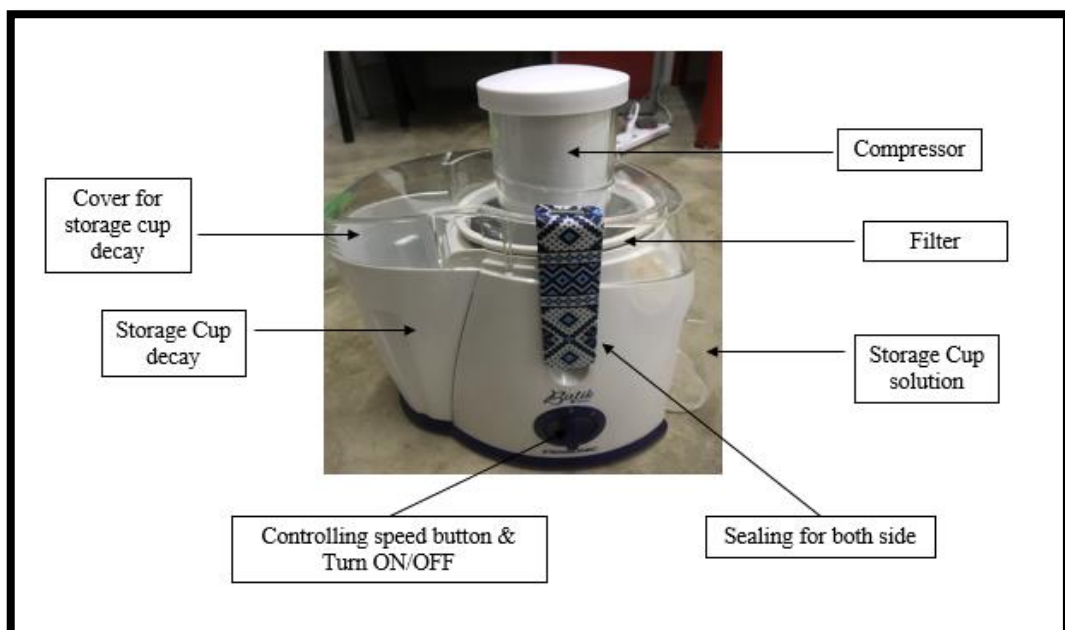


Figure 3. 14: The indicate part of mechanical extraction which is mixer

Based on the dyes extraction there are show there is not quietly show the comparison between high and low level of solution in the bottle. Since all of all fruit are uses the same mechanical extraction which is mixer are great process to get the dyes. Based on the figure above as could see there are the part mechanical extraction by mixer to crush the fruit very easily. That equipment involves the process which is the controlling the speed button and ON/OFF controlling since the power will activated. The functioning of compressor is used to press the fruit into the mechanical extract flow to the filter part since to penetrate the solution only without any pieces of fruit. In additional, for the safety reason the mechanical extraction included the sealing for the both sides to avoid any incident could be happening. After the process of extracted will flow based on the solution (dyes) will drop to the storage cup solution and all the decay from the fruit will drop to the part storage cup decay.

The advantages of this mixer use are not delay effected the time taken also the efficiency preparation compared to the dye's extraction by hand.



Figure 3. 15: All the dyes extraction is filled in the bottle

Aluminum foil has the most important element that consist in this study dye-sensitized solar cell. To provide the dyes extraction in the good condition it must be protect by used something covered. Therefore, aluminum foil is the best solution to covered the dyes extraction since aluminum foil has characteristics to avoid any material or components from any oxidation. While each of the bottle that filled the different dye such as strawberry, blueberry and water melon and cheery compulsory to wrapped by aluminum foil.



Figure 3. 16: Wrapped each of the bottle for the second batch

Finally, all the dyes extraction for the second batch has been successfully extraction and efficiently arrangement. In additional, each of the bottle has been made placed the mark or sticker to rename each dyes extraction.



Figure 3. 17: Efficiently arrangement for the second batch

3.4.4 Summarize for Flow Whole Procedure for Second Batch

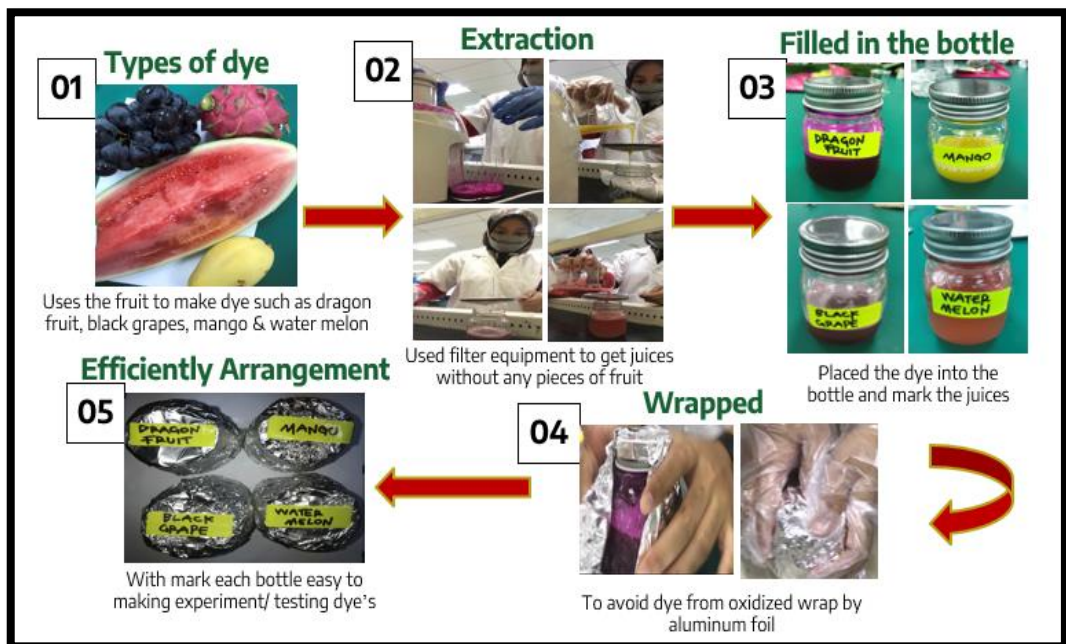


Figure 3. 18: The flow whole procedure dyes extraction second batch

3.5 Measurement of Absorbance by Ultraviolet-Visible Spectrophotometer

Foremost, the measurement absorbance is defined as the quantity of light has been absorbed by a solution. In this research, solution is conducting the dyes extraction based on several fruit are making the sample. There are such as Strawberry, Blueberry, Cherry, Water melon, Dragon Fruit, Mango and Black Grapes. Experimental are going categorization into two batch which is First Batch and Second Batch. Since, observing the result will come out based on different fruit dyes extracted

Consequently, in this study absorbance value are measure by determination using the equipment are well known as named Ultraviolet-Visible Spectrophotometer are placed at UMP Gombang which is Fakulti Teknologi Kejuruteraan Kimia & Proses Laboratory. This equipment is functioning as to measure the concentration of a sample can be calculated from its absorbance. When applied the dyes into Ultraviolet-Visible Spectrophotometer the apparatus will used insert that equipment are called cuvette. Hence, this functioning the filled in and out into cuvette and placed into the holder cuvette in Ultraviolet-Visible Spectrophotometer.

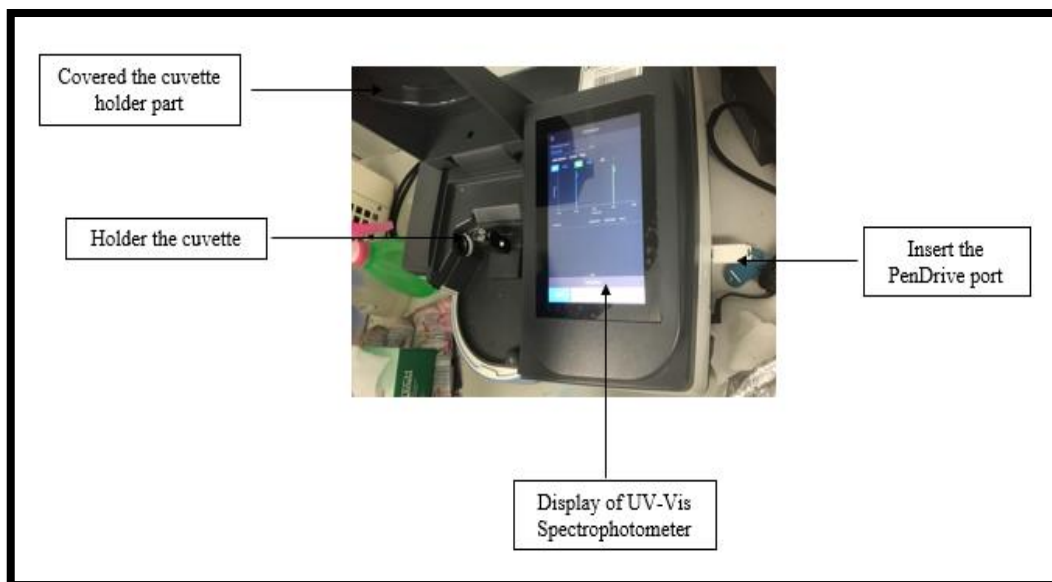


Figure 3. 19: The indicate part of Ultraviolet-Visible Spectrophotometer

3.5.1 Absorbance for Extraction Fruit First Batch

1. Initially, with preparation for dyes extraction with different fruit extract from anthocyanin-based.



Figure 3. 20: All the dyes extraction first batch is filled in the bottle

2. Continue the process with select the 'SCAN' at Ultraviolet-Visible Spectrophotometer, then click add experiment and fill at the 'RANGE'. For more information, every fruit anthocyanin-based have any range wavelength of their characteristics.



Figure 3. 21: Display on Ultraviolet-Visible Spectrophotometer

3. Pour distilled water into cuvette (Blank) started the used.

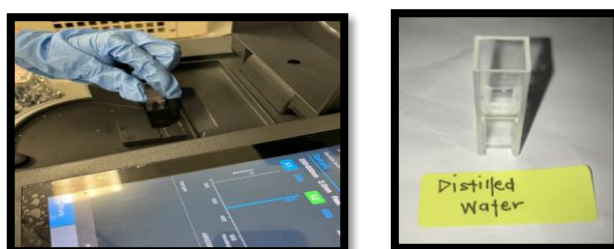


Figure 3. 22: Initial procedure with distilled water (Blank)

4. Pour the dyes into cuvette for the second round to observe the absorbance.



Figure 3. 23: Pour dyes first batch into cuvette by using dropper

5. After that, with different sample of dyes (Strawberry, Blueberry, Cherry and Water Melon) will exchange the cuvette and repeat the step 'BLANK'.

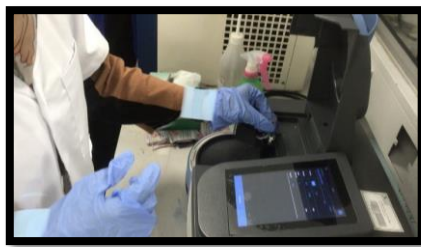


Figure 3. 24: Exchanging the cuvette with different dyes extraction

6. Likewise, after fill in the cuvette as can see the comparison color from the figure below from the different fruit experimental. Since, the many cuvette represent of dilution that have make when the graph has cut at 5 Absorbance state. In additional, before dilution process the graph are indicate the flow of graph are not in smooth graphical compare after the dilution process has made. Therefore, when the value of absorbance is very low it is the great condition since UV-Visible Spectrophotometer are easily the through the liquid (dyes).

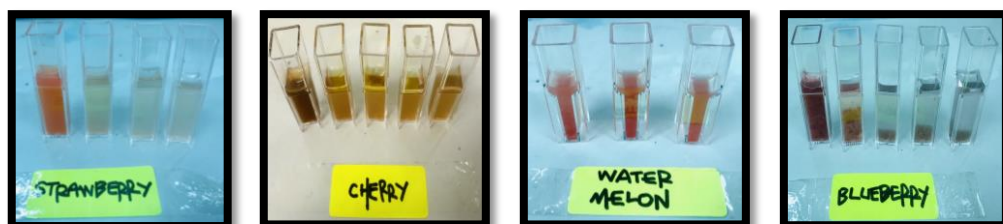


Figure 3. 25: Comparison liquid before & after dilute process first batch

7. Based on the graph representation at display Ultraviolet-Visible Spectrophotometer will come out the result on the Axis X as Wavelength while on the Axis Y as Absorbance value.

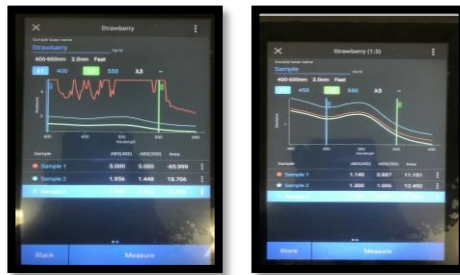


Figure 3. 26: Graphical Strawberry representation measurement absorbance



Figure 3. 27: Graphical Cherry representation measurement absorbance



Figure 3. 28: Graphical Blueberry representation measurement absorbance

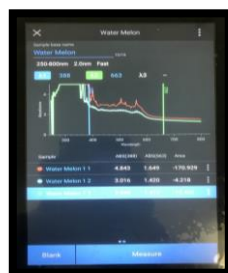
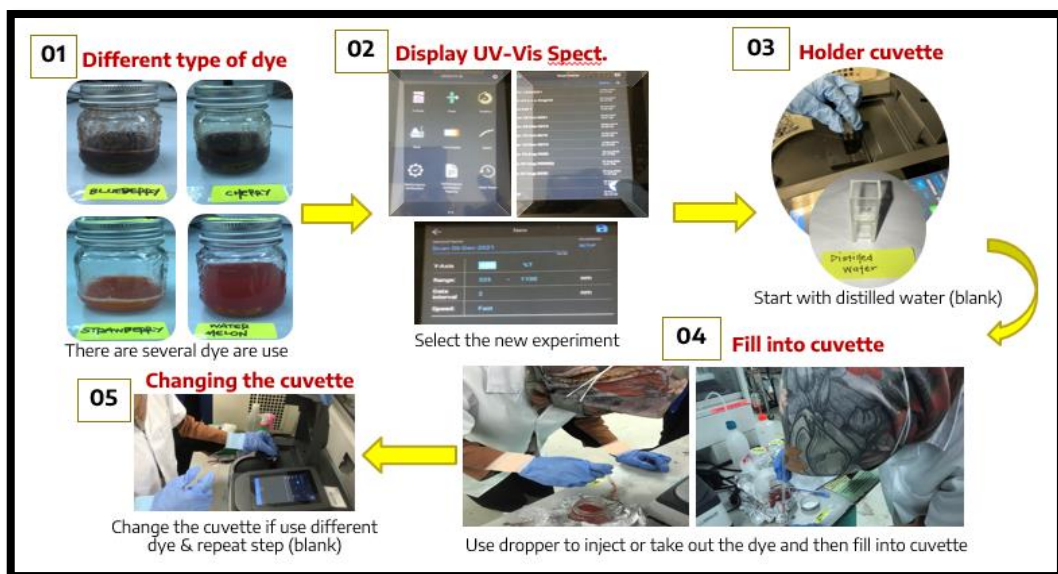


Figure 3. 29: Graphical Water Melon representation measurement absorbance

8. Based on the graph as shown the above, there are showing the comparison between both graph at representation of measurement. The reason is before making the dilute process the graph is indicate not quietly smooth and cut at the higher value which is 5 absorbance on axis y.
9. Therefore, should make the dilute process to minimize the higher value at 5 absorbance. Then, after making the dilute process the graph on the display Ultraviolet-Visible Spectrophotometer are come out the smooth graph. Hence, analyse are making when the higher concentration the liquid, the difficult of absorbance value are computation.

3.5.2 Summarize for Flow Whole Procedure for First Batch



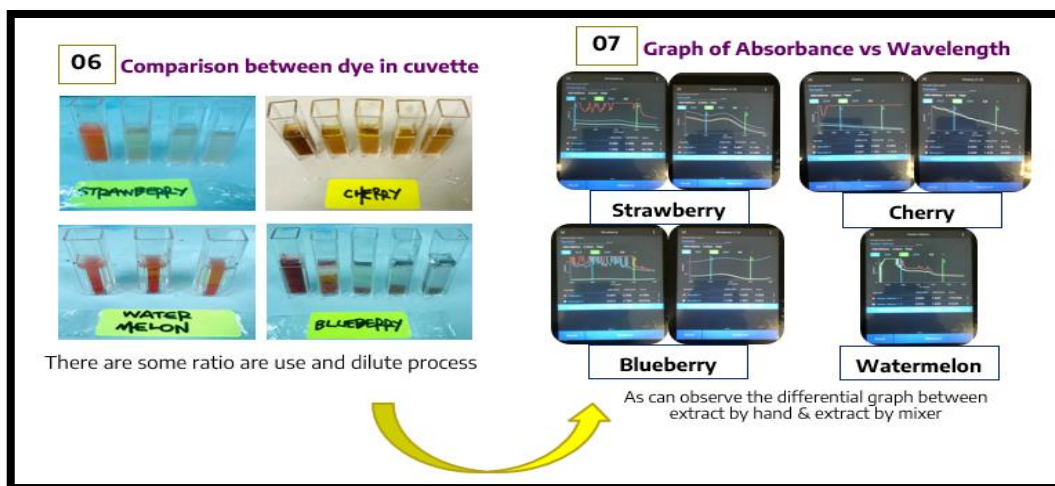


Figure 3. 30: The flow whole procedure measurement absorbance first batch

3.5.3 Absorbance for Extraction Fruit Second Batch

1. Starting the preparation of four sample dyes extraction such as Dragon Fruit, Mango, Black Grapes and Water Melon.



Figure 3. 31: All the dyes extraction second batch is filled in the bottle

2. This part is similar step of the First Batch measurement of Absorbance acquire. Select the 'SCAN' at Ultraviolet-Visible Spectrophotometer, then click add experiment and fill at the 'RANGE'. For more information, every fruit anthocyanin-based have any range wavelength of their characteristics.
3. Pour distilled water into cuvette (Blank) started the used.
4. Pour the dyes (Dragon Fruit, Black Grapes, Mango and Water melon) into cuvette for the second round to observe the absorbance.



Figure 3. 32: Pour dyes second batch into cuvette by using dropper

5. After fill in the dyes into cuvette, are compulsory to wipe the excess water are drop surrounding the cuvette.



Figure 3. 33: Wipes the surrounding the cuvette

6. Continue process, with different sample of dyes (Dragon Fruit, Black Grapes, Mango and Water Melon) will exchange the cuvette and repeat the step from the step distilled water 'BLANK'.
7. Likewise, after fill in the cuvette as can see the comparison color from the figure below from the different fruit experimental. Since, the many cuvette represent of dilution that have make when the graph has cut at 5 Absorbance state. In additional, before dilution process the graph are indicate the flow of graph are not in smooth graphical compare after the dilution process has made. Therefore, when the value of absorbance is very low it is the great condition since UV-Visible Spectrophotometer are easily the through the liquid (dyes).



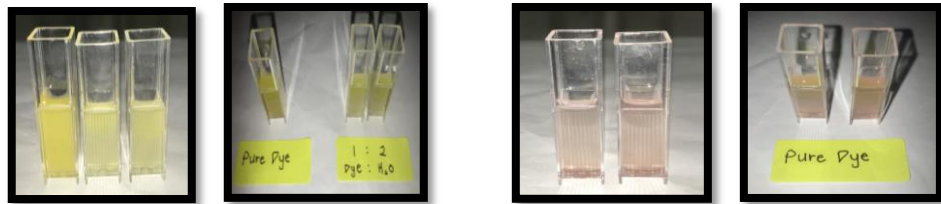


Figure 3. 34: Comparison liquid before & after dilute process second batch

8. Based on the figure above from dyes extracted (Dragon Fruit, Black Grapes and Mango) there have three cuvettes since representation of have be made the dilution process. This is because the graph has been cut at 5 Absorbance compare to the Water Melon their dyes are very not quietly concentration among the other fruit dyes sample.
9. Based on the graph representation at display Ultraviolet-Visible Spectrophotometer will come out the result on the Axis X as Wavelength while on the Axis Y as Absorbance value.



Figure 3. 35: Graphical Dragon Fruit representation measurement of absorbance



Figure 3. 36: Graphical Black Grapes representation measurement of absorbance

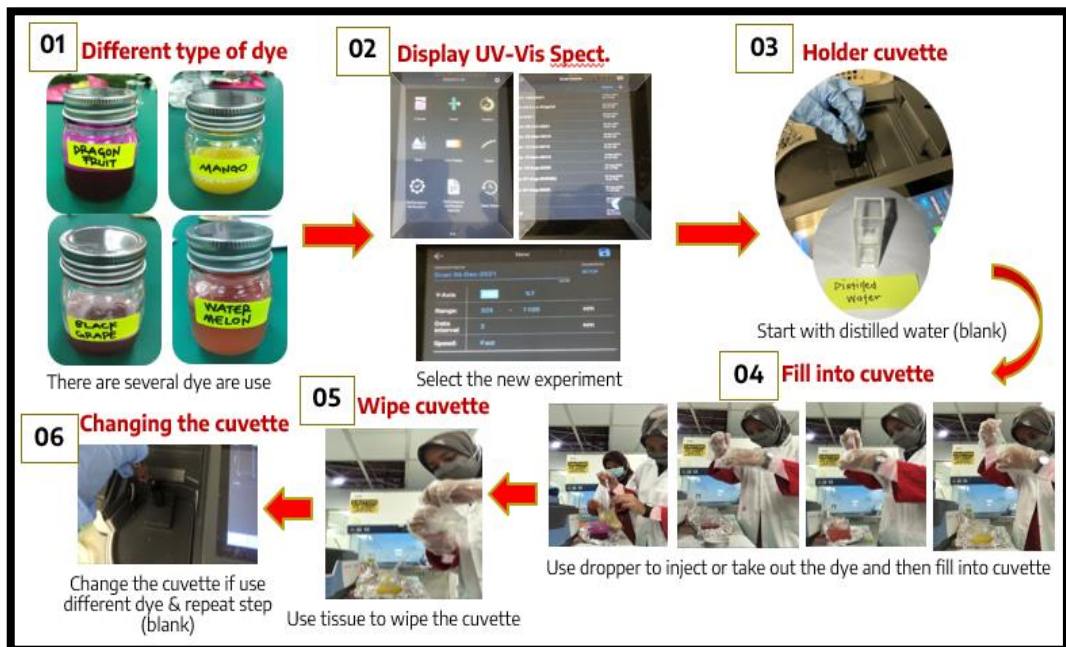


Figure 3. 37: Graphical Mango representation measurement of absorbance



Figure 3. 38: Graphical Water melon representation measurement of absorbance

3.5.4 Summarize for Flow Whole Procedure for Second Batch



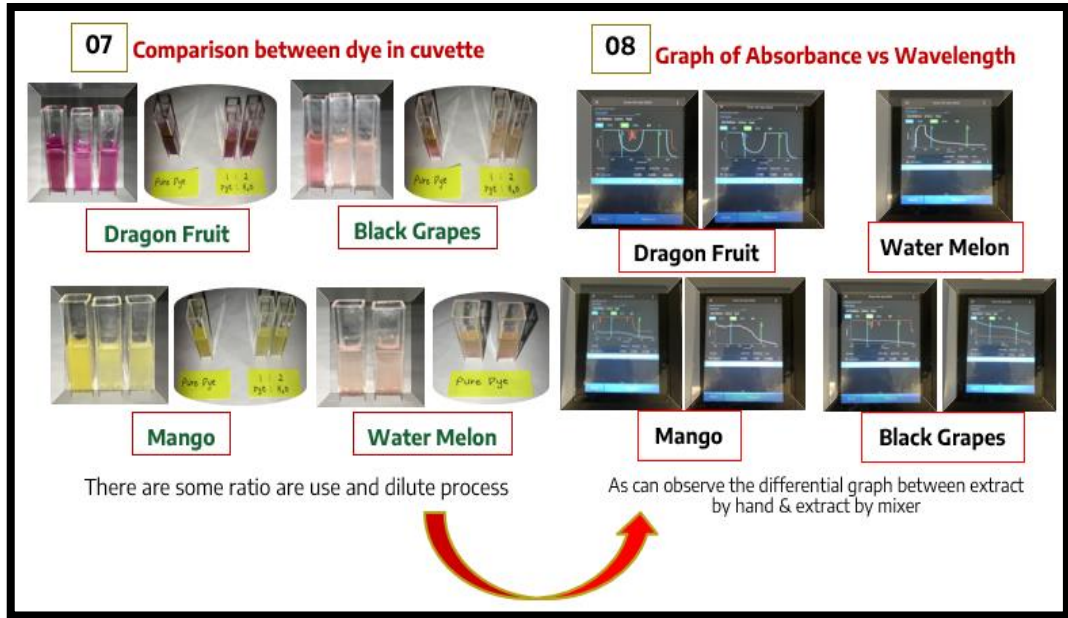


Figure 3.39: The flow whole procedure measurement absorbance second batch

3.6 Measurement of Permittivity based on Resonator

Simultaneously, this part is most important element of this project since this research are correlated with the elucidate an effect of material permittivity to current-voltage characteristics. Therefore, the measurement of permittivity is determination by used the equipment waveguide and resonator are functioning to controlled the frequency of the communication based on the radio waves generated. It is also included the having the property of transmission electric force without any conduction transferred. This study which is permittivity are related to the designed to function as a resonator for radio waves properties that confined the surrounding inside the resonator components abrupt the exchanged in permittivity at the surface area.

Moreover, the resonant are made up combination between the waveguide at the both sided of resonator hence the waves are locked to be out from the resonator while computing. Overall, the resonant frequency is determined by physical dimension resonator correlated the dielectric constant of the material that conducting the high around the relaxation of the polarisation mechanism. Finally, in this case also categorization into two divided experimental to observe the result will come out based on used the dyes extraction regarding different fruit are used.

3.6.1 Permittivity for the Extraction Fruit First Batch

First Step: Preparation start of Network Analyzer

1. Turn on the socket and power of Network Analyzer.
2. Then, compulsory delay the time of Network Analyzer around 20 minutes.
3. Connect the wire to the port of both sides (No polarity charges).

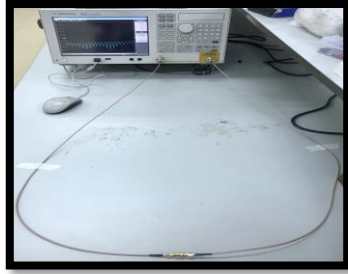


Figure 3. 40: Calibration Network Analyzer

4. To avoid the wire move, use a salotip at the both sides.
5. Tightness the port by using tight kit.

Second Step: To setup the Network Analyzer

10. Based on the screen Network Analyzer (MEASUREMENT: click S21).
11. Based on the RESPONSE: Choose button SCALE
 - Scale/Div = click 0.1, choose button (x 1) the scale will get 100 mdB/div
 - Reference Position = 5 Div
 - Reference Value = 0.0000 Db
12. Based on the RESPONSE: Choose button AVG
 - Averaging: ON
 - Smoothing: ON
13. Based on the STIMULUS: choose button START/STOP
 - Start = 4GHz
 - Stop = 6GHz
14. Based on the RESPONSE: choose button CAL. At this stage, cannot have any movement at all.
 - Click: Calibrate

- Click: Enhanced Response

15. After that, observe the Network Analyzer while calibration stage and wait around 2 minutes.

16. Each equipment must make the calibration test to avoid any uncertainty measurement value. Calibration kit such as:

- Open, Short & Load

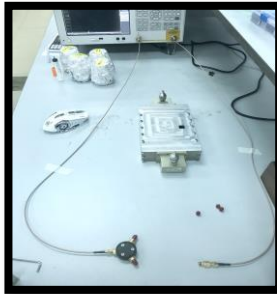


Figure 3. 41: Calibration Open, Short & Load of Network Analyzer

- Thru

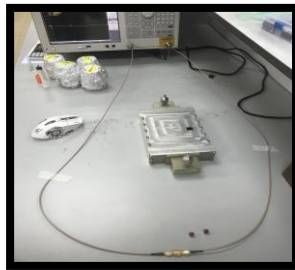


Figure 3. 42: Calibration Thru of Network Analyzer

- Isolator

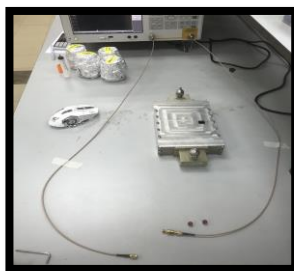


Figure 3. 43: Calibration of Isolator of Network Analyzer

17. In addition, all the calibration kit must do the tightness and wait around 5 second to provide the stable stage.
18. Based on the Enhanced Response: click tick any calibration done.
19. Repeat step 7 to 9 for all calibration kit.
20. Click DONE and because of that will appear one straight line at 0 value. So, calibration is done.

Third Step: To setup the Resonator/Waveguide

1. First of all, loose the screw at a waveguide.



Figure 3. 44: Loose the screw at waveguide

2. Connect the waveguide at the both side of resonator.

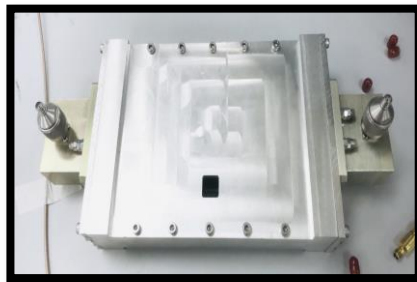


Figure 3. 45: Loose the screw at Resonator

3. Connect the wire at the both side resonator and tightness the screw at the waveguide.
4. Tightness the wire by use the tight kit.
5. Then, use the holder dye to fill the dye.

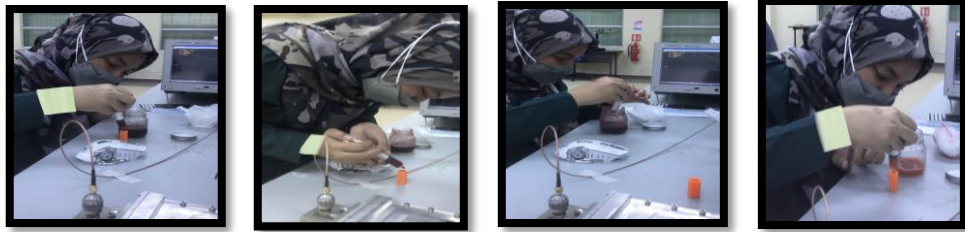


Figure 3. 46: Fill the dyes first batch into holder dye

6. Place the holder dye at resonator.

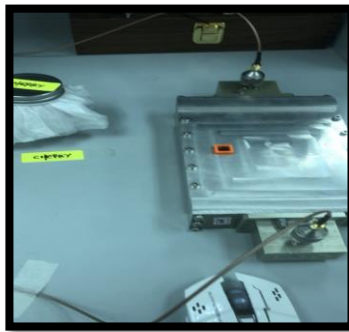


Figure 3. 47: Placed the holder dye first batch into Resonator

7. Repeat step 5 to 6 to change the different use of dye.

Forth Step: To observe the output of Network Analyzer and Resonator/waveguide

1. Based on the STIMULUS: choose button START/STOP
 - Start = 4GHz
 - Stop = 6GHz
2. First of all, we are measure Air Material (without dye).
3. Observe the wave at network analyzer and choose peak graph at 5GHz because this value is center between start (4GHz) and end (6GHz).
4. Based on the STIMULUS: choose button START/STOP
 - Start = 4.9GHz
 - Stop = 5.1GHz
5. Based on the RESPONSE: choose Scale
 - Click Autoscale

6. Place the holder dye (Cherry) at resonator.

Measurement with Material Air (Cherry)

7. Then, we use start frequency (4.9GHz) and end (5.1GHz). Observe the waves and make sure the waves are 3decibel.

8. Based on the MKR/ANALYSIS: choose Marker Search

- Click: Max
- Tracking: ON
- Bandwidth: ON

9. From the previous setting, the network analyzer will appear the information such as:

- Bw
- Cent
- Low
- High
- Q
- Loss

10. Furthermore, to bigger the size of waves we can setting the value based on the information given.

- Low as start value.
- high as end value.

11. Based on the STIMULUS: choose button START/STOP

- Start = 4.991GHz
- Stop = 4.995GHz

12. Based on the RESPONSE: choose Scale

- Click Autoscale

13. Hence, we will get output waves of air material.

14. Finally, repeat step 7 to 12 to exchanging every time used different dyes (Strawberry, Blueberry and Water Melon) solution.

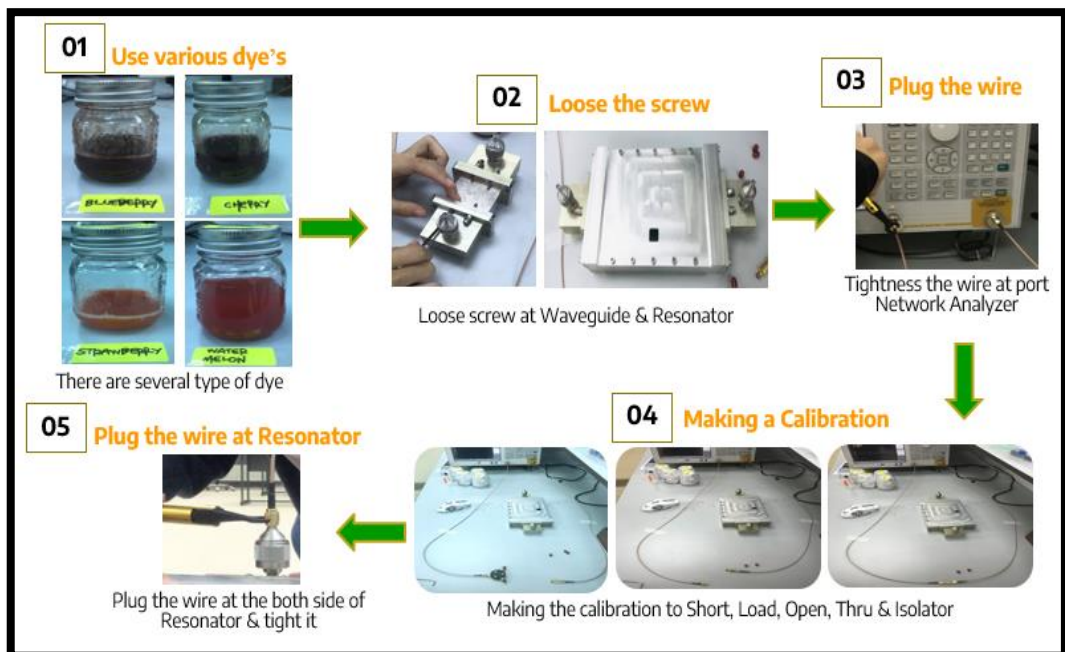
Measurement with Material dye (Cherry)

15. Repeat step 4 to 6.

16. Then, the wave will appear for material dye (Cherry).
17. Based on the STIMULUS: choose button START/STOP
 - Start = 4.994GHz
 - Stop = 5.033GHz
18. Based on the RESPONSE: choose Scale
 - Click Autoscale
19. Hence, we will get output waves of material dye (Cherry).
20. Finally, repeat step 14 to 17 to exchanging every time used different dyes (Strawberry, Blueberry and Water Melon) solution.

3.6.2 Summarize for Flow Whole Procedure for First Batch

The flow process for whole procedure permittivity for the extraction fruit first batch has been shown as the figure below:



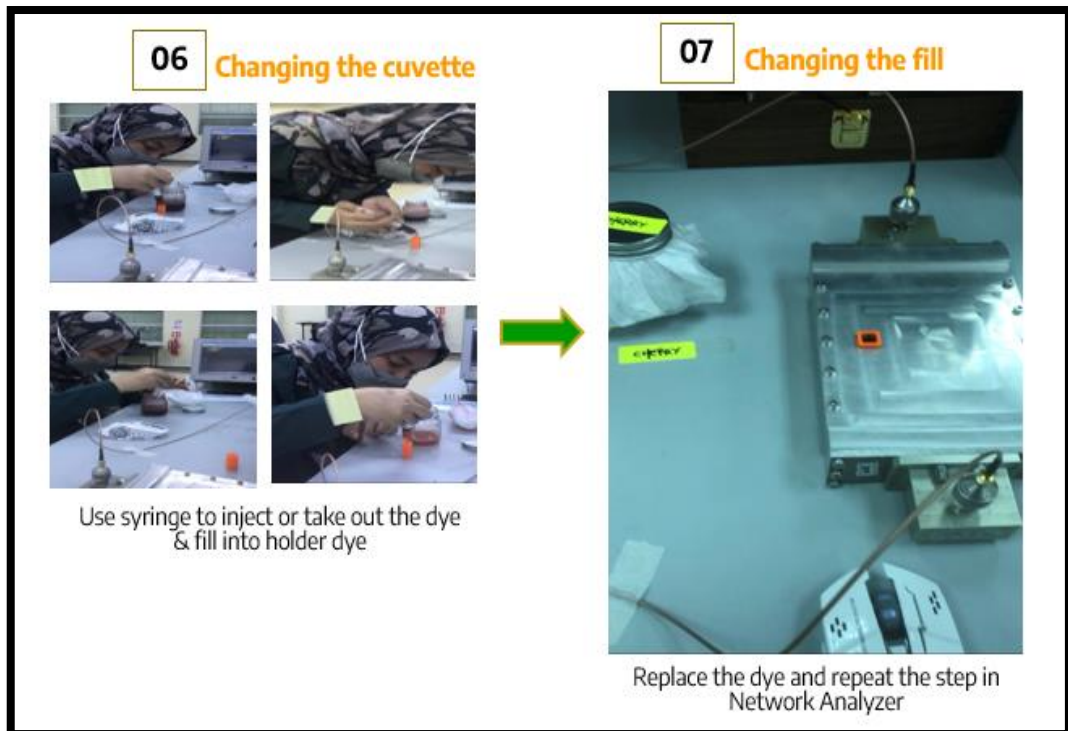


Figure 3. 48: The flow whole procedure measurement permittivity first batch

3.6.3 Permittivity for the Extraction Fruit Second Batch

First Step: Preparation start of Network Analyzer

1. Turn on the socket and power of Network Analyzer.
2. Then, compulsory delay the time of Network Analyzer around 20 minutes.
3. Connect the wire to the port of both sides (No polarity charges).
4. To avoid the wire move, use a salotip at the both sides.
5. Tightness the port by using tight kit.

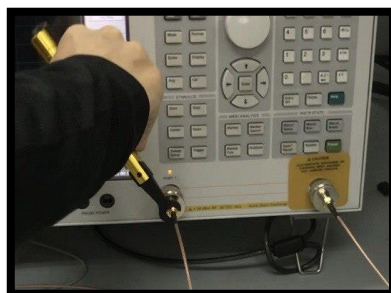


Figure 3. 49: Using tight kit to tightness port Network Analyzer

Second Step: To setup the Network Analyzer

21. Based on the screen Network Analyzer (MEASUREMENT: click S21).
22. Based on the RESPONSE: Choose button SCALE
 - Scale/Div = click 0.1, choose button (x 1) the scale will get 100 mdB/div
 - Reference Position = 5 Div
 - Reference Value = 0.0000 Db
23. Based on the RESPONSE: Choose button AVG
 - Averaging: ON
 - Smoothing: ON
24. Based on the STIMULUS: choose button START/STOP
 - Start = 4GHz
 - Stop = 6GHz
25. Based on the RESPONSE: choose button CAL. At this stage, cannot have any movement at all.
 - Click: Calibrate
 - Click: Enhanced Response
26. After that, observe the Network Analyzer while calibration stage and wait around 2 minutes.
27. Each equipment must make the calibration test to avoid any uncertainly measurement value. Calibration kit such as:
 - Open, Short & Load
 - Thru
 - Isolator
28. In addition, all the calibration kit must do the tightness and wait around 5 second to provide the stable stage.
29. Based on the Enhanced Response: click tick any calibration done.
30. Repeat step 7 to 9 for all calibration kit.
31. Click DONE and because of that will appear one straight line at 0 value. So, calibration is done.

Third Step: To setup the Resonator/Waveguide

8. First of all, loose the screw at a waveguide.

9. Connect the waveguide at the both side of resonator.
10. Connect the wire at the both side resonator and tightness the screw at the waveguide.



Figure 3. 50: Tightness the port at Resonator by using tight kit

11. Tightness the wire by use the tight kit.
12. Then, use the holder dye to fill the dye.

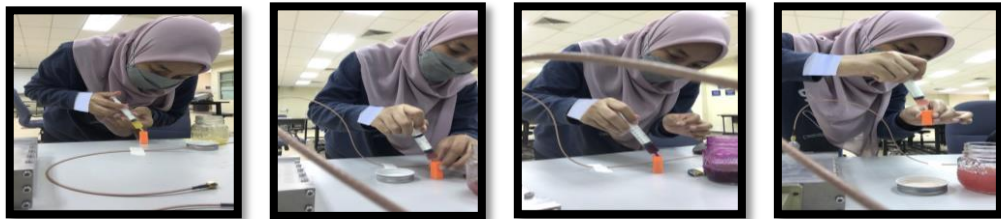


Figure 3. 51: Fill the dyes second batch into holder dye

13. Place the holder dye at resonator.

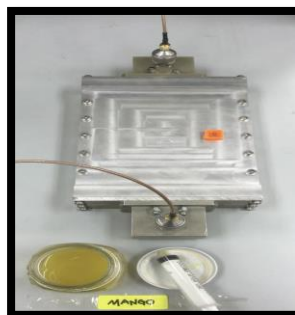


Figure 3. 52: Placed the holder dye first batch into Resonator

14. Repeat step 5 to 6 to change the different use of dye.

Forth Step: To observe the output of Network Analyzer and Resonator/waveguide

21. Based on the STIMULUS: choose button START/STOP
 - Start = 4GHz
 - Stop = 6GHz
22. First of all, we are measure Air Material (without dye).
23. Observe the wave at network analyzer and choose peak graph at 5GHz because this value is center between start (4GHz) and end (6GHz).
24. Based on the STIMULUS: choose button START/STOP
 - Start = 4.9GHz
 - Stop = 5.1GHz
25. Based on the RESPONSE: choose Scale
 - Click Autoscale
26. Place the holder dye (mango) at resonator.
Measurement with Material Air (Mango)
27. Then, we use start frequency (4.9GHz) and end (5.1GHz). Observe the waves and make sure the waves are 3decibel.
28. Based on the MKR/ANALYSIS: choose Marker Search
 - Click: Max
 - Tracking: ON
 - Bandwidth: ON
29. From the previous setting, the network analyzer will appear the information such as:
 - Bw
 - Cent
 - Low
 - High
 - Q
 - Loss
30. Furthermore, to bigger the size of waves we can setting the value based on the information given.
 - Low as start value.

- high as end value.
31. Based on the STIMULUS: choose button START/STOP
 - Start = 4.993GHz
 - Stop = 4.998GHz
 32. Based on the RESPONSE: choose Scale
 - Click Autoscale
 33. Hence, we will get output waves of air material.
 34. Finally, repeat step 7 to 12 to exchanging every time used different dyes (Dragon Fruit, Black Grapes and Water Melon) solution.

Measurement with Material dye (Mango)

35. Repeat step 4 to 6.
36. Then, the wave will appear for material dye (Mango).
37. Based on the STIMULUS: choose button START/STOP
 - Start = 4.996GHz
 - Stop = 5.028GHz
38. Based on the RESPONSE: choose Scale
 - Click Autoscale
39. Hence, we will get output waves of material dye (Mango).
40. Finally, repeat step 14 to 17 to exchanging every time used different dyes (Dragon Fruit, Black Grapes and Water Melon) solution.

3.6.4 Summarize for Flow Whole Procedure for Second Batch

The flow process for whole procedure permittivity for the extraction fruit second batch has been shown as the figure below:

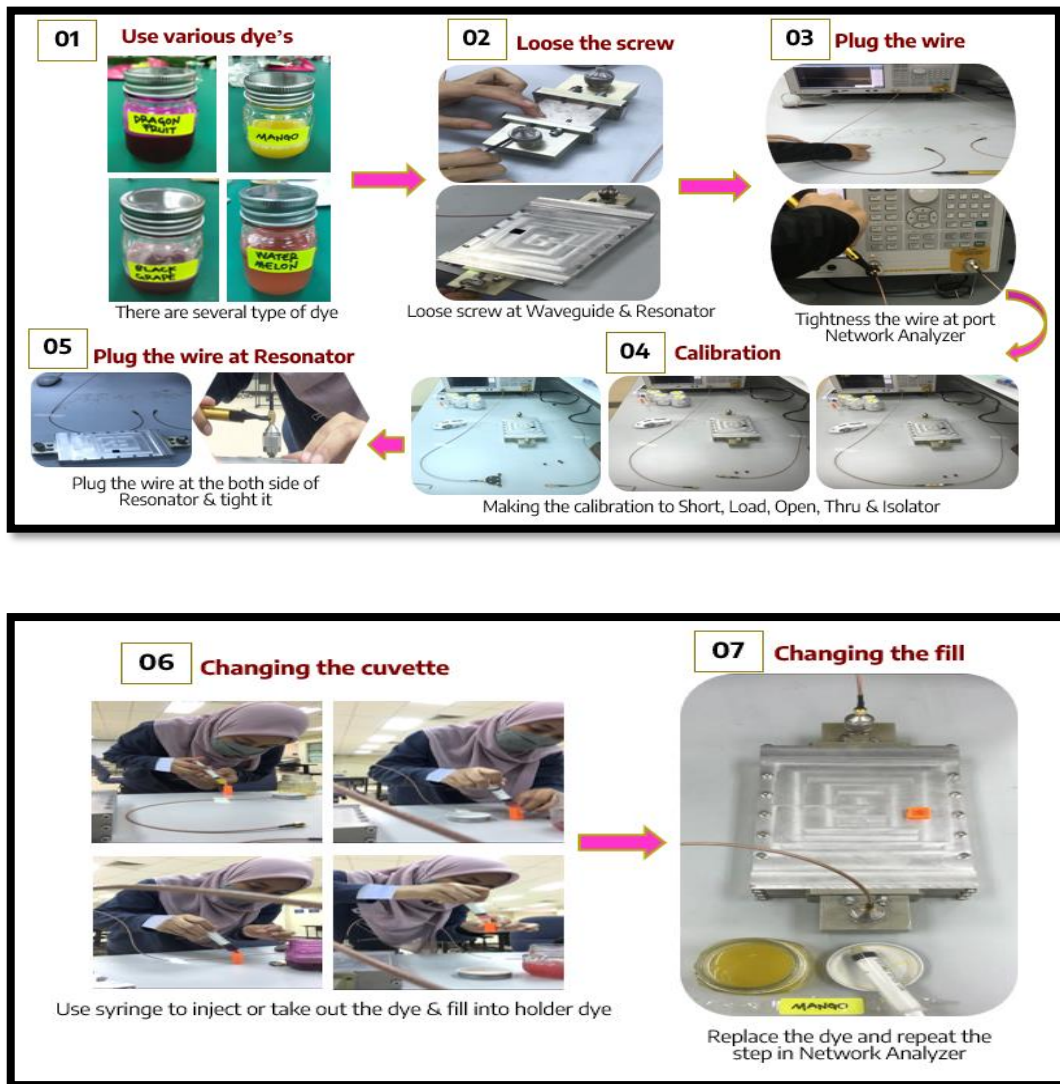


Figure 3. 53: The flow whole procedure measurement permittivity second batch

3.7 Preparation of Dye Sensitized Solar Cell (DSSC)

Dye-sensitized solar cells are element photovoltaic devices that transform light energy into electrical energy based on nanomaterial which is TiO_2 are used in this fabricated. Typically, in this study mostly are used TiO_2 that the electrons from the TiO_2 will flow toward the transparent electrode where contains too other nano-particles that included dyes extraction and other process where there are collected for powering a load.

Moreover, in this research are exactly similar to the other experimental process such as dyes extraction, measurement absorbance and measurement permittivity are also divided into two part which is First Batch and Second batch. In order to analysing the information regarding this study and correlated with other experiment also.

3.7.1 DSSC for First Batch

1. Analytical balance is used to weighing TiO_2 powder with 2gm.



Figure 3. 54: Weighing TiO_2 powder by using Analytical Balance for First Batch

2. All the fabrication work is performed under fume hood chamber at room temperature 27°C .



Figure 3. 55: Perform work in Fume Hood Chamber

3. Fluorine-doped Tin Oxide, FTO as conductive glass for DSSCs are washed with distilled water and ethanol (for dry the equipment).



Figure 3. 56: Cleansing the conductive test

4. Preparation of TiO_2 :



Figure 3. 57: Stir the mixture all together

Combined all the item below with measured and then mixture all the solution around 15minute with non-stop until the liquid turns white solution:

- Vinegar (2ml)
- TiO_2 powder (2gm)
- Ethanol (4ml)

5. Then, planning an idea to incremental the value of current short circuit (I_{sc}) of active area (TiO_2) hence, sketch at A4 paper the length & width of FTO glass.



Figure 3. 58: Planning the length & width of FTO glass

6. Checking the conductive side of FTO glass. That will be comparison value between of them.



Figure 3. 59: Checking the conductive side of FTO glass

7. Glass rod is used to perform doctor blade method with solution TiO_2 above the FTO glass until the solution become thin.



Figure 3. 60: A drop of TiO_2 on the FTO glass and using Doctor Blade Method

8. Therefore, the sketch having the various of area (LxW) and random sizing.

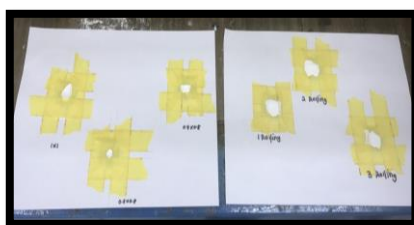


Figure 3. 61: Various area of FTO glass

9. Used the technique by hand to extract the dyes, to crush the raw materials (fruit/ flower/ leaf/ midrib etc.).
10. After that, setting the hot plate such as down below and then placed the FTO glass lining with aluminum that was rolled.



Figure 3. 62: Baked FTO glass 450°C for 45 minutes for first batch

11. Bake the FTO glass coated with TiO_2 until 45 minutes.
12. Placed out the FTO glass from hot plate and then leave it for 5 minutes to cold down.
13. Filter the juices (dyes) from the fruit crush and pour into petri dish. Then, pour dyes into petri dish and immersed the FTO glass



Figure 3. 63: Immerse the FTO glass into dyes extraction first batch

14. And then, wrap with aluminum foil in order to avoid oxidation for 24 hours.



Figure 3. 64: Keep FTO glass first batch into dark places

15. After 24 hours immerse, take it FTO glass out from petri dish and observe the active area.



Figure 3. 65: FTO glass after take it out immerse first batch

16. Continue with the part of counter electrode meanwhile should shaded with graphite (carbon from pencil).

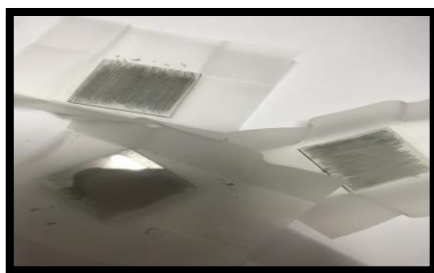


Figure 3. 66: Shaded Counter electrode for first batch with graphite

17. Assembly the combination of photoelectrode and counter electrode.

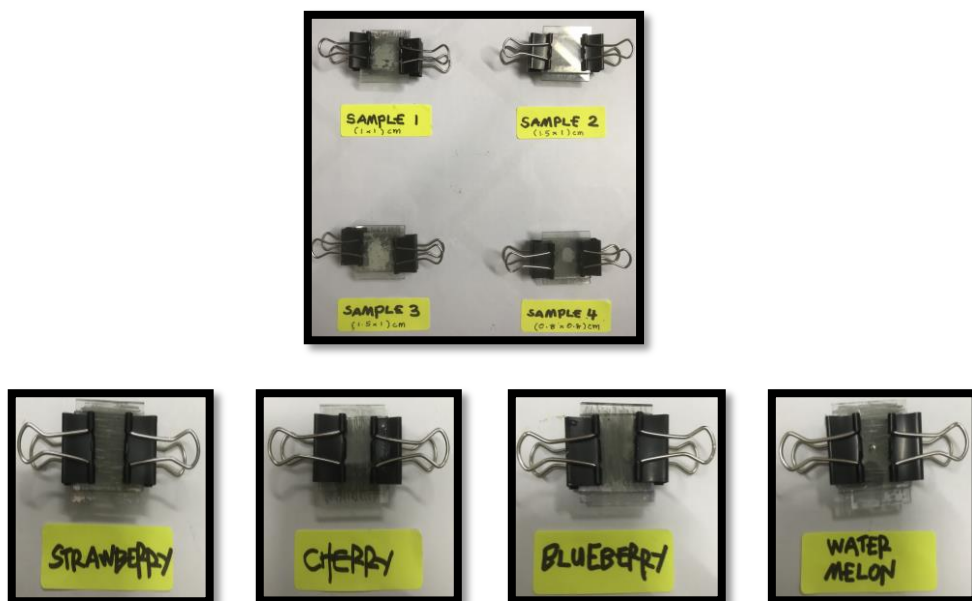


Figure 3. 67: Assembly the Photoelectrode & Counter Electrode for First Batch

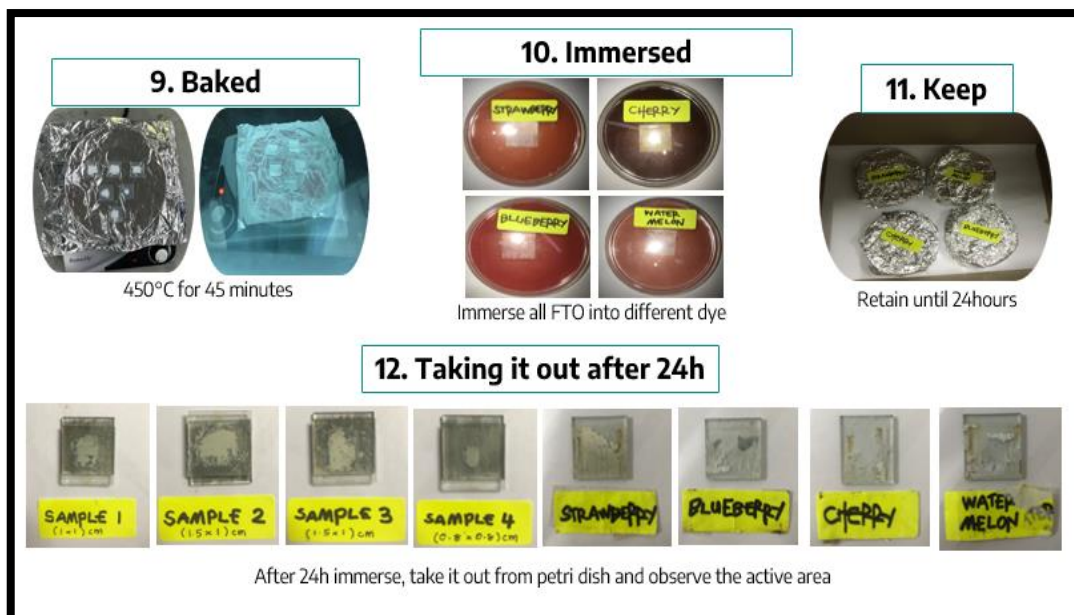
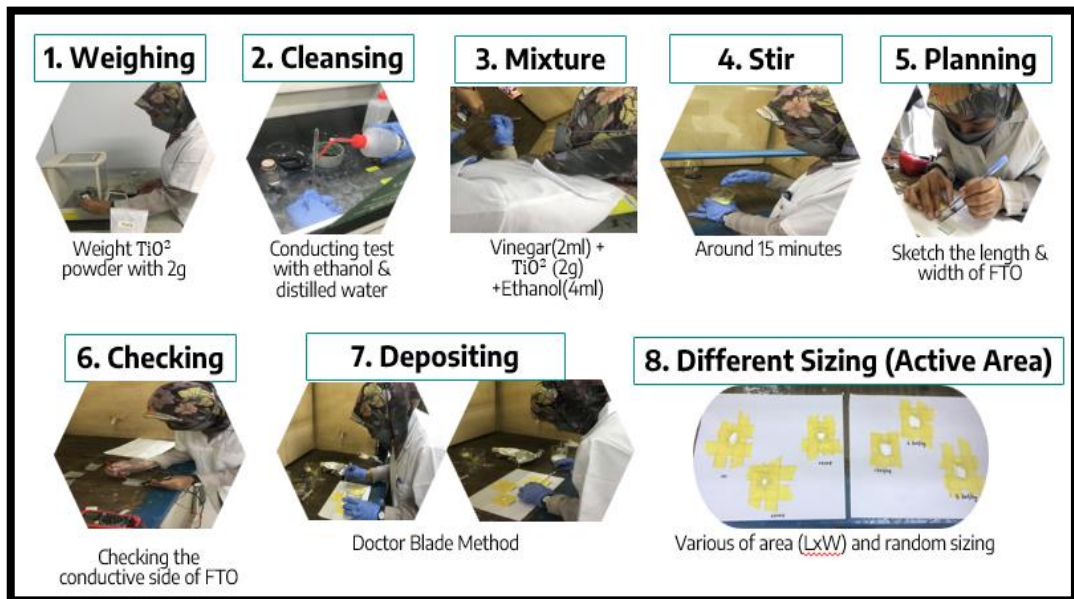
18. Finally, wrapping the combination of both to avoid from any light.



Figure 3. 68: Dye-sensitized solar cells for First Batch fabricated

3.7.2 Summarize for Flow Whole Procedure for First Batch

The flow process for whole procedure preparation of dye-sensitized solar cells for the extraction fruit first batch has been shown as the figure below:



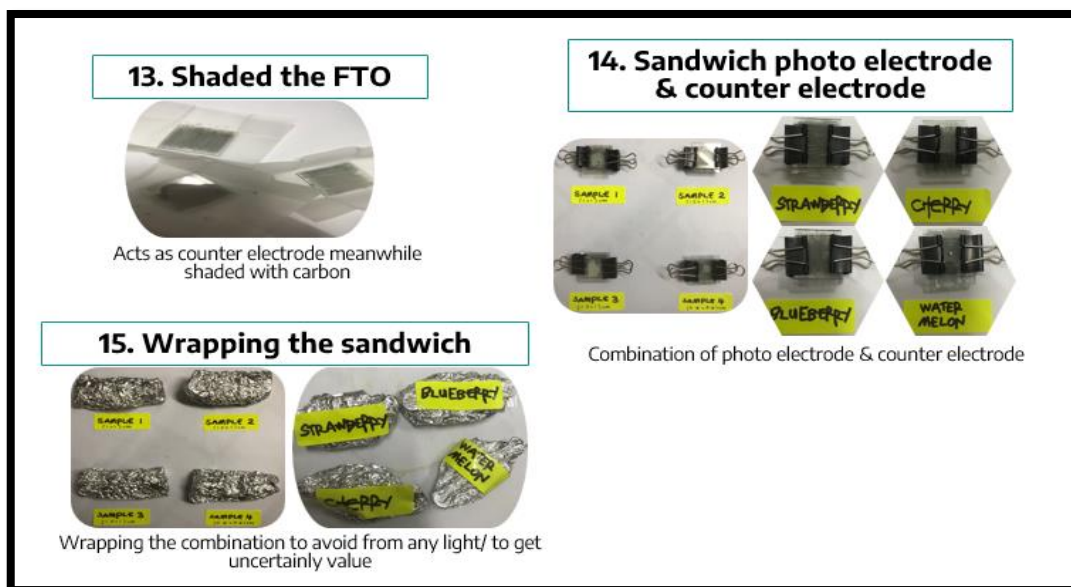


Figure 3. 69: The flow whole procedure DSSC for First Batch

3.7.3 DSSC for Second Batch

1. Preparation of Titanium Oxide (TiO_2) is done in fume hood chamber. 2g of TiO_2 powder is weighing by using analytical balance.



Figure 3. 70: Weighing TiO_2 powder by Analytical Balance for second batch

2. Before using the rod glass, wash it with distilled water and ethanol
3. 2gram of TiO_2 powder is added in the beaker with 4ml of ethanol and 2ml of vinegar.



Figure 3. 71: Stir the mixture all together for the second batch

4. Stir the mixture continuously for 15 minutes and let leave at several minute until it achieves equilibrium state.
5. FTO glass consist two sided are differently, hence the thin layer of TiO_2 paste will be coated on the conductive side of FTO glass.
6. Cylindrical rod will be used in Doctor Blade Method in order to apply the thin layer of TiO_2 paste on the conductive side of FTO glass.

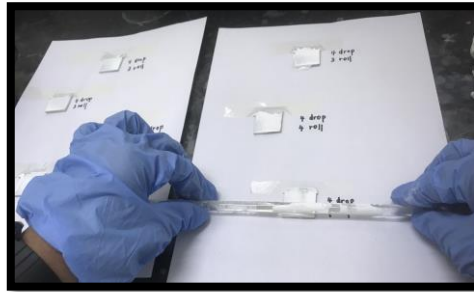


Figure 3. 72: Doctor Blade Method for second batch

7. Step of the rolling has been recording how many times rolling above the thin paste TiO_2 .

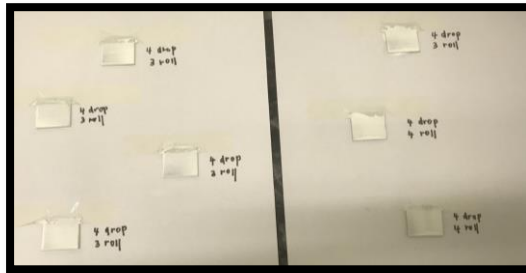


Figure 3. 73: Record how many rolling is apply

8. Bake the FTO glass that coated with TiO_2 until 45 minutes with setting the hot plate 450°C . The color of TiO_2 glass will change from white to yellow to white again.



Figure 3. 74: Baked FTO glass 450°C for 45 minutes for Second Batch

9. After that, dye solution sample are transfer into petri dish before placing the TiO_2 glass. Immerse the TiO_2 glass into dye solution carefully.

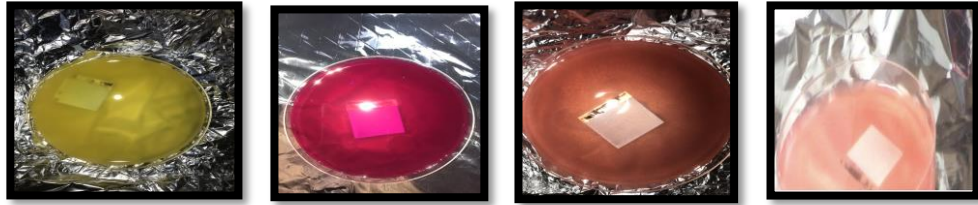


Figure 3. 75: Immerse the FTO glass into dyes extraction second batch

10. And then, wrap with aluminum foil in order to avoid oxidation for 24 hours.



Figure 3. 76: Keep FTO glass Second Batch into dark places

11. After 24 hours immersion the TiO_2 glass will be clean with distilled water. Clean carefully by use dropper to avoid any crack of TiO_2 thin layer.



Figure 3. 77: Rinse and clean the debris at FTO glass for Second Batch

12. And then, after 24 immerse the FTO glass, take it out from petri dish and observe the active area TiO_2 .

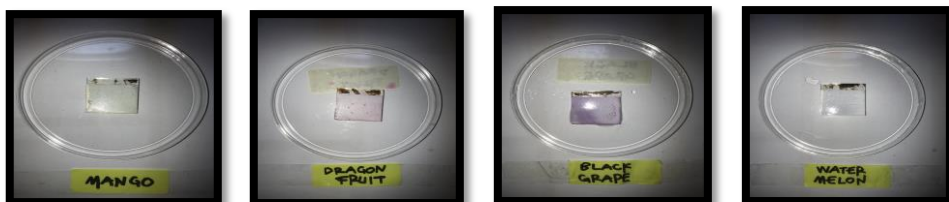


Figure 3. 78: FTO glass after take it out immerse Second Batch

13. Continue with the part of counter electrode meanwhile should shaded with graphite (carbon from pencil).



Figure 3. 79: Shaded Counter Electrode for Second Batch with graphite

14. Then, both are the glasses will be bind by using the clip



Figure 3. 80: Assembly the Photoelectrode & Counter Electrode for Second Batch

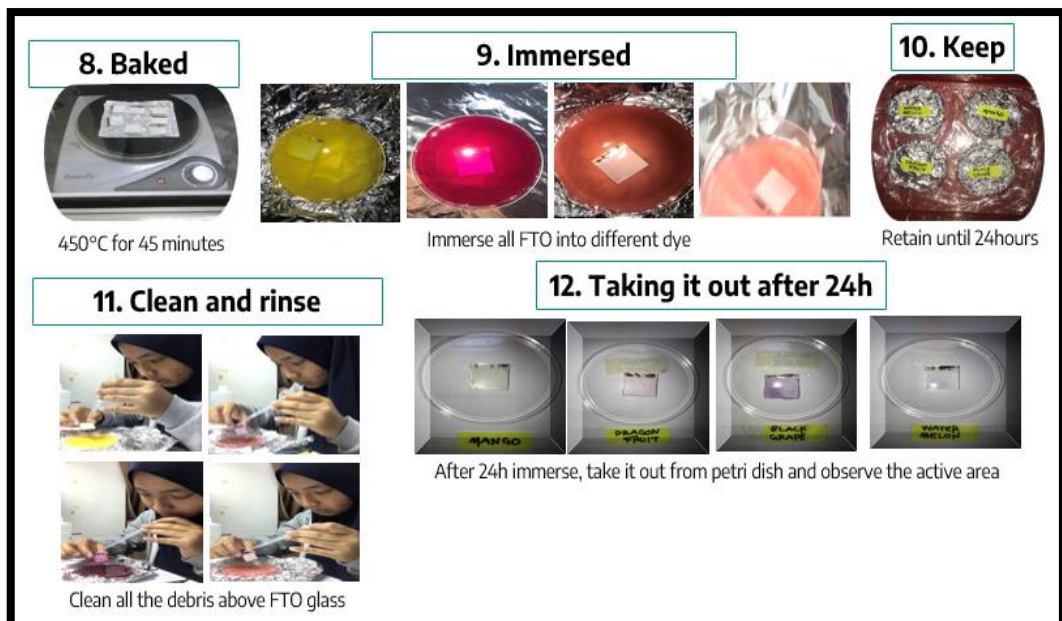
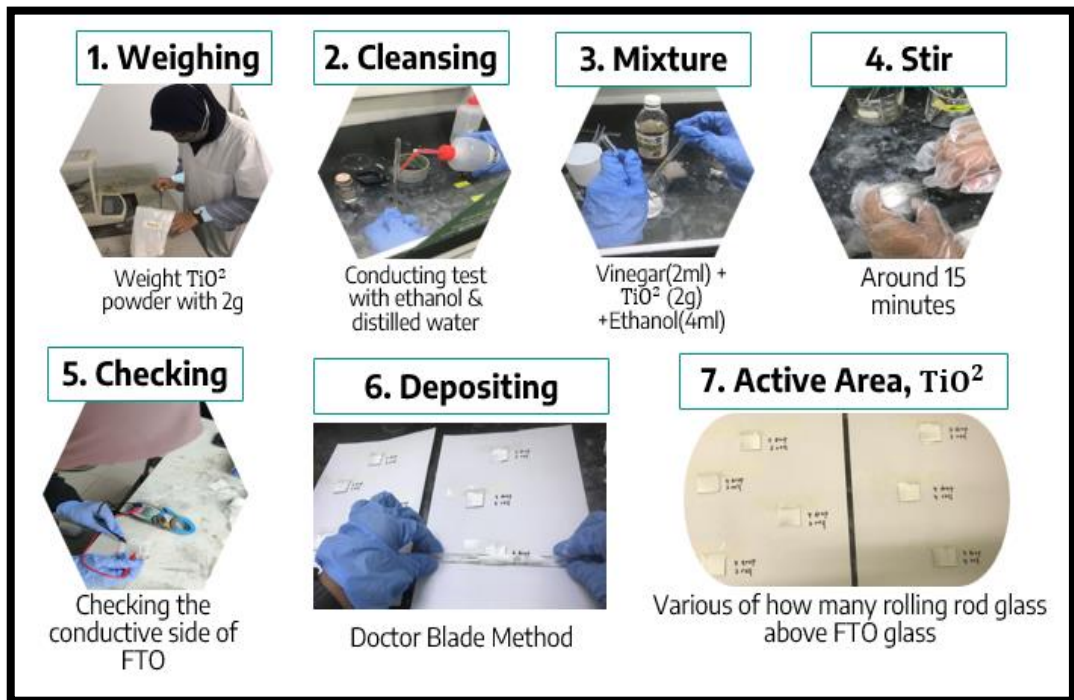
15. Lastly, dye-sensitized solar cells have been fabricated.



Figure 3. 81: Dye-sensitized solar cells for Second Batch fabricated

3.7.4 Summarize for Flow Whole Procedure for Second Batch

The flow process for whole procedure preparation of dye-sensitized solar cells for the extraction fruit first batch has been shown as the figure below:



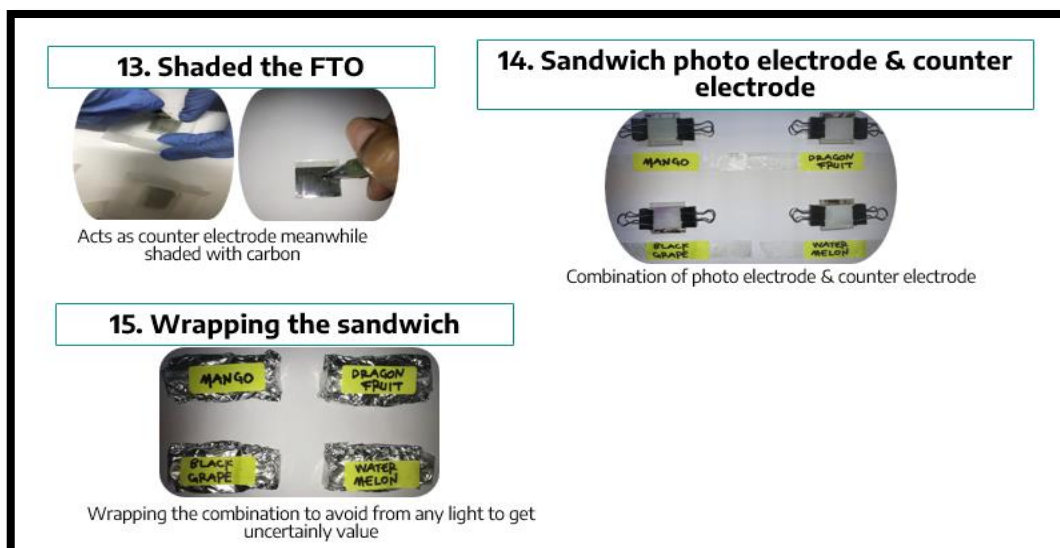


Figure 3. 82: The flow whole procedure DSSC for Second Batch

3.8 Measurement of Current-Voltage Characteristics

1. Prepared a several sample of dye-sensitized solar cells that have been fabricated before experimental.



Figure 3. 83: Several sample of Dye-Sensitized Solar Cells

2. A drop of electrolyte which is Potassium Iodide (KI) is added in between two glass TiO_2 glass and carbon glass before performing each measurement.



Figure 3. 84: A drop of Potassium Iodide

3. Conducting the measurement of current-voltage for several sample dye-sensitized solar cells under shading area, direct sunlight and uses of different equipment of solar to observing the result comparison of measurement and make a hypothesis about this study.

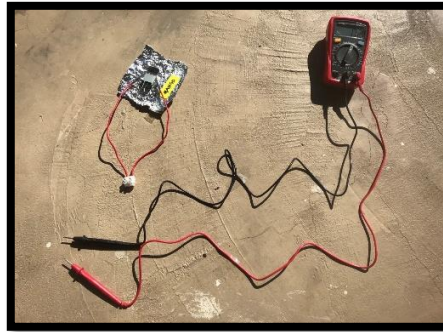


Figure 3. 85: Measurement of Voc under shading area



Figure 3. 86: Measurement of Voc under direct sunlight



Figure 3. 87: Measurement of Voc by uses differences equipment solar



Figure 3.88: Measurement of voltage at load

4. Record all the data and will analyse each of the measurement from the output. Since, all the measurement have different places of measurement, the uses of differences equipment and the differences of sample dye-sensitized solar cells.
5. In additional, for the measurement of voltage at load that have some uses of variable resistor that can varied the measurable value of resistor from the range 1k to 500k Ω . In fact, the result of that measurement will come out the many differences value depending the variable resistor.

CHAPTER 4

RESULTS AND DISCUSSION

4.1 Graphical of Absorbance by Ultraviolet-Visible Spectrophotometer

4.1.1 First Batch Graph of Absorbance versus Wavelength

Table 4. 1: The data Strawberry of three sample with different dilution

Wavelength(nm)	Pure	(1:2)	(1:3)
400	5	1.956	1.349
420	3.875	1.88	1.304
440	3.801	1.808	1.242
460	3.509	1.805	1.237
480	5	1.923	1.276
500	5	1.977	1.288
520	5	1.812	1.19
540	5	1.542	1.001
560	3.268	1.369	0.87
580	2.629	1.27	0.794
600	2.349	1.212	0.754

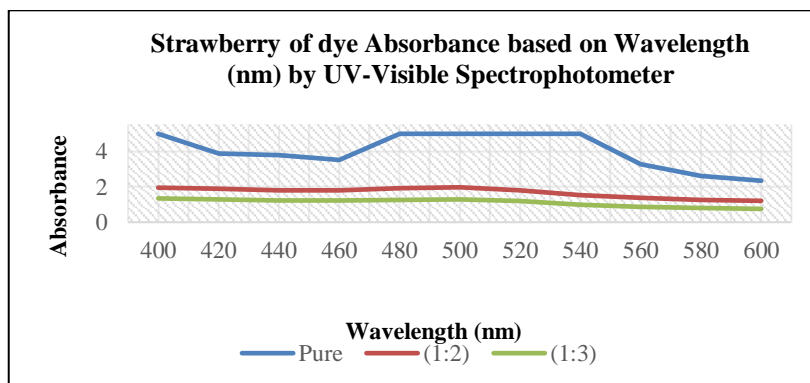


Figure 4. 1: The graph Strawberry of three sample with different dilution

Table 4. 2: The data Strawberry of the actual value and the value dilution

Sample True Value	Sample (1:3)
5.396	1.349
5.216	1.304
4.968	1.242
4.948	1.237
5.104	1.276
5.152	1.288
4.76	1.19
4.004	1.001
3.48	0.87
3.176	0.794
3.016	0.754

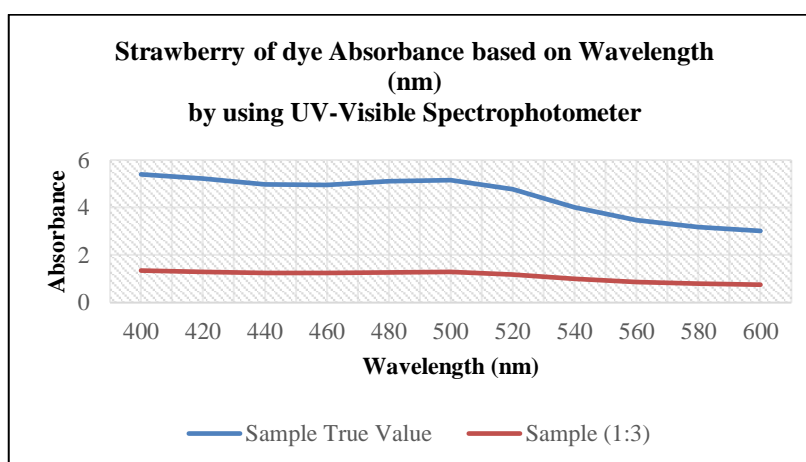


Figure 4. 2: The graph Strawberry of the actual value and value of dilution

1. Based on the graph Strawberry, the absorption peak (1:3) occurring around 500nm with absorption wavelength at the range between 460nm to 520nm.
2. Furthermore, the ratio (1:3) are chosen because it has the lowest value among the other ratio. Hence, when the lowest value achieves, it will be the great value in absorption UV-Visible Spectrophotometer.
3. Lastly, for the measurement absorbance versus wavelength by dyes extraction Blueberry, Cherry and Water Melon for the first batch has unmeasurable value and analyse.

4.1.2 Second batch Graph of Absorbance versus Wavelength

Table 4. 3: The data Mango of two sample with different dilution

Wavelength(nm)	Pure	(1:2)
350	5	2.412
400	5	2.265
450	5	2.299
500	5	1.987
550	2.501	1.584
600	2.414	1.461

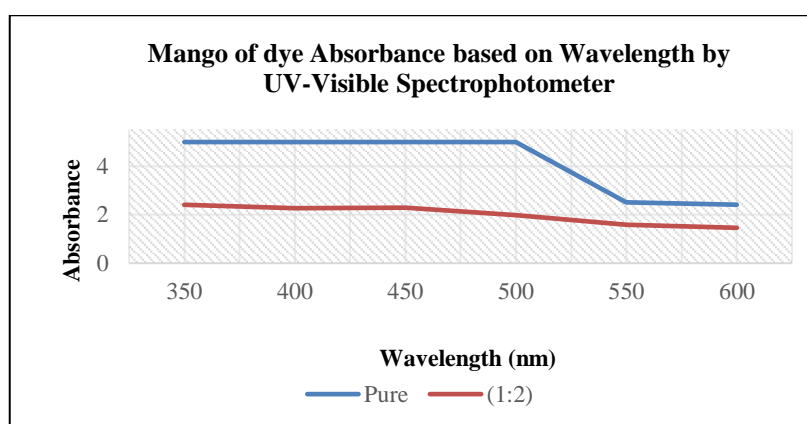


Figure 4. 3: The graph Mango of two sample with different dilution

Table 4. 4: The data Mango of the actual value and the value dilution

Sample True Value	Sample (1:2)
7.236	2.412
6.795	2.265
6.897	2.299
5.961	1.987
4.752	1.584
4.383	1.461

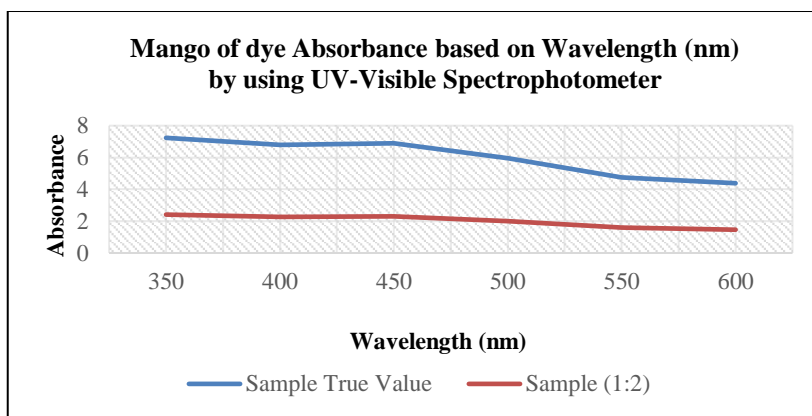


Figure 4. 4: The graph Mango of the actual value and the value dilution

1. Based on the graph Mango, the absorption peak of sample (1:2) occurring around 450nm with absorption wavelength at the range between 350nm to 600nm.

Table 4. 5: The data Dragon fruit of two sample with different dilution

Wavelength(nm)	Pure	(1:2)
250	5	5
300	5	5
350	5	2.742
400	5	1.819
450	5	2.621
500	5	5
550	5	5
600	5	2.113
650	1.955	0.918

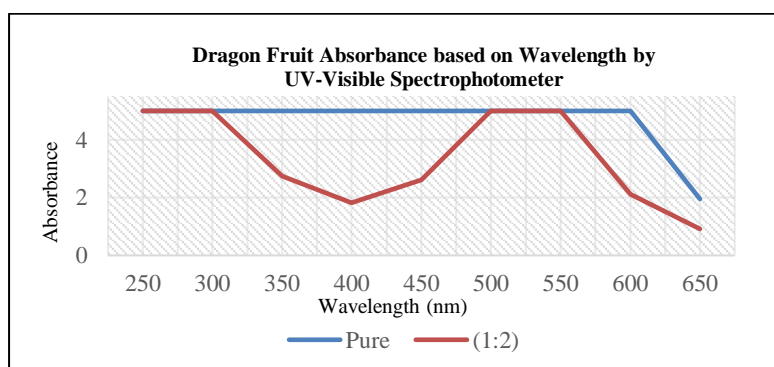


Figure 4. 5: The graph Dragon Fruit of two sample with different dilution

Table 4. 6: The data Dragon Fruit of the actual value and the value dilution

Sample True Value	Sample (1:2)
15	5
15	5
8.226	2.742
5.457	1.819
7.863	2.621
15	5
15	5
6.339	2.113
2.754	0.918

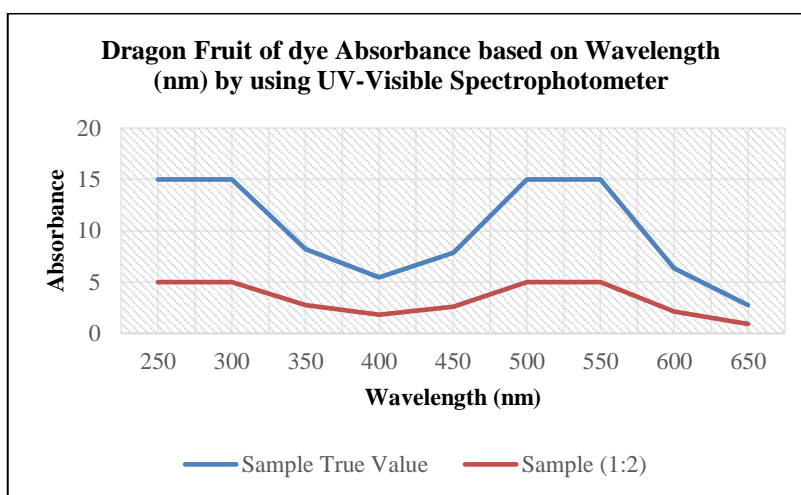


Figure 4. 6: The graph Dragon Fruit of the actual value and the value dilution

1. Based on the graph Dragon Fruit, the absorption peak of sample (1:2) occurring around 300nm, 500nm to 550nm with absorption wavelength at the range between 250nm to 650nm.

Table 4. 7: The data Black Grapes of two sample with different dilution

Wavelength(nm)	Pure	(1:2)
400	5	1.998
420	5	1.88
440	5	1.813
460	4.254	1.738
480	5	1.719

500	5	1.71
520	5	1.672
540	5	1.6
560	5	1.504
580	5	1.396
600	3.136	1.304

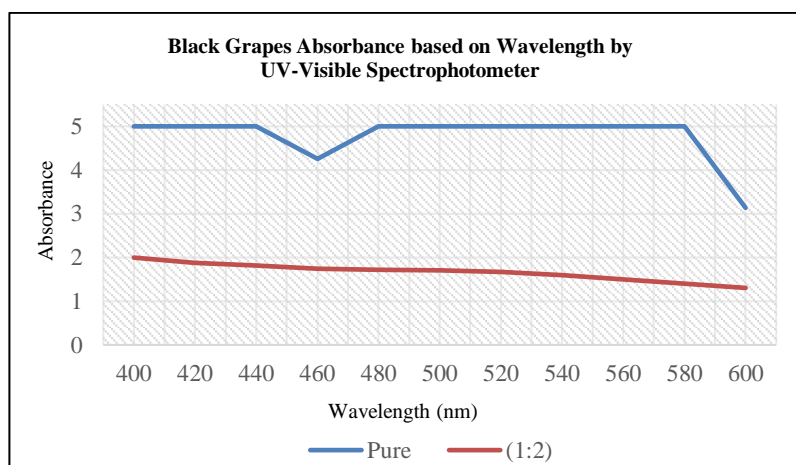


Figure 4. 7: The graph Black Grapes of two sample with different dilution

Table 4. 8: The data Black Grapes of the actual value and the value dilution

Sample True Value	Sample (1:2)
5.994	1.998
5.64	1.88
5.439	1.813
5.214	1.738
5.157	1.719
5.13	1.71
5.016	1.672
4.8	1.6
4.512	1.504
4.188	1.396
3.912	1.304

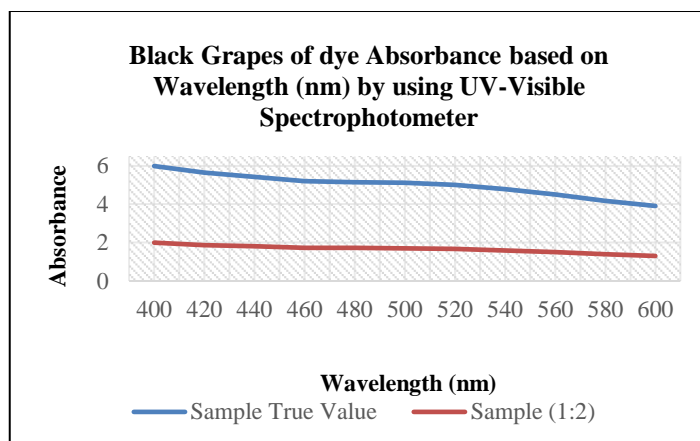


Figure 4. 8: The graph Black Grapes of the actual value and the value dilution

1. Based on the graph Black Grapes, the absorption peak of the sample (1:2) occurring around 525nm with absorption wavelength at the range between 400nm to 600nm.

Table 4. 9: The data Water Melon of two sample with same dye without dilution

Wavelength(nm)	Sample 1	Sample 2
350	1.795	1.78
400	1.679	1.578
450	0.876	0.755
500	0.998	0.942
550	0.678	0.576

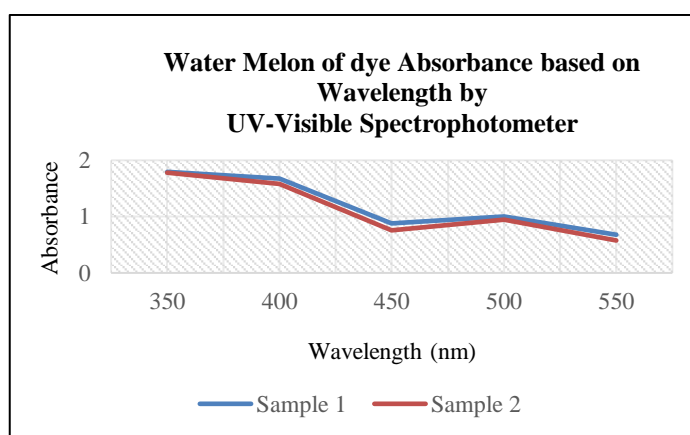


Figure 4. 9: The graph Water melon of two sample with same dye without dilution

1. Based on the graph Water Melon, the absorption peak of sample occurring around 400nm with absorption wavelength at the range between 350nm to 550nm.
2. Therefore, in second batch of the measurement all the dyes extraction is measure able compare to the first batch has some dyes are unmeasurable.

4.1.3 Summarized of Measurement Absorbance

Table 4. 10: The data for overall measurement absorbance

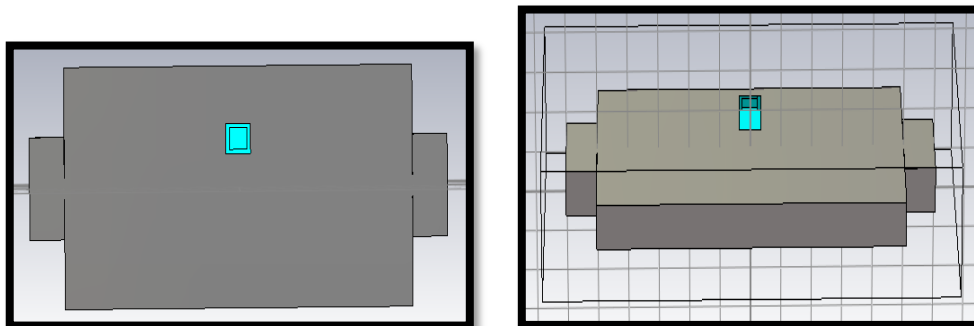
Fruit	References		Result	
	Wavelength	Absorbance	Wavelength	Absorbance
Strawberry	400nm to 600nm	520nm	460nm to 520nm	500nm
Mango	350nm to 600nm	475nm	400nm to 520nm	450nm
Dragon Fruit	250nm to 650nm	535nm	300nm to 570nm	525nm
Black Grapes	400nm to 600nm	530nm	470nm to 530nm	525nm
Water Melon	350nm to 550nm	520nm	400nm to 550nm	400nm

1. Based on the table above, Dragon Fruit and Black Grapes have a highest peak value of absorption by a solution which is dyes.
2. This is because Dragon Fruit and Black Grapes have a highest concentration in dyes extraction.

4.2 Software CST Studio Suite 2019

CST Studio Suite 2019 are functioning as designing, analysing and optimizing an electromagnetic (EM). Hence, in this study are conducting several dyes extracted to observe the output from this software.

4.2.1 Dimensioning of Resonator



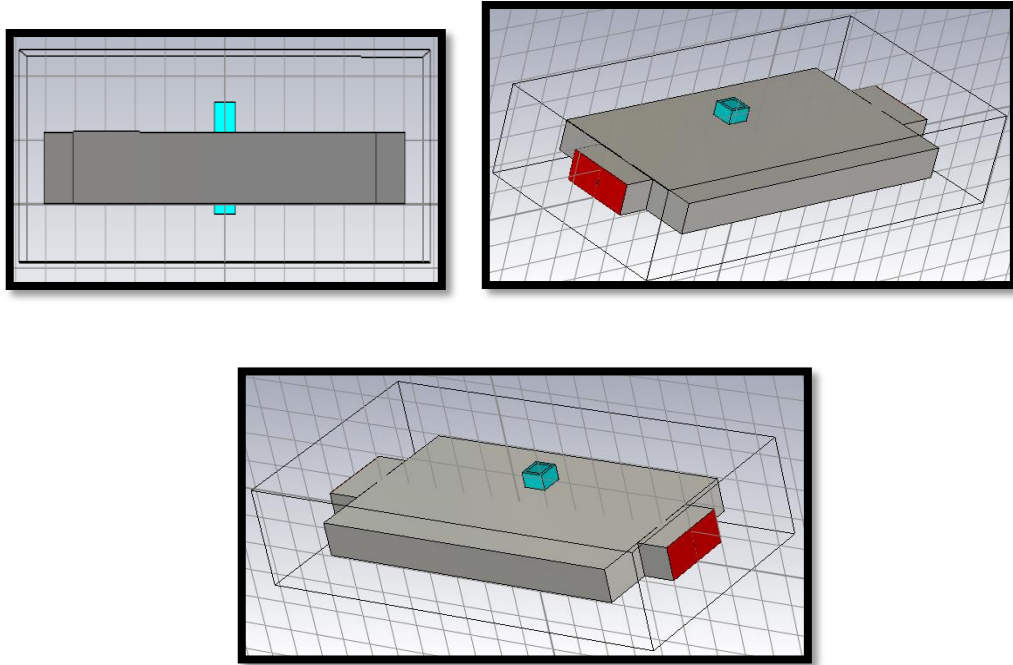


Figure 4. 10: The design of Sensor Resonator

4.2.2 Measurement of Resonator

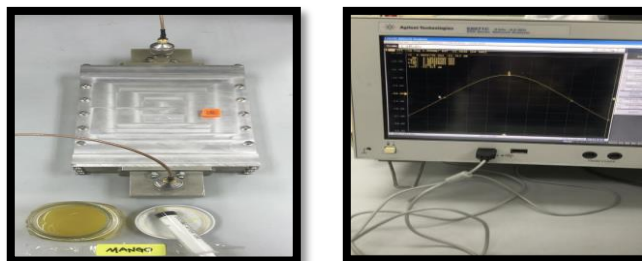


Figure 4. 11: Measurement Permittivity with Material Dye

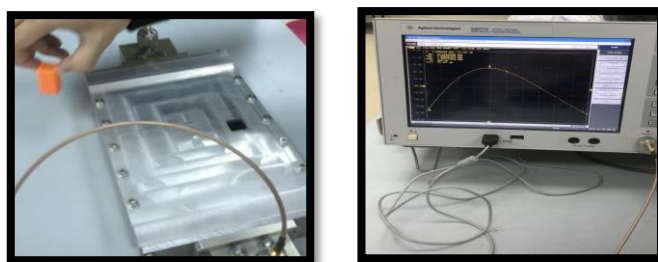


Figure 4. 12: Measurement Permittivity with Material Air

Table 4. 11: The data from Network Analyzer Material Dye & Air

	Mango		Water Melon		Dragon Fruit		Black Grapes	
	Air	Dye	Air	Dye	Air	Dye	Air	Dye
Bw	3.1279MHz	31.8206MHz	3.1284MHz	28.1322MHz	3.1291MHz	31.8306MHz	3.1297MHz	30.7306MHz
Cent	4.9955GHz	5.0119GHz	4.9957GHz	5.0135GHz	4.9962GHz	5.0114GHz	4.9965GHz	5.0129GHz
Low	4.9939GHz	4.9966GHz	4.9942GHz	4.9971GHz	4.9945GHz	4.9932GHz	4.9946GHz	4.9956GHz
High	4.9971GHz	5.0273GHz	4.9974GHz	5.0285GHz	4.9978GHz	5.0283GHz	4.9981GHz	5.0284GHz
Q	1597.1	163.09	1603.4	162.15	1611.1	163.32	1615.4	163.37
Loss	-11.311 dB	-32.120 dB	-11.316 dB	-33.116 dB	-11.322 dB	-32.120 dB	-11.325 dB	-32.154 dB

Table 4. 12: The calculation of differences frequency

Fruit	Frequency High (Material Dye)	Frequency Low (Material Air)	Differences
Mango	5.0273GHz	4.9939GHz	0.0334
Water Melon	5.0285GHz	4.9942GHz	0.0343
Dragon Fruit	5.0283GHz	4.9945GHz	0.0338
Black Grapes	5.0284GHz	4.9946GHz	0.0338

Table 4. 13: The calculation of differences Q factor of a resonant

Fruit	Q Factor (Material Dye)	Q Factor (Material Air)	Differences
Mango	163.09	1597.1	5.5054m
Water Melon	154.23	1124	5.5941m
Dragon Fruit	201.51	1868.3	4.4273m
Black Grapes	190.17	1615.4	4.6394

Table 4. 14: The data excel from CST Studio Suite 2019

Fruit	Low Frequency	Centre Frequency	High Frequency	Resonant Frequency	Q Factor
Mango	5.002	5.0026	5.0046	5.0026	1924.076923
Water Melon	5.0023	5.0033	5.0044	5.0033	2382.52381
Dragon Fruit	5.0025	5.0033	5.0042	5.0033	2943.117647
Black Grapes	5.0022	5.0033	5.0044	5.0033	2274.227273

4.2.3 Summarized of Measurement Permittivity

Table 4. 15: The data for Overall Measurement Permittivity

Fruit	References		Result	
	Permittivity, ϵ	Loss	Permittivity, ϵ	Loss
Mango	79	30	78	29
Water Melon	69	38	68	27
Dragon Fruit	89	34	88	34
Black Grapes	75	30	73	31

1. Resonant Frequency is determined by overall physical dimension Resonator.
2. Measurement of Resonator based on Dragon Fruit is the highest Permittivity, ϵ and Loss among the other fruit.
3. Measurement of Resonator based on Water Melon is the lowest Permittivity, ϵ and Loss among the other fruit.

4.3 Summarize of Completeness of Titanium Oxide on FTO glass

This part is most important element that required the successfully the dye-sensitized solar cell experimental. Hence, when the completeness is not fully recovered the measurement of current-voltage are affected as well.

4.3.1 Completeness TiO_2 for the First Batch



Figure 4. 13: Before immerse from First Batch



Figure 4. 14: After immerse from First Batch

1. Foremost, in this research and analysing the experimental dye-sensitized solar cell the completeness of TiO_2 for the first batch have some issue.

2. This is because, the short time taken to baked the FTO glass, the hot plate is not functioning very well. In additional, all the apparatus for the conducting test are not cleansing very done.
3. Therefore, the completeness of the TiO₂ for the first batch are not fully achievement.

4.3.2 Completeness TiO₂ for the Second Batch

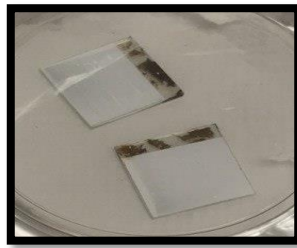


Figure 4. 15: Before immerse from Second Batch

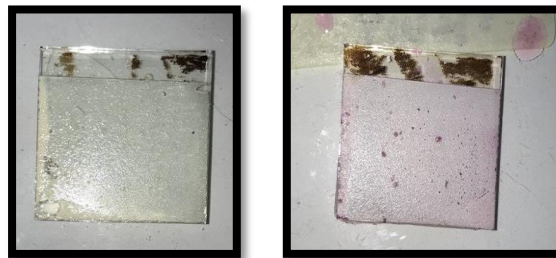


Figure 4. 16: After immersed from Second Batch

1. Consequently, in this research and analysing the experimental dye-sensitized solar cell the completeness of TiO₂ for the second batch there is no have some issue.
2. Since, the time taken to baked the FTO glass are exactly 450°C, all the apparatus for the conducting test are cleansing very well, step of depositing is recorded and solution in TiO₂ are concentrated milky look likes.
3. Therefore, the completeness of the TiO₂ for the second batch are fully achievement compare completeness of the TiO₂ first batch.

4.4 Measurement of Open-Circuit Voltage, V_{oc}

After dye-sensitized solar cell fabricated, the next process will compute with measurement of open circuit voltage, V_{oc} that included the multimeter to measure the output. Therefore, there are several experiments are conducting to observe and analyse the result.

4.4.1 First Batch on Open Circuit Voltage, V_{oc}

Measurement open circuit voltage, V_{oc} are experimental with the acquirer of time of measure from 6:00pm to 6:25pm that sky condition at that time are late evening. In additional, an expected irradiance is estimate around 180 to 280 w/m^2 .



Strawberry, $V_{oc} = 46.7mV$



Blueberry, $V_{oc} = 24.5mV$



Cherry, $V_{oc} = 46.7mV$



Water Melon, $V_{oc} = 24.5mV$

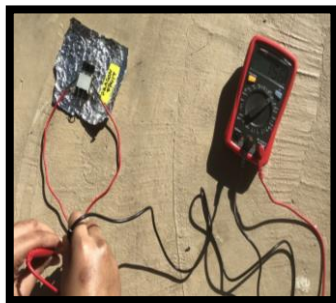
Figure 4. 17: Open Circuit Voltage for First Batch

4.4.2 Second Batch on Open Circuit Voltage, Voc

Thereby, in second batch the completeness of TiO_2 are fully recovered on the FTO glass. Therefore, has several conditions has been testing to observe the result and making the comparison between of that.

4.4.2.1 Condition 1 from Second Batch Sample

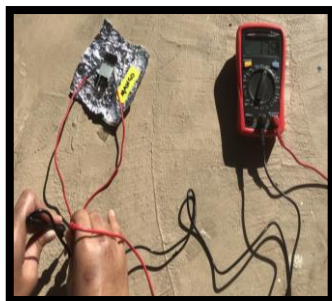
Measurement open circuit voltage, Voc are experimental with the acquirer of time of measure from 4:00pm to 4:25pm that sky condition at that time are late evening. For this sample are conducting at shading area with building at FTKEE. In additional, an expected irradiance is estimate around 180 to 280 w/m^2 . Regarding the result measurement open circuit voltage, measurement under shading area are achieved the lowest measurement compare to the under direct sunlight. Since, under direct sunlight there is no block from surrounding compare the shading area.



Dragon Fruit, Voc = 156mV



Black Grapes, Voc = 24.7mV



Mango, Voc = 156mV

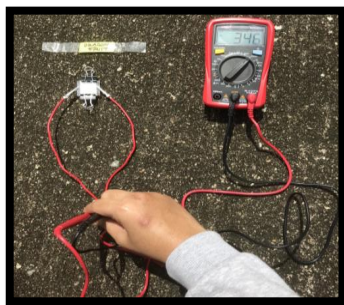


Water Melon, Voc = 24.7mV

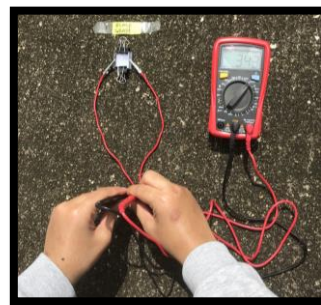
Figure 4. 18: Measurement Open Circuit Voltage for Condition 1

4.4.2.2 Condition 2 from Second Batch Sample

Measurement open circuit voltage, V_{oc} are experimental with the acquirer of time of measure from 2:00pm to 2:55pm that sky condition at that time are clear sky. For this sample are conducting at under direct sunlight in front hostel. In additional, an expected irradiance is estimate around 450 to 600 w/m^2 . Based on the result, Dragon Fruit has achieved a higher open circuit voltage among the other while Water Melon has achieved a lowest open circuit voltage among the other. Since, Dragon Fruit has a higher concentration in anthocyanin-based compare to the Water Melon.



Dragon Fruit, $V_{oc} = 346mV$



Black Grapes, $V_{oc} = 343mV$



Mango, $V_{oc} = 173.7mV$



Water Melon, $V_{oc} = 57.5mV$

Figure 4. 19: Measurement Open Circuit Voltage for Condition 2

4.4.2.3 Condition 3 from Second Batch Sample

Measurement open circuit voltage, V_{oc} are experimental with the acquirer of time of measure from 2:15pm to 3:00pm that sky condition at that time are clear sky. For this sample are conducting with several equipment of solar to observe the measurement form different dyes extraction. In additional, an expected irradiance is estimate around 450 to

600 w/m². Based on the result, Black Grapes has achieved a higher open circuit voltage among the other while Water Melon has achieved a lowest open circuit voltage among the other. Since, Black Grapes has a higher concentration in anthocyanin-based compare to the Water Melon.

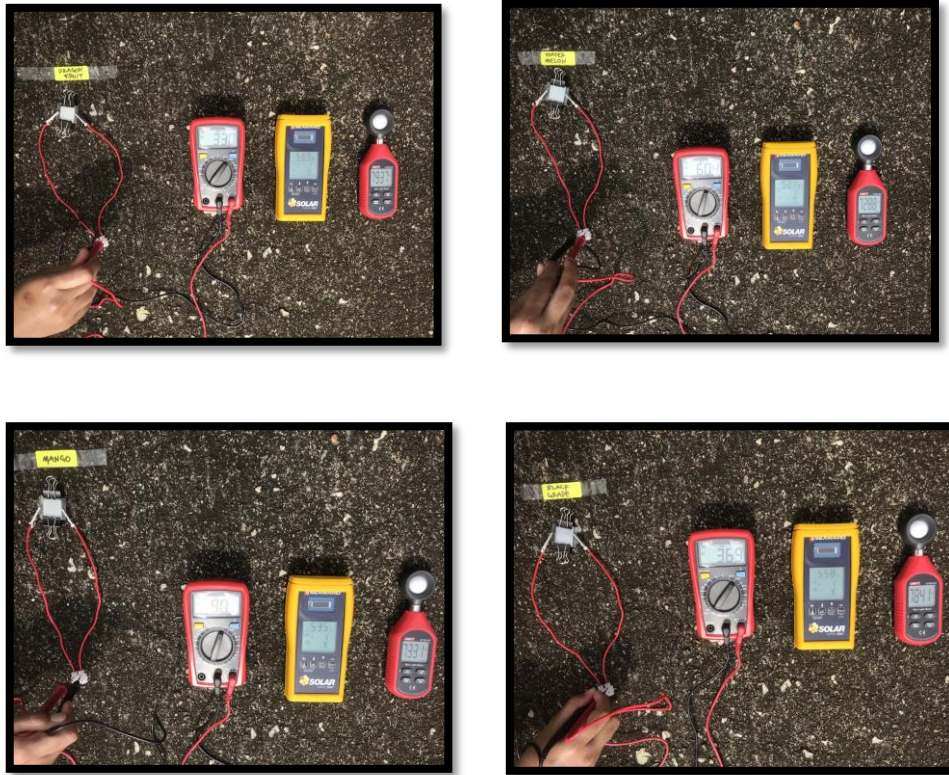


Figure 4. 20: Measurement Open Circuit Voltage with difference equipment Solar

4.4.3 Summarize for Measurement Dye-sensitized Solar Cells

Table 4. 16: Differences value Voc depends on the difference's places measured

Fruit	Voltage Open Circuit, Voc		Time Measure
	Condition 1 (Shading with building at FTKEE)	Condition 2 (Under direct sunlight in front of hostel)	
Dragon Fruit	156mV	346mV	2:15pm to 2.25pm
Black Grapes	24.7mV	343mV	2:30pm to 2:40pm
Mango	17.9mV	173.7mV	2:00pm to 2:10pm
Water Melon	13.5mV	57.5mV	2:45pm to 2:55pm

1. The value of open circuit voltage without shading is higher compare with shading area.
2. The time measure is contributing to the measurement dye-sensitized solar cells.

Table 4. 17: Differences value Voc depend on differences equipment

Fruit	Condition 3 (Open Circuit Voltage, Voc)	Solar Irradiance (w/m ²)	Lux Meter	Time Measure
Dragon Fruit	330mV	569	79370	2:15pm to 2:25pm
Black Grapes	369mV	558	78410	2:30pm to 2:40pm
Mango	90mV	535	73310	2:45pm to 2:50pm
Water Melon	60.4mV	521	72880	2:55pm to 3:00pm

1. In conclude, the higher value of solar irradiance the higher the value voltage open circuit, Voc.

4.4.4 Open Circuit Voltage at Load

Table 4. 18: The value of Current-Voltage Characteristics

Sample of DSSC	Resistor (Ω)	Voltage (mV)	Current (mA)
Black Grapes	3.3	297	90
	305	305	1
	17.99k	307	17.065
	122.8k	318	2.5896
	180.5k	329	1.8227
Dragon Fruit	3.3	54.5	0.017
	330	47	0.000142
	18.87k	41.3	0.00000219
	20.9k	25.5	0.00000122
	181.3k	16.4	0.00000009
Mango	3.3	74.6	0.0226
	365	71	0.000195
	19.06k	78.9	0.00000414
	121.6k	75.7	0.000000622
	181.5k	77.8	0.000000428
Water Melon	3.3	75.9	0.023
	314	71.9	0.000229
	18.93k	71.2	0.00000376
	121.3k	73.5	0.000000605
	181.9k	78.9	0.000000433

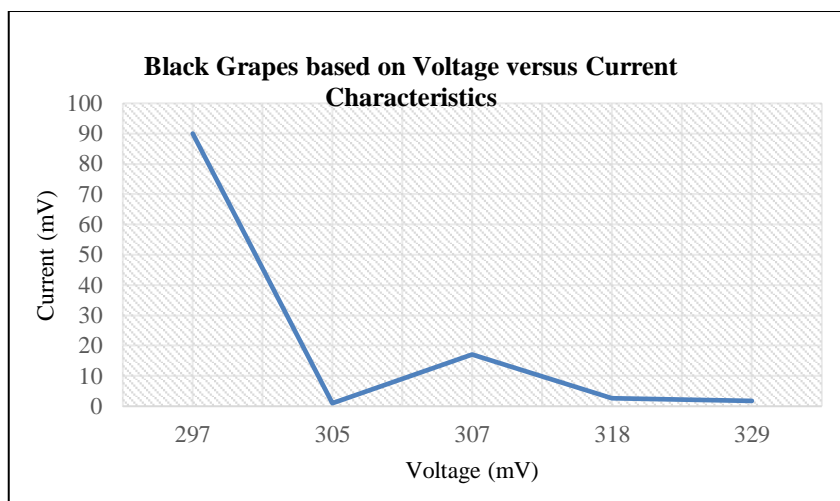


Figure 4. 21: The value of Black Grapes in I-V characteristics

4.5 Summarize of Measurement Project

Table 4. 19: Summarize of the Measurement Project

Fruit	Measurement UV-Vis Spectrophotometer	Measurement Resonator		Voltage at load (mV)			Measurement of DSSC	
	Maximum Value of Absorbance	Permittivity, ϵ	Loss	Resistor (Ω)	Voltage (mV)	Current (A)	Voltage Open Circuit (Voc)	Solar Irradiance $\frac{W}{m^2}$
Black Grapes	5.994	88	34	3.3	297	90m	369mV	558
				305	305	1n		
				17.99k	307	17.0650m		
				122.8k	318	2.5896m		
				180.5k	329	1.8227m		
Dragon Fruit	8.226	73	31	3.3	310	93.9394m	330mV	569
				330	316	957.5758m		
				18.87k	318	16.8521m		
				20.9k	324	15.5024m		
				181.3k	330	1.8202m		
Mango	7.236	78	29	3.3	72	21.8182m	90mV	535
				365	77	210.9589m		
				19.06k	81	4.2497m		
				121.6k	87	0.7155m		
				181.3k	93	0.3124m		
Water Melon	1.78	68	27	3.3	30	15.1515m	60.4mV	521
				314	33	168.7898m		
				18.93k	37	3.0111m		
				121.3k	61	0.5029m		
				181.9k	67	0.3683m		

1. From the extracted dyes, Dragon Fruit is the highest the Permittivity value, that correlated with performance current-voltage characteristics.
2. Permittivity value effected the measurement of dye's absorption that Dragon Fruit is the achieve the maximum value of absorbance.

CHAPTER 5

CONCLUSION AND RECOMMENDATION

This experiment was conducted objectively to elucidate an effect of material permittivity based on physical dimension resonator by the dielectric constant of the material that related with the measurement of Resonator and Waveguide to achieves the output of measurement permittivity, ϵ . Therefore, for the measurement of current-voltage performance are affected regarding to the dye-sensitized solar cells based on several extracted dyes' fabrication. Hence, there are various experimental are conducting such as measurement of absorbance by using Ultraviolet-Visible Spectrophotometer, measurement of permittivity by using the Network Analyzer in additional uses the software of CST Studio Suite 2019 and measurement of open circuit voltage, V_{oc} based on several condition to achieves an objective in this project. Furthermore, an objective of this project is successfully achieved by related to the analyse the relationship between the material's permittivity and dyes' absorption. Consequently, based on the result it is should be further in studies and research of the permittivity measurement related to the extracted varied of the flower that contain the pigment of the various colour and based which in anthocyanin and chlorophyll. Since, the result in this research are about anthocyanin it may be gain the knowledge more into depth the permittivity measurement. It is was recommended to conduct further research on extraction of anthocyanin-based by using vegetables and flower dyes extraction. In order, to research has into another factor type may also increase the high yield anthocyanin-based in concentration. Finally, the correlated with dye-sensitized solar cells are included since that have the extracted regarding various pigment of flower and vegetables.

REFERENCES

- Guiming Fu, Eun Ji Cho, Xiuting Luo, Jungkeun Cha, Ji Hoon Kim, Hyung Woo Lee and Soo Hyung Kim, Enhanced light harvesting in panchromatic double dye-sensitized solar cells incorporated with bilayered TiO₂ thin film-based photoelectrodes, *IEEE Journal of Solar Energy*, VOL. 218, April 2021, Pages 346-353
- Sabastine C. Ezike, Clement N. Hyelnasinyi, Mufutau A. Salawu, John F. Wansah, Amarachukwu N. Ossai and Nnabuike N. Agu, Synergistic effect of chlorophyll and anthocyanin Co-sensitizers in TiO₂-based dye-sensitized solar cells, *IEEE Journal of Surfaces and Interfaces*, VOL.22, February 2021, 100882
- N., Prabavathy, R., Balasundaraprabhu, Arne S. Kristoffersen, G., Balaji, S., Prasanna, K., Sivakumaran, M.D., Kannan, Svein R. Erga and Dhayalan Velauthapillai, Enhanced photostability of anthocyanin dye for increased efficiency in natural dye sensitized solar cells *IEEE Journal of Optik*, VOL.227, February 2021, 166053
- Alfred Blaszczyk, Katarzyna Joachimiak-Lechman, Sylwia Sady, Tomasz Tanski, Marek Szindler and Aleksandra Drygala, Environmental performance of dye-sensitized solar cells based on natural dyes, *IEEE Journal of Solar Energy*, VOL. 215, February 2021, Pages 346-355
- Emre Guzel, Baris Seckin Arslan, Veysel Durmaz, Mert Cesur, Omer Faruk Tutar, Tugba Sari, Mehmet Isleyen, Mehmet Nebioglu and Ilkay Sisman, Photovoltaic performance and photostability of anthocyanins, isoquinoline alkaloids and betalains as natural sensitizers for DSSCS, *IEEE Journal of Solar Energy*, VOL.173, October 2018,Pages 34-41
- Tahmineh Jalali, Parisa Arkian, Malihe Golshan, Mandana Jalali and Shahriar Osfour, Performance evaluation of natural native dyes as photosensitizer in dye-sensitized solar cells, *IEEE Journal of Optical Materials*, VOL.110, December 2020,11041
- Daiyaan Kabir, Taseen Forhad, William Ghann, Balvin Richards, Mohammed M. Rahman, MDd. Nizam Uddin, Md. Refat J. Rakib, Mohammad Hossain Shariare, Faisal I., Dye-sensitized solar cell with plasmonic gold nanoparticles modified photoanode,*IEEE Journal of Nano-Structure & Nano0Objects*, VOL.26, April 2021, 100698
- P.S. Mukherjee, A.K.Das, B. Dutta, A.K. Meikap, Role of silver nanotube on conductivity, dielectric permittivity and current voltage characteristics of polyvinyl alcohol-silver nanocomposite film, *IEEE Journal of Physics and Chemistry of Solids*, VOL. 111, December 2017, Pages 266-273

M.F. Coelho, M.A. Rivas, E.M. Nogueira, T.P. Iglesias, Permittivity of (40nm and 80nm) alumina nanofluids in ethylene glycol at different temperatures, IEEE Journal of Chemical Thermodynamics, VOL.158, July 2021, 106423

S. Mandalunis, P.A. Sorichetti, S.D. Romano, Relative permittivity of bioethanol, gasoline and blends as a function of temperature and composition, IEEE Journal of Fuel, VOL.293, 1 June 2021, 120419

Yang Yu, Yu Zhao, Yu-Long Qiao, Yu Feng, Wei-Li Li, Wei-Dong Fei, Effect of direct-current biasing on the adjustable radio-frequency negative permittivity characteristics of Bi₂SiO₅/multiwall carbon nanotube metacomposites, IEEE Journal of Ceramics International, VOL. 47, Issue 1, 1 January 202, Pages 1389-1398

Toton Haldar, Utkarsh Kumar, B.C. Yadav, V.V. Ravi Kanth Kumar, Effect of direct-current biasing on the adjustable radio-frequency negative permittivity characteristics of Bi₂SiO₅/multiwall carbon nanotube metacomposites, IEEE Journal of Ceramics International, VOL. 47, Issue 1, 1 January 202, Pages 1389-1398

Zhiniu Xu, Yi Zhang, Yijie Zhang, The influence of parameters of disk electrode with guard electrode system and sample on permittivity error caused by equivalent electrode area calculation and its correction method, IEEE Journal of Measurement, VOL. 129, December 2018, Pages 37-50

Kai Sun, Jiahao Xin, Yaping Li, Zhongyang Wang, Qing Hou, Xiaofeng Li, Xinfeng Wu, Runhua Fan, Kwang Leong Choy, Negative permittivity derived from inductive characteristics in the percolating Cu/EP metacomposites, IEEE Journal of Materials Science & Technology, VOL.35, Issue 11, November 2019, Pages 2463-2469

Janne Peltonen, Matti Murtomaa, Kelly Robinson, Jarno Salonen, The electrical resistivity and relative permittivity of binary powder mixtures, IEEE Journal of Powder Technology, VOL.325, 1 February 2018, Pages 228-233

Sofyan A. Taya, Nael Doghmosh, Anas A. Alkanoo, Vigneswaran Dhasarathan, NR Ramanujam, IS A miri, Waveguides including negative permeability and simultaneously negative permittivity and permeability materials for sensing applications, IEEE Journal of Optik, VOL.228, February 2021, 166147

Mustafa Suphi Gulsu, Fulya Bagci, Sultan Can, Asim Egemen Yilmaz, Baris Akaoglu, Metamaterial-based sensor with a polycarbonate substrate for sensing the permittivity of alcoholic liquids in a WR-229 waveguide, IEEE Journal of Sensors and Actuators A: Physical, VOL. 312, 1 September 2020, 112139

A.H. Seltzman, S. Wukitch, Precision measurement of relative permittivity of aluminum oxide for a high power resonant waveguide window with low retn loss,IEEE Journal of Fusion Engineering and Design, VOL. 147, October 2019, 111226

Ugur Cem Hasar, Yunus Kaya, Noniterative complex permittivity retrieval using calibration-independent waguide measurements, Sensors and Actuators A: Pysical,VOL.263, 15 August 2017, Pages 654-666

Hassan Aghayari, Javad Nourinia, Changiz Ghobadi, Bahman Mohammadi, Realization of dielectric loaded waveguide filter with substrate integrated waveguide technique based on incorporation of two substrates with different relative permittivity, IEEE Journal of AEU - International Journal of Electronics and Communiations, VOL.86, March 2018, Pages 17-24

Mejica, G. F. C., Unpaprom, Y., Balakrishnan, D., Dussadee, N., Buochareon, S., & Ramaraj, R. (2022, January 10). *Anthocyanin pigment-based dye-sensitized solar cells with improved ph-dependent photovoltaic properties*. Sustainable Energy Technologies and Assessments. Retrieved February 11, 2022,

APPENDIX A GANTT CHART

Elements	Week 1	Week 2	Week 3	Week 4	Week 5	Week 6	Week 7	Week 8	Week 9	Week 10	Week 11	Week 12	Week 13	Week 14
Introduction of Project														
Brief explanation														
Plan the dye used														
Decide the technique & wavelength														
Methodology														
Mechanical Extraction & by hand														
Measurement of Permittivity by Waveguide Resonator														
Absorbance value by UV-Visible Spectrophotometer														
Fabricate FTO glass the (Dye-sensitized Solar Cell)														
Results														
Anthocyanin Analysis														
Resonance Frequency														
Absorption light (Absorbance versus Wavelength)														
Open Circuit Voltage, Voc (Dye-Sensitized Solar Cell)														
Presentation														
Presentation Slide														
Thesis														
Completion of Logbook														

APPENDIX B LITERATURE REVIEW

Author	Title	Journal	Glass	Counter Electrode	Photoelectrode	Electrolyte	Dyes	Evaluated parameters	Measurement Tools	Findings
Gaoming Fu, Fan Ji, Chu, Xiang, Liu, Jingchen, Chen, Ji, Hoon Kim, Hyung Wook Lee and Sun-Hong Kim	Enhanced light harvesting in panchromatic double dye-sensitized solar cells incorporated with bilayered TiO ₂ nanofilm-based photoelectrodes	IEEE Journal of Solar Energy, VOL. 218, April 2021, Pages 346-353	FTO/Glass	Pt-coated	TiO ₂ (Top layer & Bottom layer)	Iodide/triiodide(I ⁻ /I ₃ ⁻)	N719 & N749	1. Schematic of the fabrication of a bilayered TiO ₂ nanofilm-based photoelectrode 2. To verify the light absorbance of the N719 & N749 3. Cross-sectional N719 & N749	1. Solar Simulator (PEC-L11) 2. Keithley 5400 source meter	1. Dye N719 broader light absorbance 2. Narrow light absorbance electrolyte in DSSC
Suboctic C. Ede, Clemer N. Hjeltnings, Mattias A. Salama, John F. Wansah, Amarschakwu N. Oso and Nsohke N. Anu	Synergistic effect of chlorophyll and anthocyanin Co-sensitizers in TiO ₂ -based dye-sensitized solar cells	IEEE Journal of Surfaces and Interfaces, VOL. 22, February 2021, 100882	FTO	Pt-coated	TiO ₂ Photoanode & ZnO Photoanode	Iodide/triiodide(I ⁻ /I ₃ ⁻)	1. Tallium trisulfonate 2. Tallium oxocyanide (chlorophyll pigments) 3. Caspalhin puckerium (anthocyanin pigment)	1. UV-Vis spectroscopy 2. Electrochemical impedance spectroscopy (EIS) 3. Current-voltage (I-V)	1. Onus weighing balance(HF A100) 2. Whisman filter paper (Cat No 1001 150)	1. Caspalhin puckerium flower & Tallium oxocyanide highest photovolt 2. Anthocyanin & chlorophyll effective improvement DSSC
N. Pabuarthy, R. Balasubramanian, Ame S. Krishnaiah, G. Babji, S. Prasanna, K. Sriramam, M.D. Kannan, Sriniv R. Eppa and Dhyanlal Velamuri	Enhanced photostability of anthocyanin dye for increased efficiency in natural dye-sensitized solar cells	IEEE Journal of Optik, VOL.227, February 2021, 166053	FTO	Pt-coated	Photoanolytic activity (PCA)	Iodide/triiodide(I ⁻ /I ₃ ⁻)	1. Red color amaranthum pigment 2. Co-sensitizer with anthocyanins extracted from rose petals	1. UV source for photo catalytic 2. Cyclic measurement of concentrated dye	1. Sapphire laser (Coheren Chambon Ultra 2. Generating femtosecond pulses (pulse width 140fs) 3. Microscope (Leica TCS SP5) 4. PMT detector (Hamamatsu R3310-02)	1. PCA improve photostability performance 2. Performance anthocyanins enhanced concentration 3. Astaxanthin perfect shielding for anthocyanin
Alfred Blazynski, Katarzyna Jochimiak-Lechman, Sylwia Sady, Tomasz Tanski, Marek Sander and Aleksandra Dyrkacz	Environmental performance of dye-sensitized solar cells based on natural dyes	IEEE Journal of Solar Energy, VOL. 215, February 2021, Pages 346-355	FTO	Pt-coated	TiO ₂	Iodide/triiodide(I ⁻ /I ₃ ⁻)	1. Juice 2. Pomace 3. Leaves of black chokeberries 4. Systemic N719 sensitizer	1. DSSC based on natural dye 2. Scarcity of metals 3. Lengthy purification steps 4. High-system costs	Vibr-Cell ultrasonic processor (130W, 20kHz) & MSC9000 painting machine	1. Energy efficiency lower but with N719 dye 2. Outweighs the environmental benefits using natural dyes
Emre Guzel, Baki Seclan Arslan, Veyis Durmaz, Mert Cezar, Omer Frank Tuzar, Tugba Sait, Mehmet Iskyen, Mehmet Nebegün and İhsan Sisman	Photovoltaic performance and photostability of anthocyanins, isocyanine alkaloids and betanin as natural sensitizers for DSSCs	IEEE Journal of Solar Energy, VOL. 173, October 2018, Pages 34-41	FTO	Pt-coated	TiO ₂ Photoanode	Iodide/triiodide(I ⁻ /I ₃ ⁻)	1. Anthocyanin (FBV) 2. Alkaloid (RPV) 3. Betanin (PPA/SPA)	1. Electrochemical properties of natural dyes 2. Photovoltaic performance of DSSCs 3. Photostability of DSSCs	Solar Simulator	1. Betanin highest efficiency & better light harvesting 2. Anthocyanin highest stability
Tahmineh Jahak, Parisa Arslan, Mahdi Ghorban, Mandana Jahak and Shahrzad Ostad	Performance evaluation of natural dyes as photosensitizer in dye-sensitized solar cells	IEEE Journal of Optical Materials, VOL. 110, December 2020,1044	FTO	Pt-coated	TiO ₂ Photoanode/ photoanolyte	Iodide/triiodide(I ⁻ /I ₃ ⁻)	1. Crocus saffron Saffron 2. Alism corpa 1. (red color) 3. Maha oshenya (Maha) 4. Oregon (Origanum vulgare)	1. DSSC operation process 2. Material & method 3. UV-Visible spectrometer	Incubator shaker (PFSKT-801L, Korea) 2. Centrifuge (Sigma, Model-409)	1. WBAK natural plants increase the biocompatibility of the DSSCs 2. Anthocyanin & chlorophyll very excellent light harvesting & effective charge carrier 3. UV-Vis Spectrometry 3. Transmission Electron Microscopy 3. Dynamic Light Scattering
Danuwan Kabir, Tassem Farhat, Wilham Chama, Bahin Richards, Mohammed M. Rahman, M.D. Nizam Uddin, Md. Reza J. Kabir, Mohammad Hosain Shurair, Faisal Chowdhury, Mohammad Mahabub Raihan, Newaz M. Babakar and Jamal Uddin	Dye-sensitized solar cell with plasmonic nanoparticles modified photoanode	IEEE Journal of Nano-Structures, VOL.26, April 2021, 100998	FTO	Pt-coated	TiO ₂ photoanode	Iodide/triiodide(I ⁻ /I ₃ ⁻)	N719 & an unmodified photoanode	1. UV-Visible spectroscopy 2. Dynamic light scattering 3. Performance solar cells via photoanode & photoanode	FT-IR spectroscopy	1. UV-Visible spectroscopy 2. Dynamic light scattering 3. Performance solar cells via photoanode & photoanode

Author	Title	Journal	Sample	Conduction mechanism	Temperature variation	Frequency	Material	Evaluated parameters	Measurement tools	Findings
P.S. Makhjee, A.K. Das, B. Datta, A.K. Meikap	Role of silver nanosphere on conductivity, dielectric permittivity and current voltage characteristics of polyvinyl alcohol-silver nanocomposite film	IEEE Journal of Physics and Chemistry of Solids, VOL. 111, December 2017, Pages 266-273	AR/D & FEMEM	Dielectric relaxation and current voltage behavior of Polyvinyl alcohol (PVA)	Range 303 ≤ T ≤ 423K (conductivity & dielectric response)	Range 20Hz ≤ f ≤ 1 MHz	1. Silver nitrate (AgNO ₃ 99.9%) 2. Ethylene glycol (EG, 99.8%, molecular weight: 62.07) 3. Polyvinylalcohol (PVP, molecular weight: 10,000) 4. Polyvinyl alcohol (PVA, molecular weight: 85,000-86,999)	1. Revised refined NRD pattern for Ag nanosphere 2. FEMEM micrograph and EDS study of the Ag nanosphere 3. TGA of PVA-Ag composite film determined in nitrogen atmosphere	1. Microscope (FE-SEM, Carl Zeiss Sigma) 2. Agilent E-4980A precision LCR meter 3. Keithley 2450 SMT 4. kikitast software	1. Semiconducting behavior with low activation energy 2. DC conductivity has been explained by adiabatic small polaron model 3. Dielectric property enhances & follow modified Cole-cole model 4. The current density vs. voltage characteristics obeys back to back Schottky diode
M.F. Coelho, M.A. Reis, E.M. Nogueira, T.P. Iglesias	Permittivity of (40nm and 80nm) alumina nanofibers in ethylene glycol at different temperatures	IEEE Journal of Chemical Thermodynamics, VOL. 158, July 2021, 106423	Alumina nanofibers (alumina oxide) in ethylene glycol - size: (40nm & 80nm)	The largest growth Water-based nanofibers	six different temperatures (from 298.15K to 348.15K)	Factor of frequency (104Hz and 107Hz)	Alpha-alumina nanoparticles (α-AD3)	1. Relative permittivity of the nanofibers 2. Permittivity enhancement for the nanofibers 3. Relative permittivity mixing for the system	1. Karl Fisher coulometer (Mettler Toledo BR32) 2. Bandelin Sonotrope HD2000 ultrasonic homogenizer	1. Relative permittivity decrease with increasing temperature and increase with increasing concentration 2. Permittivity measurement increases while increasing both temperature and concentration
S. Mandilani, P.A. Sorchetti, S.D. Romano	Relative permittivity of bioethanol, gasoline and blends as a function of temperature and composition	IEEE Journal of Fuel, VOL.293, 1 June 2021, 120419	Bioethanol, gasoline, and their blends	Bioethanol-gasoline blends	Range between 298K and 323K	100kHz	1. Gasoline (E0) 2. Sulphur content 3. Bioethanol	1. Relative permittivity as a function of temperature and composition 2. Estimation of blends composition from permittivity and temperature	1. Thermostat; bath 2. Measuring cell 3. LCR meter (Tonghui TH2822C)	1. Real part permittivity vs frequency well with a decreasing linear dependence with temperature 2. Permittivity dependence with composition, temperature range
Yong Yu, Yu Zhou, Yo Long Qiao, Yu Feng, Wei LiLi, Wei Dong Pei	Defect engineering of rutile TiO ₂ ceramics: Route to high voltage stability of colossal permittivity	IEEE Journal of Materials Science & Technology, VOL.84, 10 September 2021, Pages 10-15	(Ti-Al-La) co-doped TiO ₂ ceramics with colossal permittivity (CP)	Co-doped TiO ₂	25°C to 500°C	100-1M Hz	TiO ₂ , Ta2O5, ADO3 and La2O3	1. The relationship between the applied dc voltages and dielectric properties of TAIT 2. Leakage current density	1. PANanalytical Empower X-ray diffractometer 2. Scanning electron microscopy (SEM) 3. Materials studio CASTEP	1. Dielectric loss of ~0.02 above excellent temperature stability 2. Induced by defect dipoles formed by dopants with different ionic radius
Toton Haldar, Ukesh Kumar, B.C. Yadav, V.V. Ravi Varth Kumar	Effect of direct-current biasing on the adjustable radio-frequency negative permittivity characteristics of B2SO5/multiwall carbon nanotube nanocomposites	IEEE Journal of Ceramics International, VOL. 47, Issue 1, 1 January 2021, Pages 1389-1398	Multwall carbon nanotube (MWCNT)	B2SO5 (BSO/MWCNT) nanocomposites	MWCNT growth, 500nm for 3h raising temperature up to 650°C	Resonance in the frequency range 1MHz to 1GHz	1. Chemical vapor deposition (CVD) 2. sol-gel 3. Ethanol	1. Microstructural analysis of the BSO/MWCNT nanocomposites 2. Morphology and compositional analysis 3. Alternating current conduction and percolation threshold of the BSO/MWCNT nanocomposites	1. X-ray diffraction (XRD) 2. X-ray diffractometer 3. FEMEM (JEOL-ISM 15kV)	1. BSO/MWCNT nanocomposite can exhibit negative permittivity 2. Plasmun frequency increase with increase of MWCNT 3. BSO/MWCNT absorb energy from external dc bias

Author	Title	Journal	Sample	Standards	Conduction mechanism	Frequency	Evaluated parameters	Measurement tools	Findings
Zhanu Xu, Yi Zhang, Yifei Zhang	The influence of parameters of disk electrode with guard electrode system and sample on permittivity error caused by equivalent electrode area calculation and its correction method	IEEE Journal of Measurement, VOL. 129, December 2018, Pages 37-50	Disk electrode with guard electrode	1. IEC60250 Standard 2. GB/T 1409 Standard 3. ASTM D150 Standard	Sample and disk electrode with guard electrode on the permittivity error	0.01Hz to 1kHz	1. Disk electrode with guard electrode and calculation of permittivity 2. Modelling of disk electrode with guard electrode and its analysis 3. Accuracy in permittivity measurement and its influencing factors analysis	Insulation Diagnostics System (IDAX300)	1. Permittivity errors nearly negative & maximum related error larger than 50% 2. Error decreases with increasing sample thickness 3. Error increases with guarded electrode potential
Kai Sun, Jiahao Xin, Yaping Li, Zhongyong Wang, Qing Hou, Xinofeng Li, Xifeng Wu, Ruanhan Fan, Kwang Leong Choy	Negative permittivity derived from inductive characteristics in the percolating Cu/EP nanocomposites	IEEE Journal of Materials Science & Technology, VOL.35, Issue 11, November 2019, Pages 2463-2469	Copper dispersed in epoxy (EP)	None	Percolating composites with Cu/EP by polymerization method	10kHz to 1MHz	1. TGA curve 2. Electrical conductivities of the Cu/EP 3. Permittivity spectra of the Cu/EP	1. Electron microscopy (SEM, FEI Quanta 650) 2. Keysight E4980AL LCR meter 3. Synchronous thermal analyzer	1. Permittivity did not increase monotonously with the increase of Cu content, due to the presence leakage current 2. Positive permittivity (capacitive) & negative permittivity (inductive)
Janne Peltonen, Matti Martonen, Kobby Robinson, Jarmo Salonen	The electrical resistivity and relative permittivity of binary powder mixtures	IEEE Journal of Powder Technology, VOL. 325, 1 February 2018, Pages 228-233	Electrical resistivities & relative permittivities of binary powder mixtures	None	Resistivity & permittivity of the pure component materials, the particle sizes and sticking between different particles	None	1. AccuPyc 1330 pycnometer 2. Keithley 6517B electrometer 3. Fluke 289 Multimeter	1. Resistivity measurement 2. Static relative permittivity	1. The larger particles were covered by the small particles of the powder 2. Smaller particles size was dominant

Author	Title	Journal	Keywords	Sample	Conduction	Evaluated Parameter	Measurement Tool	Finding
Sofyan A. Taya, Nael Doghmosh, Anas A. Alkano, Vigneeswaran Dhasarathan, NR Ramamurjan, IS A niri	Waveguides including negative permeability and simultaneously negative permittivity and permeability materials for sensing applications	IEEE Journal of Optik, VOL.228, February 2021, 166147	Slab waveguide, Negative permeability, Fresnel coefficient, Optical sensor	Four-layer slab waveguide sensor	Conventional structure substrate, a guiding film, & cladding	1. Reflectance from negative μ structure 2. Reflectance from simultaneously negative μ and ϵ structure 3. Application of the two structures as optical sensors	1. Ellipsometer 2. Optical film thickness (Fibronics)	1. Both structures shows a dip at a resonance angle 2. Sharpness, depth and angular position depend structure 3. Sharpness & depth corresponding with negative μ layer
Mustafa Sapha Gaba, Fuyla Bagci, Sahar Can, Asim Egenen, Yilmaz, Baris Aksoylu	Metamaterial-based sensor with a polycarbonate substrate for sensing the permittivity of alcoholic liquids in a WR-229 waveguide	IEEE Journal of Sensors and Actuators A: Physical, VOL. 312, 1 September 2020, 112139	Dielectric sensor, Complex permittivity, Metamaterial, Microwave waveguide	Alcoholic liquid	The complex permittivity (ethanol-water & methanol-water mixture)	1. Design, modeling and fabrication 2. Ethanol-Water mixture 3. Methanol-Water mixture	1. WR-229 waveguide 2. Rohde-Schwarz ZVL-13 network analyzer	1. Electromagnetic waves, sensor enables characteristics the complex permittivity 2. Determine resonance frequency
A.H. Sezman, S. Wuklich	Precision measurement of relative permittivity of aluminum oxide for a high-power resonant waveguide window with low return loss	IEEE Journal of Fusion Engineering and Design, VOL. 147, October 2019, 111226	Aluminum oxide, Permittivity, Dielectric, Lower hybrid current drive, RF window, Resonant window	Aluminum oxide	Estimating permittivity & window thickness with high precision	1. Ceramic material analysis 2. Measurement of dielectric properties 3. Error contribution and sensitivity	Waveguide resonant cavity per ASTM D2520-13	Waveguide cavity resonator provides measurement permittivity at several frequency at different resonant mode
Ugur Cem Hasar, Yunus Kayu	Noniterative complex permittivity retrieval using calibration-independent waveguide measurements	Sensors and Actuators A: Physical, VOL.263, 15 August 2017, Pages 654-666	Calibration-independent, Explicit determination, Sample shifting, Complex permittivity, Waveguide measurement	Calibration-independent nonresonant	1. Eliminate errors arising from inaccurate 2. Determine complex permittivity explicitly	1. Measurement 2. Repeatability analysis 3. Uncertainty analysis	Keysight Instruments (N9928A)	1. Parasitic oscillations eliminated aperture averaging 2. Sensitive measurement errors coming from geometry knowledge
Hassan Aghayari, Javad Nourinia, Changiz Gholbadi, Bahman Mohammadi	Realization of dielectric loaded waveguide filter with substrate integrated waveguide technique based on incorporation of two substrates with different relative permittivity	IEEE Journal of AEU - International Journal of Electronics and Communications, VOL.86, March 2018, Pages 17-24	SIW, Dielectric-loaded waveguide, H-plane filter, Transition circuit	Incorporated substrate integrated waveguide (ISIW)	Waveguide filter & dielectric loaded waveguide filter realized with SIW & ISIW	1. Structural analysis of incorporated substrate integrated waveguide 2. Design strategy 3. Fabrication and measurement	E8363C PNA network analyser	1. ISIW filter more insertion loss & return loss than waveguide filter 2. ISIW structure is much easier & less costly